EXPERIMENTAL INVESTIGATION OF PHASE DISTRIBUTION IN A HORIZONTAL TEE JUNCTION

by

Mark T. Rubel

A thesis
presented to the University of Manitoba
in partial fulfillment of the
requirements for the degree of
Master of Science
in
Mechanical Engineering

Winnipeg, Manitoba

ISBN Ø-315-33897-Ø

EXPERIMENTAL INVESTIGATION OF PHASE DISTRIBUTION IN A HORIZONTAL TEE JUNCTION

BY

MARK T. RUBEL

A thesis submitted to the Faculty of Graduate Studies of the University of Manitoba in partial fulfillment of the requirements of the degree of

MASTER OF SCIENCE

I hereby declare that I am the sole author of this thesis.

I authorize the University of Manitoba to lend this thesis to other institutions or individuals for the purpose of scholarly research.

Mark T. Rubel

I further authorize the University of Manitoba to reproduce this thesis by photocopying or by other means, in total or in part, at the request of other institutions or individuals for the purpose of scholarly research.

Mark T. Rubel

The University of Manitoba requires the signatures of all persons using or photocopying this thesis. Please sign below, and give address and date.

ABSTRACT

A two-phase flow apparatus was designed and constructed to generate phase-distribution data for steam-water flow through a horizontal tee junction with a horizontal branch of equal diameter (37.6-mm I.D.). For low system pressures (100 - 200 kPa) and low inlet mass fluxes (15 - 50 $kg/m^2.s$), a wide range of inlet qualities (20 - 80 percent) and extraction rates (0.2 - 0.8) were tested. These inlet flow conditions led to the observation of stratified, wavy, semiannular-wavy and semiannular flow patterns at the tee junction inlet. The results showed that in general, the phases did not distribute themselves evenly between the branch and run sides. All stratified flow data were below the line of even phase distribution; that is, the branch quality was less than the inlet quality. Most of the wavy and semiannular-wavy flow data were above this line while the semiannular flow data were both above and below it.

The phase-distribution results were presented in a number of ways in order to examine the individual effects of important inlet flow parameters on the phase distribution. The results indicate that for a fixed inlet mass flux, the ratio of the branch to inlet quality decreased with increasing inlet quality except, however, at the lowest inlet mass fluxes

in which case the reverse was true. For a fixed inlet flow pattern and inlet quality, there was no apparent effect of the mass flux on the phase distibution. For any constant superficial vapor velocity, the fraction of the total vapor that entered the branch increased with increasing superficial liquid velocity, irrespective of the inlet flow pattern. These trends in the present data are similar to trends observed by other investigators using different operating conditions and junction geometries.

The phenomenological model developed by Azzopardi and Whalley [7] for annular flow poorly predicted the present data (which did not include annular flow). Predictions became increasingly better, however, as the inlet quality and the ratio of the superficial vapor velocity to the superficial liquid velocity increased. The empirical correlation derived by Seeger et al. [14] predicted the present data remarkably well for all inlet conditions and for extraction rates greater than 0.3. This correlation failed to predict any of the present data where the extraction rate was less than 0.3.

ACKNOWLEDGEMENTS

I would like to express my deepest gratitude and respect to Dr. H. M. Soliman and Dr. G. E. Sims for their continuous encouragement, guidance and support. I would also like to thank Dr. J. R. Cahoon for spending so much time setting up some of the electrical equipment in the lab.

Although it would be impossible to thank all my friends and colleagues who have helped me in so many ways, your help will not be forgotten.

I am deeply gratefull to Miss Melody Munz for her always present smile, her encouraging words and for giving her summer to type this thesis. I could not have finished on time without her.

I would like to thank my friend and colleague Mr. Fawzy Rashwan for always being there to listen, or advise, and for helping me endlessly in the design and construction of the lab.

Finally, I would like to thank my family who have supported me throughout my entire studies. Without all of you behind me, my career could not have been possible. To you I dedicate this thesis.

TABLE OF CONTENTS

LIST OF FIGURES

LIST OF TABLES

NOMENCLATURE

English

a	Constant used by Seeger et al. [14], defined by equation (4.5)
c_p	Specific heat of water, kJ/kg.K
D_1	Inside diameter of inlet tube, m
D_2	Inside diameter of run tube, m
D_3	Inside diameter of branch tube, m
E_1	Liquid fraction entrained by the vapor phase
F_{BG}	Fraction of the total inlet gas (vapor) entering the branch, defined by equation (3.14)
F_{BL}	Fraction of the total inlet liquid entering the branch, defined by equation (3.15)
G_1	Inlet mass flux, defined by equation (3.10), $kg/m^2.s$
G_2	Run mass flux, $kg/m^2.s$
G_3	Branch mass flux, defined by equation (3.11), $kg/m^2.s$
g	Gravitational acceleration, m/s^2
h_f	Enthalpy of saturated liquid, kJ/kg
h_{fg}	Latent heat of vaporization, kJ/kg
h_{in}	Precondenser inlet enthalpy, kJ/kg
h_{out}	Precondenser outlet enthalpy, kJ/kg
P_{in}	Precondenser inlet pressure, kPa
P_{out}	Precondenser outlet pressure, kPa

P_1	Pressure at tee-junction inlet, kPa
P_2	Pressure at tee-junction outlet (run side), kPa
P_3	Pressure at tee-junction outlet (branch side), kPa
S_1	Slip ratio, used by Seeger et al. [14], defined by equation (4.6)
$T_{CW,in}$	Cooling-water temperature at precondenser inlet, °C
$T_{CW,out}$	Cooling-water temperature at precondenser outlet, °C
T_{in}	Precondenser inlet temperature, °C
T_{out}	Precondenser outlet temperature, °C
V_{GS}	Superficial gas (vapor) velocity, defined by equation(3.12), m/s
$\bar{V}_{GS}$	Nominal superficial gas (vapor) velocity, m/s
V_{LS}	Superficial liquid velocity, defined by equation (3.13), m/s
$\bar{V}_{LS}$	Nominal superficial liquid velocity, m/s
V_{rel}	Relative velocity, used by Seeger et al. [14], defined by equation (4.8), m/s
W_{CW}	Cooling-water mass flow rate into the precondenser, kg/s
W_1	Inlet mass flow rate, kg/s
W_2	Run mass flow rate, kg/s
W_3	Branch mass flow rate, kg/s
x_1	Inlet quality, defined by equation (3.5)

x_2 Run quality

x_3 Branch quality, defined by equation (3.6)

Greek

ρ_G Density of gas (vapor), kg/m^3

ρ_H Homogeneous mixture density, defined by equation (4.7), kg/m^3

ρ_L Density of liquid, kg/m^3

σ Liquid surface tension, N/m

Chapter 1

INTRODUCTION

Two-phase flow is a topic of rapidly increasing importance, particularly in its application to the power and process industries. Two-phase flow is present in systems such as conventional steam power plants, evaporators and condensers of refrigeration systems, boiling-water nuclear reactors, pressurized-water nuclear reactors, and a wide variety of chemical and petroleum applications, to name a few. Quite often, the complex piping networks in these systems require the two-phase flow to pass through branching junctions (e.g. wyes and tees). Until very recently, a commonly made assumption was that the phases were distributed evenly through the junction; that is, the quality in each downstream side of the junction was equal to the inlet quality. Observations have shown that this can be very far from the actual situation, even in a junction as simple as a tee. Under certain inlet conditions single-phase vapor may be present in the branch section, while other conditions can lead to single-phase liquid in the branch. This severe maldistribution can lead to serious consequences in many applications, one being the main cooling system of light-water nuclear reactors during hypothetical loss-of-coolant accidents.

In regards to the problem of phase distribution at junctions, a great deal of attention has been focussed on attempting to develop generalized mathematical models, capable of predicting the downstream side qualities in a wye or tee junction, for any inlet flow pattern. A truly generalized model (not flow pattern specific) would accommodate any combination of inlet pressure, mass flow rate and quality for any fluid combination, junction orientation and dimensions, as well as any extraction rates. A review of the literature (Chapter 2) indicates that, to date, no model has been published which satisfies the above requirements. Furthermore, there is no complete agreement amongst researchers in this field as to the important parameters that influence the physics occurring at the junction itself. A fundamental prerequisite to the development of such a mathematical model is the availability of a wide range of experimental data against which to test any proposed model. Unfortunately, only a small amount of phase-distribution data has been published, and of these data most exist for air-water (two-phase, two-component) flow at low pressures. Few studies using steam-water (two-phase, one-component) flow have been carried out, none of which involved low system pressures and low flow rates. It is the intent of this work, therefore, to generate a data base at these last-mentioned conditions to aid in the understanding and model development of phase distribution during two-phase flow through tee junctions.

The following is a list of objectives which the present investigation has undertaken:

1. To design and construct a two-phase flow apparatus, in the existing two-phase flow laboratory located on the University of Manitoba campus, capable of generating steam-water phase-distribution data through a horizontal tee junction with a horizontal branch of equal diameter (37.6-mm I.D.).
2. To generate phase-distribution data for a system pressure of about 150 kPa, a range of inlet mass fluxes between 15 and 50 $kg/m^2.s$, an inlet quality range from 20 to 80 percent and extraction rates between 0.2 and 0.8.
3. To investigate the influences of the inlet mass flux, inlet quality, extraction rate and inlet flow pattern on phase distribution through the tee junction.
4. To compare some of the existing phase-distribution correlations against the generated experimental results to test their prediction capabilities at the present conditions.

Chapter 2

LITERATURE REVIEW

Figure 2.1 shows a schematic diagram of a tee junction with the relevant geometrical and flow parameters. These include: the inlet, run and branch pressures (P_1, P_2 and P_3, respectively); the inlet, run and branch mass flow rates (W_1, W_2 and W_3, respectively); the inlet, run and branch qualities (x_1, x_2 and x_3, respectively); the inlet and run (main) tube diameters (D_1 and D_2, which have been equal in most investigations) and the branch tube diameter (D_3).

The design engineer is often faced with the following question: Given the junction geometry (D_1, D_2 and D_3), the inlet flow conditions (P_1, W_1 and x_1) and one of the flow parameters in the run or branch (e.g. W_3), what would be the value of the remaining flow parameters in the run and branch (i.e. W_2, x_2, x_3, P_2 and P_3)? So far, there is no complete answer to this question over the whole range of inlet flow conditions, geometry and extraction rates (W_3/W_1). Previous investigations have succeeded in providing answers only over narrow ranges of conditions and it is hoped that the present investigation increases our understanding of the flow phenomena by examining previously untested flow conditions. Emphasis in this study is directed towards phase distribu-

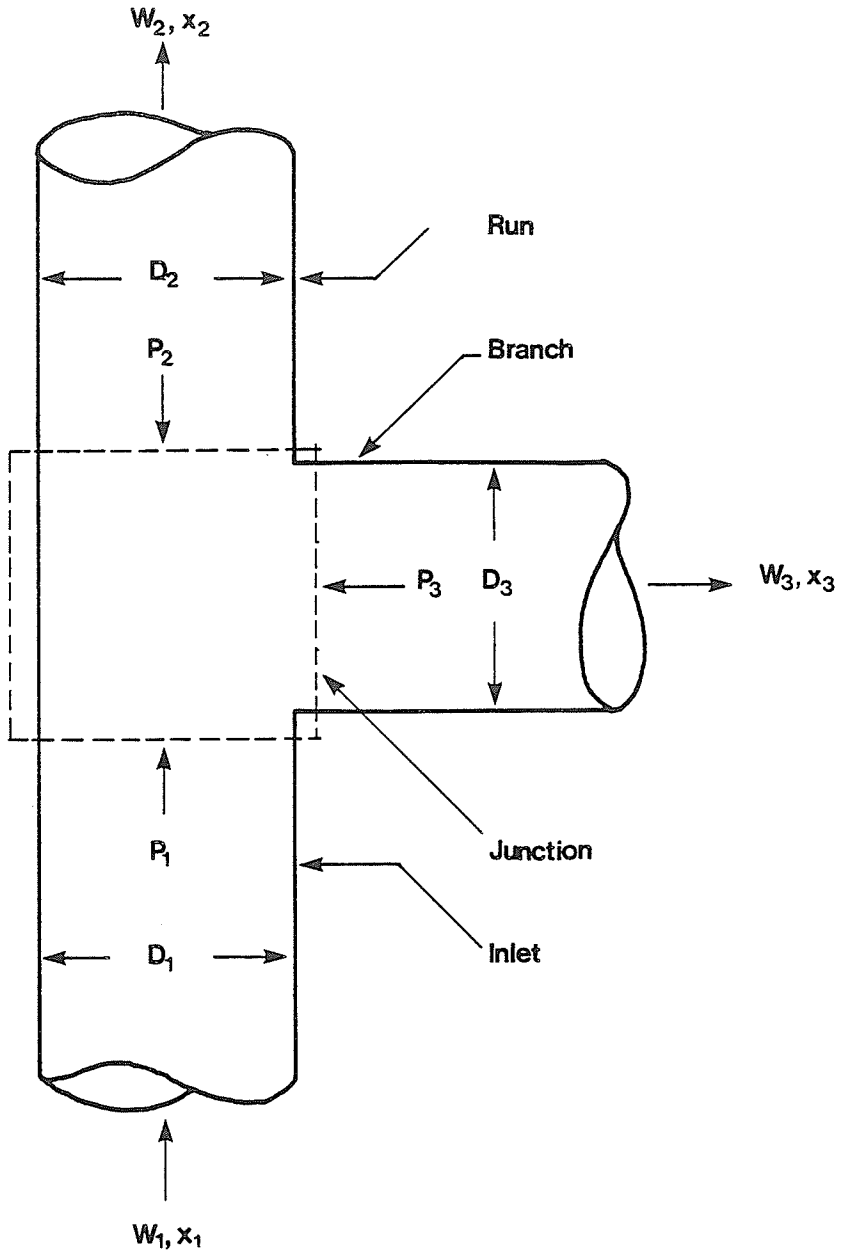

Fig. 2.1 Geometry and relevant parameters of a tee junction

tion at the tee junction, i.e. values of x_2 and x_3 relative to x_1 at different operating conditions.

Table 2.1 summarizes the previously published data for phase distribution at tee junctions. Inspection of this table indicates that, to date, only a limited range of geometrical and flow conditions have been covered. For example, most of the data correspond to air-water at 150 kPa. For the sake of completeness, Table 2.1 includes data obtained for both horizontally and vertically orientated main tubes. Only studies where the main tube was horizontal will be reviewed later in this chapter unless the results have some relevance to a horizontal main tube. A broader review of literature which includes wyes and tees with different orientations was recently published by Azzopardi [1].

Quite often in the literature, if particular terminology has not been clearly defined, ambiguities between authors can arise. As well, the method by which authors present their data can differ from one to another. It is often the case that the method by which data are presented depends upon the parameters of interest to that particular investigation. In the following discussion, an attempt will be made to define clearly the terminology used throughout this thesis. The term "phase distribution" refers to the redistribution of the incoming vapor and liquid in the inlet pipe between the run and branch pipes, after the junction has

Table 2.1 Summary of phase distribution data in tee junctions

Junction Orientation		D_1	D_3	Test Fluids	P_1	G_1	x_1	W_3/W_1	Inlet Flow Pattern	Author(s)
main	branch	(mm)	(mm)		(kPa)	($kg/m^2.s$)	(%)			
horiz.	horiz.	23.4	23.4	air-water	100	550-1000	0-45	0.0-1.0	-	Tsuyama and Taga [2]
horiz.	horiz.	38	25	air-water	300	136	2.1-50	0.05-0.9	-	Collier [3]
horiz.	vert. up horiz. vert. down	9.5	9.5	air-water	150	15-80	25-97	0.1-1.0	annular wavy	Hong [4]
horiz.	vert. up horiz. vert. down horiz.	51	51	air-water	250-400	69-841	.5-99.9	0.1-1.0	stratified slug annular-mist	Johansen [5]
		51	38.1							
horiz.	horiz.	100	20	air-water	150	200-850	10-60	0.0-0.06	annular	Henry [6]
vert. horiz.	horiz. vert. up vert. down	31.8	12.7	air-water	150 250	80-180	35-80	0.0-0.92 0.0-0.4	annular	Whalley and Azzopardi [8]
vert.	horiz.	31.8	19 6.35	air-water	150	80-180	35-80	0.0-0.92	annular	Whalley and Fells [9]
vert.	horiz.	31.8	12.7	air-water	150	80-110	10-30	0.0-0.92	churn	Azzopardi and Baker [10]
vert.	horiz.	31.8	25.6 31.8	air-water	150	80-180	35-80	0.0-0.5	annular	Azzopardi [11]
horiz.	horiz.	38.1	38.1	air-water	150	1355-2711	0.1-1.0	0.3-0.7	bubbly	Saba and Lahey [12]
horiz.	vert. up horiz. vert. down	50	50	air-water	700	1000-7000	0-100	0.0-1.0	annular slug dispersed-bubble	Seeger et al.[14]
horiz.	horiz.	50	50	steam-water	2500-10000	1000-2500	0-100	0.0-1.0	slug annular	
vert.	horiz.	38.1	38.1	air-water	150	1355-2711	0.1-1.0	0.3-0.7	bubbly	Honan and Lahey [15]

been encountered. Figure 2.2a illustrates one method which is used to present phase-distribution data. In this figure, the ratio of the branch quality to the inlet quality (x_3/x_1) appears as the ordinate. The ratio of the branch mass flow rate to the inlet mass flow rate (W_3/W_1), or the "extraction rate," appears as the abscissa. Line BC represents the limiting case where single-phase liquid is flowing in the run ($x_2 = 0$) and all the incoming vapor (plus some liquid) is diverted into the branch. From a simple mass balance on the vapor phase the equation of this line can be written as: $x_3/x_1 = W_1/W_3$. Line AB represents the limiting case of single-phase vapor in the branch ($x_3 = 1$) and all the incoming liquid (plus some vapor) continuing into the run. Point B corresponds to "total phase separation"; that is, single-phase vapor in the branch and single-phase liquid in the run. These limiting flow conditions are useful to identify since they represent upper limits on the value of x_3/x_1. In other words, no data can exist above the line ABC in Fig. 2.2a. The horizontal line CD at $x_3/x_1 = 1$ is the "even-phase-distribution" line (branch quality is equal to the inlet quality).

Figure 2.2b illustrates another form of presenting phase-distribution data with points A, B, C and D labelled. In this figure, the fraction of inlet vapor entering the branch (F_{BG}) is the ordinate and the fraction of the inlet liquid entering the branch (F_{BL}) is the abscissa.

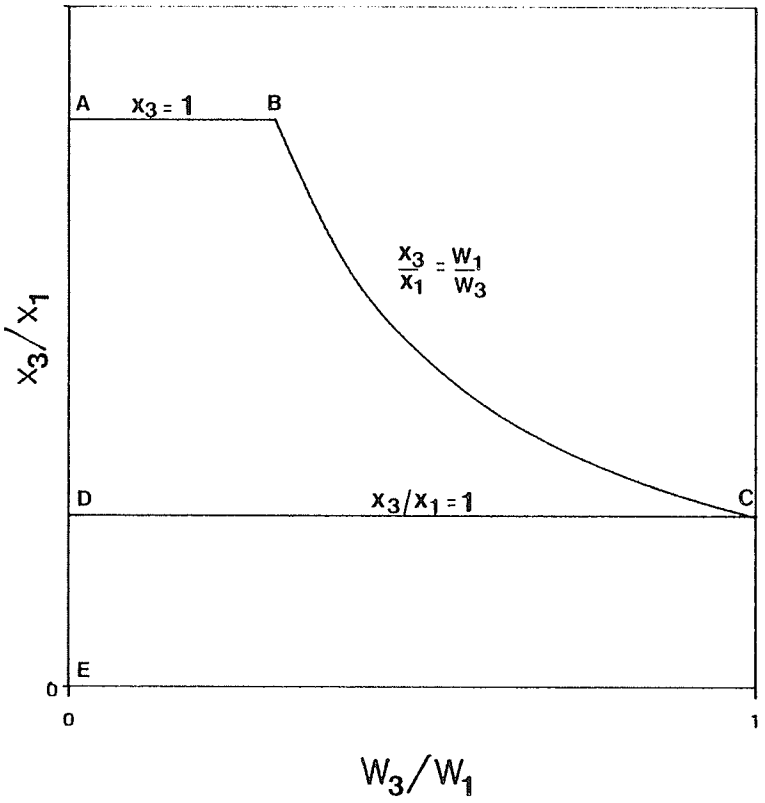

(a)

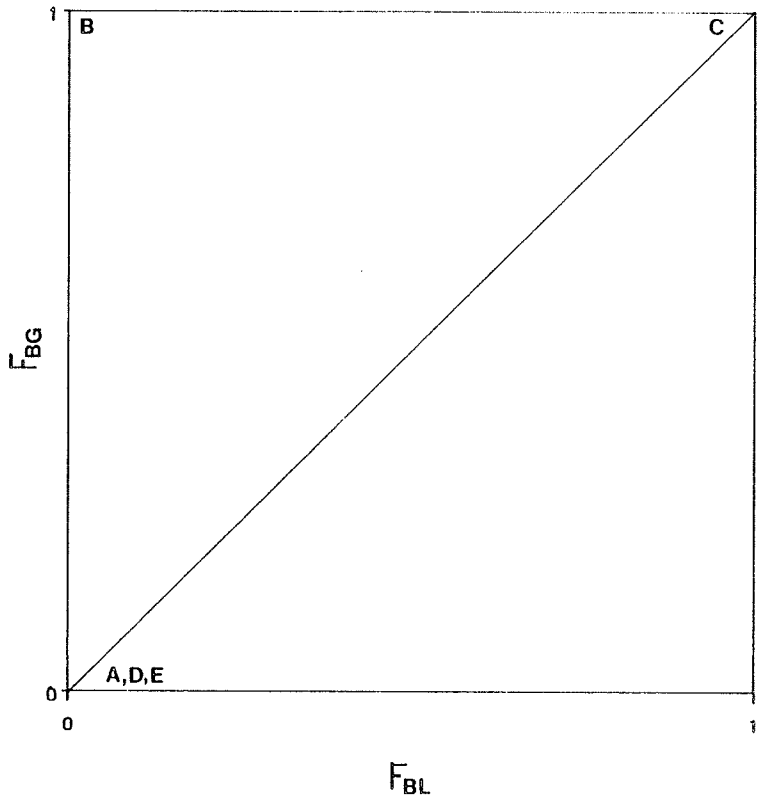

(b)

Fig. 2.2 Methods of presenting phase-distribution data

One of the earliest experimental investigations was conducted in 1959 by Tsuyama and Taga [2]. They reported their findings on the pressure differences ($P_2 - P_1$) and ($P_1 - P_3$), as well as the phase distribution for two-phase flow through a horizontal tee junction with equal tube diameters (23.4-mm I.D.). Tests were performed with an air-water mixture at isobaric and isothermal conditions. The results showed that the phase distribution after the junction could be classified into three categories: one in which both the branch and run contained a two-phase mixture, one in which the branch contained single-phase liquid, and one in which the run contained single-phase liquid. Since the investigation was quantitatively concerned with the pressure differences at the tee junction and only qualitatively concerned with the phase distribution, the authors did not discuss the conditions which led to each of the three categories.

Collier [3], in 1964, obtained phase-distribution data for a horizontal main tube (38-mm I.D.) with a horizontal branch (25-mm I.D.). For a fixed inlet mass flux (136 $kg/m^2.s$), wide ranges of inlet qualities (2.1 to 50 percent) and extraction rates (0.05 to 0.9) were investigated. Collier's [3] objective was to study the effect of inlet quality on the phase distribution. The data showed that except for very low extraction rates, the gas tended to flow preferentially into the branch; that is, $x_3/x_1 > 1$. Also, values of x_3/x_1 depended on the inlet quality in a complex man-

ner. The values of x_3/x_1 were first seen to increase and then decrease with increasing quality.

Hong [4] studied phase distribution of air-water through a tee junction with equal (9.5-mm I.D.) branch and main tube diameters. In his investigation, the inlet and run (main) tube was horizontal with the branch orientated vertically upwards, horizontal and vertically downwards. The range of inlet mass flux was 15 to 80 $kg/m^2.s$ and the inlet quality ranged between 25 and 97 percent. These inlet conditions led to the observation of wavy and annular flows. During each set of inlet conditions, the extraction rate ranged between 0.1 and 1.0. The intent of his investigation was to examine the effect of superficial gas velocity (for fixed superficial liquid velocity), superficial liquid velocity (for fixed superficial gas velocity), liquid viscosity, inlet flow pattern and branch orientation on the phase distribution at the tee junction. Most of the data that Hong [4] obtained showed the liquid phase flowing preferentially into the branch. The results indicated that for a fixed superficial gas velocity (V_{GS}) the fraction of gas entering the branch (F_{BG}), for a certain fraction of liquid in the branch (F_{BL}), increased with increasing superficial liquid velocity (V_{LS}). Conversely, for a fixed V_{LS}, F_{BG} (at a certain F_{BL}) decreased with increasing V_{GS}. The results also showed that F_{BG} decreased (at a fixed F_{BL}) with increasing liquid viscosity. Hong [4] also concluded that the inlet flow pattern

had no clear effect on phase distribution. Finally, the data showed that for a fixed combination of inlet superficial gas and liquid velocities and at a given F_{BL}, F_{BG} was dependent on the branch orientation. The maximum F_{BG} occurred when the branch was orientated vertically upwards and decreased to a minimum for the vertically downwards orientation.

Johansen [5] performed an experimental investigation using an air-water mixture flowing through a tee junction. The tee junction consisted of a 51-mm I.D. horizontal main tube with two different branch diameters. A 51-mm I.D. branch diameter was orientated vertically upwards, horizontal and vertically downwards whereas a 38.1-mm I.D. branch was orientated only horizontally. The inlet mass flux ranged between 69 and 841 $kg/m^2.s$ with inlet qualities between 0.5 and 99.9 percent. These inlet conditions led to stratified, slug and annular-mist flows being observed at the junction inlet. The results showed that all data points at low mass fluxes fell below the line of even phase distribution ($x_3 = x_1$). At the highest mass flux, all data points were above this line, although very close to it. Unfortunately, the author did not discuss the individual effects of inlet flow pattern, branch diameter and extraction rates on the phase-distribution results.

Later, Henry [6] published phase-distribution data for an air-water mixture flowing through a horizontal tee junction with a 100-mm I.D. main tube and a horizontal branch of 20-mm I.D. The inlet mass flux ranged between 200 and 850 $kg/m^2.s$ and the inlet quality ranged between 10 and 60 percent. There was a maximum of only 6 percent of the total inlet mass extracted through the branch during the experiments (i.e. $W_3/W_1 \leq 0.06$). The results that Henry [6] obtained, indicated that the branch quality increased with increasing extaction rate and eventually reached a plateau. This plateau occurred at an extraction rate approximately proportional to the inlet mass flux. The data also indicated that an even phase distribution was more likely to occur at high inlet mass fluxes. A low mass flux, on the other hand, resulted in severe maldistribution of the phases with air preferentially entering the branch. The value of x_3/x_1 was seen to approach unity as the flow became more homogeneous; that is, dispersed. This same trend was found to occur as the extraction rate increased. Based on the collected data, Henry [6] proposed an empirical correlation to predict the branch quality. This correlation was found to predict his data, and the data of Collier [3], favorably considering the simplicity of the method of correlation. The author suggested caution when the correlation is to be used at conditions outside those from which it was derived.

In 1982, Azzopardi and Whalley [7] published results which combined the works of Whalley and Azzopardi [8], Whalley and Fells [9] and Azzopardi and Baker [10]. The investigations included an air-water mixture flowing in both vertical (P_1 = 150 kPa) and horizontal (P_1 = 250 kPa) main tubes of 31.8-mm I.D. Horizontal branch diameters of 6.35, 12.7 and 19 mm gave branch diameter ratios (D_3/D_1) of 0.2, 0.4 and 0.6, respectively. The range of the inlet mass flux was between about 80 and 180 kg/m^2.s with a range of inlet quality between about 10 and 80 percent. The experimental investigations studied the effect of inlet flow patterns on the fraction of liquid in the branch (F_{BL}) as a function of the fraction of gas in the branch (F_{BG}). For the range of inlet conditions investigated, annular and churn flow patterns were present at the junction inlet. The results showed that the liquid preferentially flowed into the branch during annular and churn flow conditions. Azzopardi and Whalley [7] suggested that in annular flow, there exists three levels of momentum flux: the liquid film where the momentum flux is low (high density but low velocity), the gas core which has a low momentum flux (high velocity but low density) and the entrained drops which have a high momentum flux (high density and high velocity). Therefore, during annular flow, the liquid from the film can be expected to be diverted while the entrained drops by-pass the branch. In bubbly flow, on the other hand, there exists a

liquid layer near the wall which possesses a momentum flux close to that of the bubbles. Since the liquid core has a much higher momentum flux, the slow liquid layer near the wall could be expected to enter the branch with the bubbles. The experimental data also showed that the liquid flow rate in the branch was approximately linearly dependent on the branch gas flow rate except at low gas flow rates.

Based on the above results, Azzopardi and Whalley [7] developed a simple phenomenological model for annular flow, where the liquid flow rate through the branch was dependent on both the branch gas flow rate and the apparent angle over which the film flow rate had been extracted. This model will be discussed in more detail in Chapter 4 and compared to the present experimental results.

Later, Azzopardi [11] proposed a correction term to take into account the branch-to-inlet-diameter ratio (D_3/D_1). For the same inlet conditions as above, the experimental results were extended to include diameter ratios of 0.8 and 1.0 for extraction rates between 0.0 and 0.5. The data showed that although no clear cut branch-to-inlet-diameter-ratio dependence was evident, in general, the greater D_3/D_1 was, the greater the liquid take-off was (i.e. the lower the branch quality was).

Azzopardi and Baker [10] developed a phenomenological model applicable to various inlet flow patterns for a verti-

cal main tube which reduced to that of Azzopardi and Whalley [7] during annular flow. The approach was based on observations which showed that the fluid taken through the branch comes from the segment of the tube closest to the branch. The probability that the liquid will enter the branch depends on the ratio of the gas and liquid momentum fluxes.

In 1984 Saba and Lahey [12] reported phase-distribution data for air-water bubbly flow through a horizontal tee junction with equal diameter tubes (38.1-mm I.D.). Inlet mass fluxes of 1355, 2041 and 2711 $kg/m^2.s$ were used with a maximum inlet quality of 1.0 percent. For each inlet condition, extraction rates of 0.3, 0.5 and 0.7 were tested. The experimental investigation also included branch and run pressure losses due to the tee junction. The phase-distribution results indicated that air preferentially entered the branch; in fact, the data closely followed line BC of Fig. 2.2a. Although the extraction rate had a great effect on the phase distribution (x_3/x_1 increased with decreasing W_3/W_1), the results showed little dependence on the inlet mass flux. Saba and Lahey [12] also proposed a physically based model, with some empirical coefficients, for predicting the phase distribution at the tee junction. This model was later shown to be suitable only for bubbly flow with extraction rates greater than 30 percent [13].

Seeger et al. [14], in 1985, presented phase-distribution data during air-water and steam-water flows through a tee junction. The tee junction consisted of equal diameter tubes (50-mm I.D.) with the main tube horizontal. During steam-water flow the branch was always horizontal, while the branch orientation was horizontal, vertically upwards and vertically downwards during air-water flows. Very high inlet mass fluxes (1000 - 7000 $kg/m^2.s$) were used during air-water tests with a system pressure of 0.7 MPa. The system was designed to allow extraction rates between 0.0 and 1.0 as well as inlet qualities between 0 and 100 percent. Over the tested range of inlet mass flux and inlet quality, it was possible to have annular, slug and dispersed-bubble flows present at the tee-junction inlet. During steam-water flow, the system pressure ranged between 2.5 and 10 MPa with inlet mass fluxes between 1000 and 2500 $kg/m^2.s$. Similar to the air-water experiments, a full range of extraction rates and inlet qualities were tested; however, only annular and slug flows were present at the tee-junction inlet.

The results from the above investigation showed that for a vertically upwards orientated branch, high values of x_3/x_1 occurred. When the quality ratio (x_3/x_1) was plotted against the extraction rate (W_3/W_1), all data points fell very close to line BC of Fig. 2.2a, except however, when the inlet flow pattern was dispersed bubble in which case deviations from line BC were the greatest. The authors found

little phase-distribution dependence on the inlet parameters for a vertically upwards orientated branch and did not, therefore, investigate a wide range of inlet conditions. For a horizontal branch, both air-water and steam-water data points fell quite close to line BC at high values of W_3/W_1. After reaching a maximum at about $W_3/W_1 = 0.3$, a sharp decrease occurred in x_3/x_1 with decreasing W_3/W_1. The authors speculated that during annular flow, the extrapolated value at $W_3/W_1 = 0$ is $x_3/x_1 = 0$. For a constant superficial liquid velocity, x_3/x_1 was found to decrease with increasing superficial gas velocity, which corresponded to an increasing gas momentum flux. In comparing the phase-distribution data between air-water and steam-water flows, the authors presented data with close superficial gas and liquid velocities. The results showed that x_3/x_1 decreased with increasing pressure, again corresponding to an increasing gas momentum flux. For a downward orientated branch, high values of W_3/W_1 gave, in general, values of x_3/x_1 higher than the even-phase-distribution line, indicating that the inertia effect is greater than the gravity effect. At lower values of W_3/W_1, x_3/x_1 was below the even-phase-distribution line and reached $x_3/x_1 = 0$ at some finite value of W_3/W_1. The intercept was found to increase as the inlet flow pattern became more stratified.

Based on the above experimental data, empirical correlations for the phase distribution, for each branch orienta-

tion, were derived. As well, the expressions took into account the different inlet flow patterns. The equation derived for a horizontally orientated branch will be discussed in more detail in Chapter 4 and compared to the present experimental data.

From the above discussion, it is evident that no generalized model has yet been developed to predict accurately the phase distribution through a tee junction. As well, there is no complete understanding of the phenomena, or the important parameters affecting two-phase flow at tee junctions. Since the parameters of importance are not fully known, there is also no accepted method for presenting phase-distribution data, although either Fig. 2.2a or Fig. 2.2b has been used by most authors. Finally, to date the available phase-distribution data does not cover a very wide range of inlet conditions against which to test any proposed phase-distribution models. It is necessary, therefore, to widen the range of experimental phase-distribution data in order to improve our understanding of the phenomena occurring at tee junctions and to aid in the development of models used to predict the phase distribution at tee junctions.

Chapter 3

EXPERIMENTAL INVESTIGATION

The objective of the present experimental investigation was to generate phase-distribution data for two-phase, one-component flow through a horizontal tee junction. The apparatus required to obtain this data incorporated a horizontal branch, equal in size to the main tube (37.6-mm I.D.), and was designed for the following operating conditions: steam-water mixtures at pressures ranging between 100 and 250 kPa, inlet mass fluxes between 15 and 50 kg/m^2.s, inlet qualities ranging between 20 and 80 percent, and extraction rates from 0.2 to 0.8. In this chapter, the design and construction of the required apparatus is discussed and the test procedure and method of data reduction are presented.

3.1 Overview of Experimental Facility

The test apparatus which was constructed for this investigation is shown schematically in Fig. 3.1. The following description is a brief overview of the flow through different components of the test apparatus. A more detailed presentation of the design, construction and operation of the major components will be provided later in this chapter.

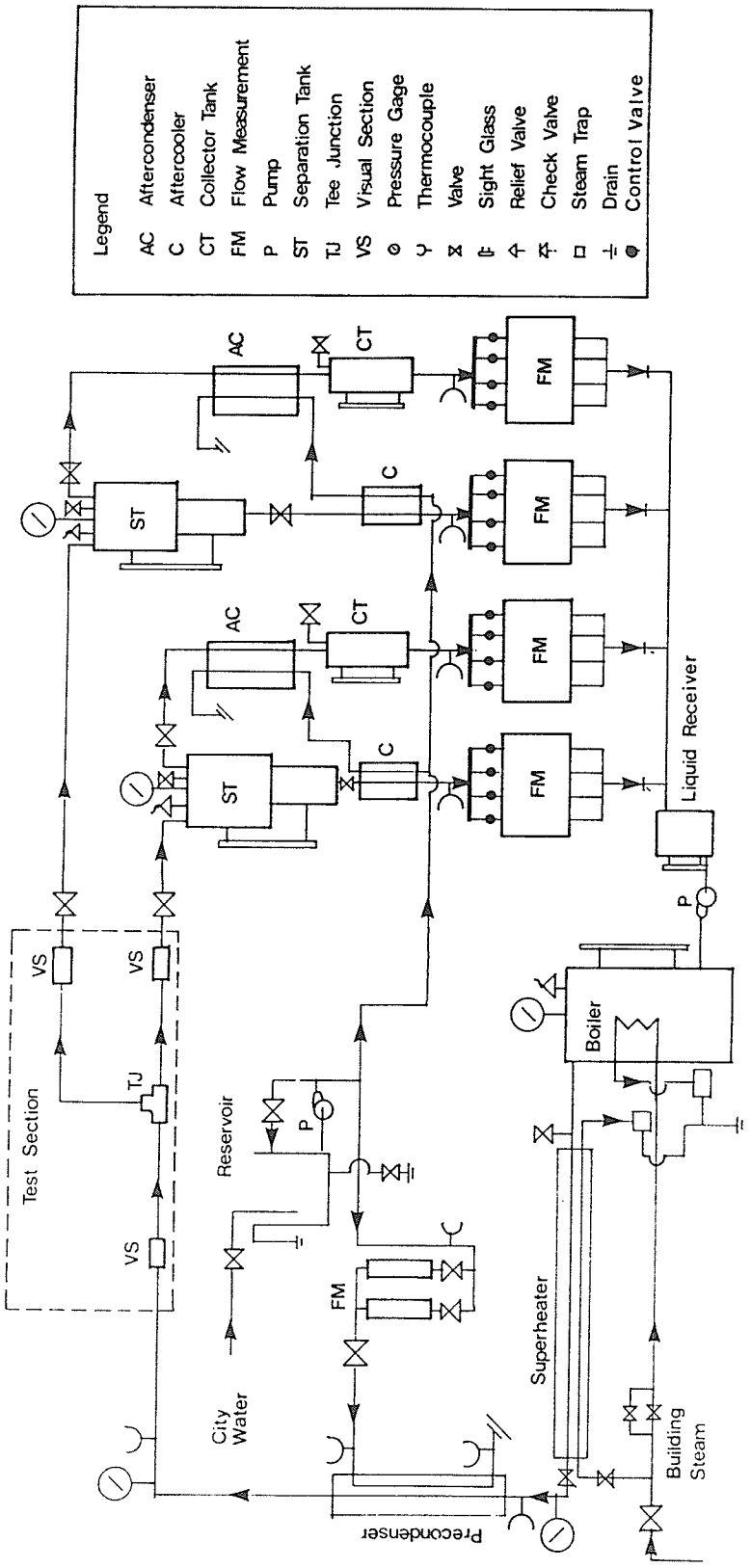

Fig. 3.1 Schematic diagram of the experimental facility

A controllable amount of steam was generated in the boiler from distilled water. Building steam, at a regulated pressure of 850 kPa, was used as the heat source in the boiler. The generated steam was first passed through a superheater which allowed control on the degree of superheat at its exit. After measuring the pressure and temperature, the superheated steam was passed through a precondenser where cooling water was used to partially condense the steam to any desired quality. The pressure and temperature were again measured at the exit of the precondenser. The two-phase mixture was then allowed to develop in a straight adiabatic length for 37 tube diameters after which the inlet flow pattern was observed through a specially designed visual section. A further 56 tube diameters of straight adiabatic developing length was provided before the flow reached the tee junction. Throttling valves, located far downstream in both the branch and run sides, controlled the fractions of the two-phase mixture entering each side. After the flow patterns in both the branch and run had been observed through visual sections, each of the two-phase mixtures entered its respective separation tank. In these tanks the steam and water were separated, while maintaining a steady liquid level in each tank. The steam from each tank was passed through an aftercondenser and the resulting condensate flow rate was measured by the appropriate (one or any combination of a possible four) flowmeters, arranged in par-

allel. The liquid phase from each separation tank passed through an aftercooler and the flow rate was also measured by one or more of four flowmeters in parallel. The two lines of condensate and two lines of liquid were then rejoined and collected in a liquid receiver tank before returning back to the boiler to complete the cycle.

3.2 Cooling-Water Circuit

All condensing units used in this apparatus were double-pipe, counter-current flow heat exchangers with the test fluid flowing through the inner pipe and the cooling water passing through the jacket. The following is a description of the cooling-water circuit which is illustrated in Fig. 3.1.

A steady level of water was maintained in a 0.2 m^3 reservoir tank. The water was circulated by a 7.5 kW centrifugal pump which had a maximum capacity of 0.142 m^3/min. and a maximum head of 155 m. A by-pass line, located downstream of the pump, was used to control the total amount of cooling water supplied to the cooling-water circuit. A fraction of this cooling water was sent to the precondenser with the flow rate being measured by either one of two variable-area flowmeters arranged in parallel ("Brooks" 0.025 m^3/min. maximum capacity and "Brooks" 0.15 m^3/min. maximum capacity). The amount of cooling water through the precondenser was one of the major independent parameters used to control

the quality of the steam exiting the precondenser. After the cooling water flow rate had been measured, it was fed directly to the precondenser inlet where its temperature was measured. At the exit of the precondenser, the temperature was again measured before the water was sent to the drain.

The fraction of cooling water which did not pass through the precondenser was divided into two streams, each of which flowed through the aftercooler and aftercondenser of the branch or run and was then rejected to the drain. Flow measurements and temperature measurements of these two cooling-water streams were not required since they did not appear in the mass- and heat-balance calculations.

All temperature measurements in this apparatus were obtained using iron-constantan thermocouples. All thermocouples were connected to a selector switch, which in turn, was connected to a "Fluke" 2170A digital potentiometer. The digital potentiometer was capable of resolving to 0.2 °C over a temperature range between -99.8 and 777.8 °C.

3.3 Steam Circuit

3.3.1 Boiler

The boiler was comprised of two main components: an outer shell, and internal heating coils. The outer shell was constructed from galvanized steel with an inside diameter of 0.914 m with a 38.1-mm wall thickness. The overall height

of the shell was 1.83 m. The heating coils were constructed from commercial pipe (9.53-mm nominal schedule 40 standard). The coils were 100 m in total length which provided enough surface area for heat transfer. The outside surface of the shell was insulated with 63.5-mm thick fiberglass insulation. A safety relief valve (set at 445 kPa absolute), as well as a pressure gage were mounted on the top cover of the shell. A sight glass was mounted on the side and shielded by a thick-walled plastic tube. The sight glass aided in ensuring that a constant liquid level existed inside the boiler during operation. The amount of steam generated in the boiler was controlled by throttling the amount of building steam entering the coils.

3.3.2 Superheater

The generated steam exited the boiler at near saturation conditions, although its exact quality was unknown. In order to facilitate the performance of a heat balance on the precondenser, the steam was first passed through a superheater. The superheater was a 3.0-m long, double-pipe, counter-current flow heat exchanger. The construction of the superheater consisted of a 37.6-mm I.D. 41.3-mm O.D. type K copper tube for the inner pipe and a 49.8-mm I.D. 54.0-mm O.D. type K copper tube for the outer pipe. Since the temperatures, and periodically the temperature gradients, imposed on the superheater were quite high, all welded

joints were sealed with silver solder and the entire unit was insulated with 63.5-mm thick fiberglass pipe insulation. Building steam at 850 kPa was used as the heating fluid and its flow rate was controlled by a needle valve. The building steam from both the superheater and the boiler was passed through steam traps before the resulting was rejected to the drain.

3.3.3 Precondenser

The superheated steam was partially condensed in a precondenser to a saturated mixture by exchanging heat with cooling water. The precondenser was a 1.6-m long, double-pipe, counter-current flow heat exchanger. The precondenser consisted of a 37.6-mm I.D. 41.3-mm O.D. type K copper tube for the inner pipe and a 49.8-mm I.D. 54.0-mm O.D. type K copper tube for the outer pipe. Similar to the superheater in assembly, all welded joints were sealed with silver solder and the entire unit was insulated with 63.5-mm thick fiberglass pipe insulation. The temperature and pressure of the superheated steam entering, and the temperature and pressure of the saturated mixture exiting the precondenser were measured. All pressure measurements in the experimental apparatus were performed by Bourdon tube pressure gages.

3.3.4 Test Section

A schematic diagram of the test section used in this investigation is shown in Fig. 3.2. The following is a discussion of the construction details of the major components in the test section.

Visual Sections

The inlet, run and branch visual sections were identical in design. Each visual section (shown in Fig. 3.3) consisted basically of a 254-mm long glass tube supported at both ends by specially machined stuffing boxes. The design of the visual sections were such that the inside diameter of the glass tube and stuffing boxes were identical to the inside diameter of the copper tubing entering and exiting each visual section. This eliminated any disturbance to the flow development. Since the inside diameter of commercial (off-the-shelf) glass tubing did not match that of the copper tubing, custom-manufactured glass tubing was used. This also allowed for the selection of a thick-wall (3.45-mm) tubing in order to eliminate the possibility of cracks due to thermal stresses. In assembling each visual section, extreme care was taken to ensure alignment and coaxiality between the copper tubing, stuffing boxes and the glass tube. The entire assembly was enclosed by a formed, plastic protective shield to guard against injuries in case of any fracture of the glass tubing.

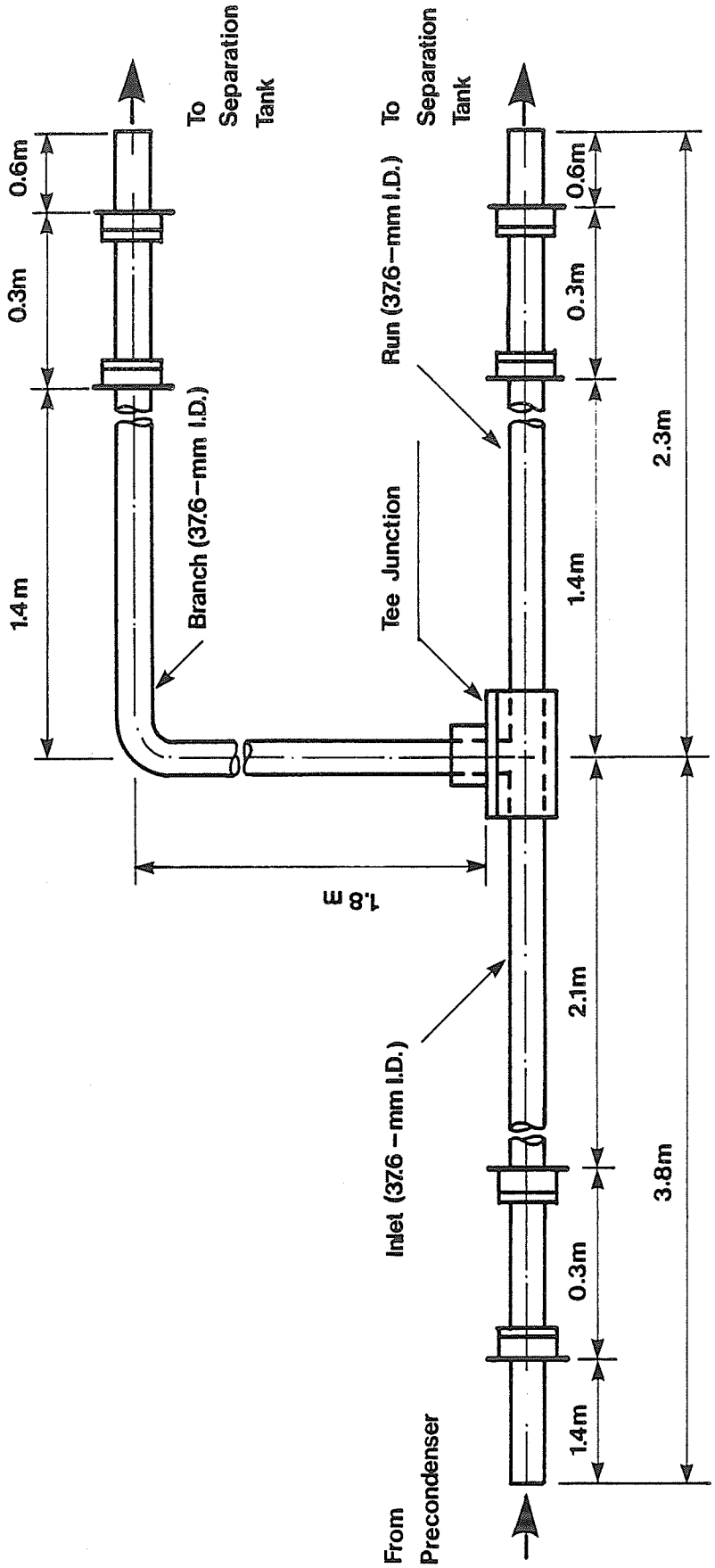

Fig. 3.2 Schematic diagram of the test section

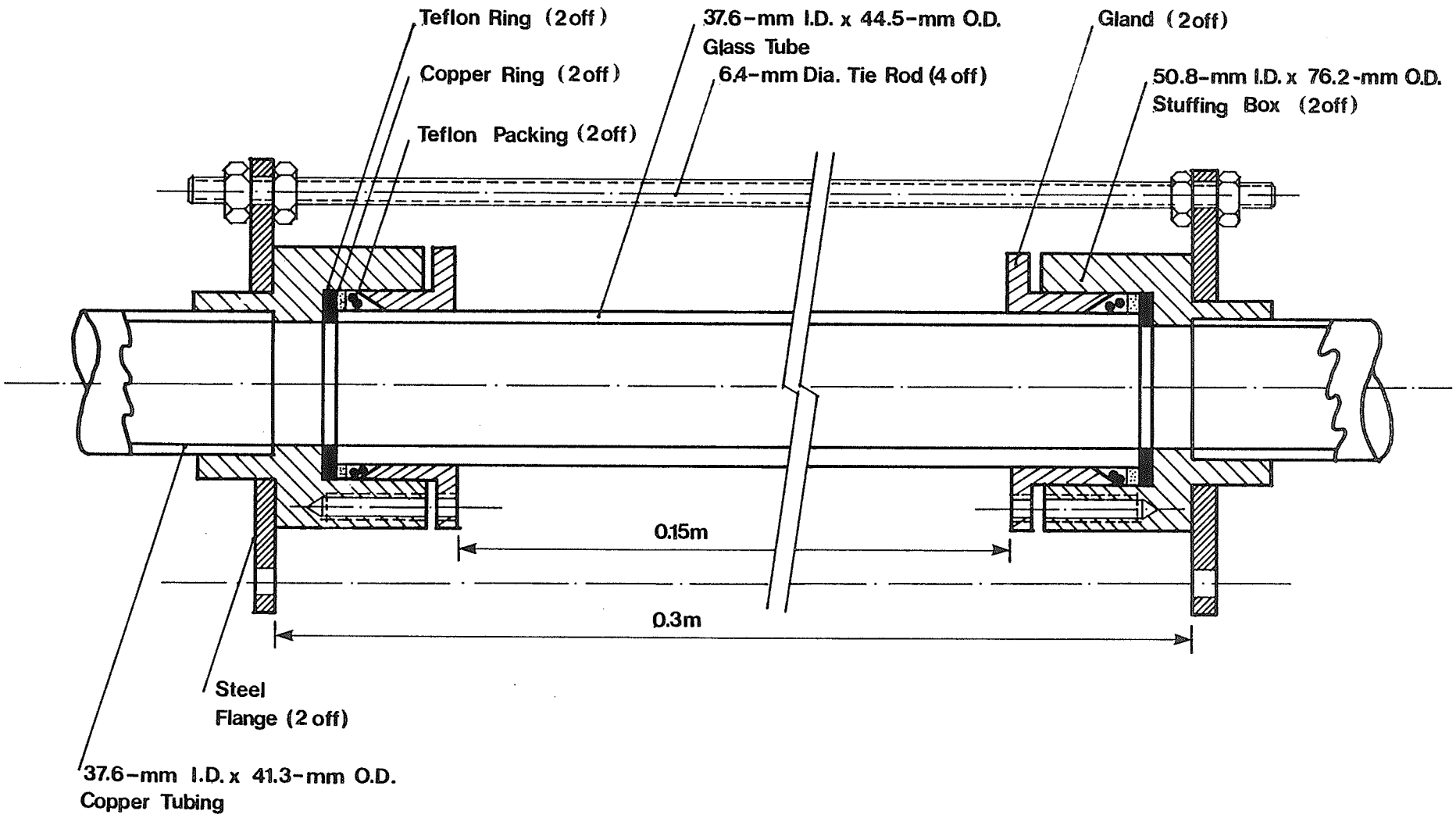

Fig. 3.3 Construction details of one visual section

In order to ensure consistency with other research laboratories, a square-edged tee was designed and constructed. This required precision machining, thereby eliminating any rounded edges or interior burrs and ensuring close tolerances. The tee junction, as shown in Figs. 3.4 and 3.5, consisted of two main components: a main body and a branch section. The main body was machined from a 63.5 mm square brass bar, 127-mm long. This length was chosen to allow the inlet and run copper tubing to mate with the tee junction for 38 mm, thus maintaining the coaxiality of the assembly. The branch section was machined from a 76-mm diameter brass rod, 44.5-mm long. On assembly, the branch section fit into the main body as shown in Fig. 3.4. Four concentric holes were drilled through the branch section and into the run, where the holes were tapped. An O-ring, placed between the branch and run sections, eliminated any leaks when four bolts securely tightened the two sections together.

Since the heat required to solder the copper tubing into the tee junction could have resulted in permanent deformation, a high temperature sealing compound ("LOCTITE" RC/620) was used to bond the tubes into the brass. Previous testing of this compound showed excellent sealing of copper tubing with steam up to 850 kPa.

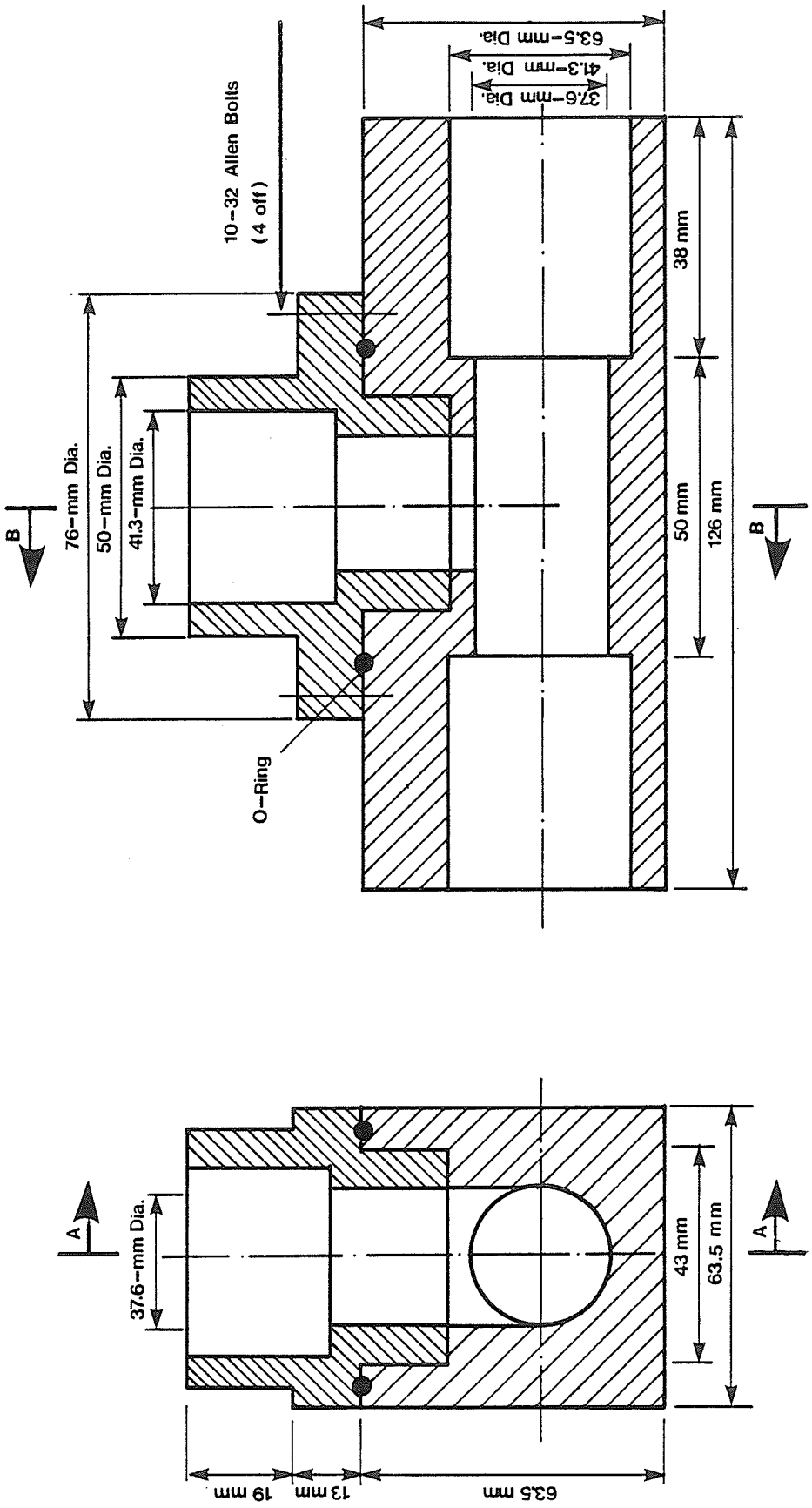

Fig. 3.4 Cross-sectional views of the tee junction

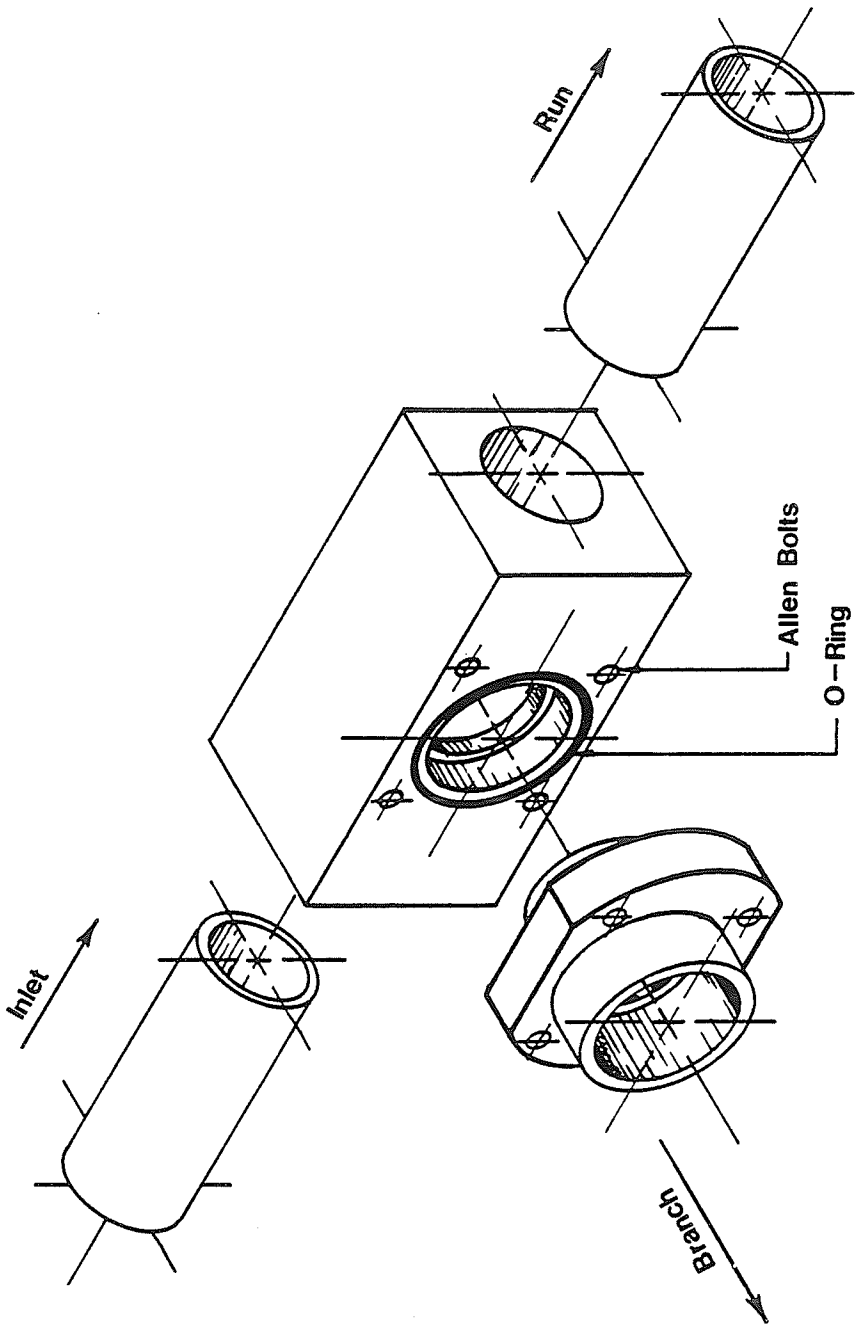

Fig. 3.5 Isometric view of the tee junction

The entire test section, including the precondenser was supported by a rigid steel frame. A survey level was used to ensure horizontality of the test section. The entire test section, except for the visual sections, was insulated with 63.5-mm thick fiberglass pipe insulation.

3.3.5 Separation Tanks

The two-phase mixture, in both the branch and run sides, discharged into separation tanks downstream from the test section. These tanks, shown in Fig. 3.6, were both identical in design. The tanks incorporated an abrupt change in cross-sectional area at about mid height. If the flow rate into one particular tank was low, high errors in the flow rate measurement could have occurred if the vapor-liquid interface was maintained in the larger diameter section of the tank. For any inlet condition or extraction rate resulting in a low liquid flow rate into either tank, the vapor-liquid interface in that particular tank was maintained in the smaller diameter section. Conversely, the larger diameter section was used for high liquid flow rates into that tank.

The separation tanks were constructed from steel pipes with steel plates welded to each end. A 305-mm nominal diameter with a 6.35-mm thick wall was used for the larger diameter section whereas a 152-mm nominal diameter with a 4.8-mm thick wall was used for the smaller diameter section. The two sections were connected by a 25.4-mm nominal diame-

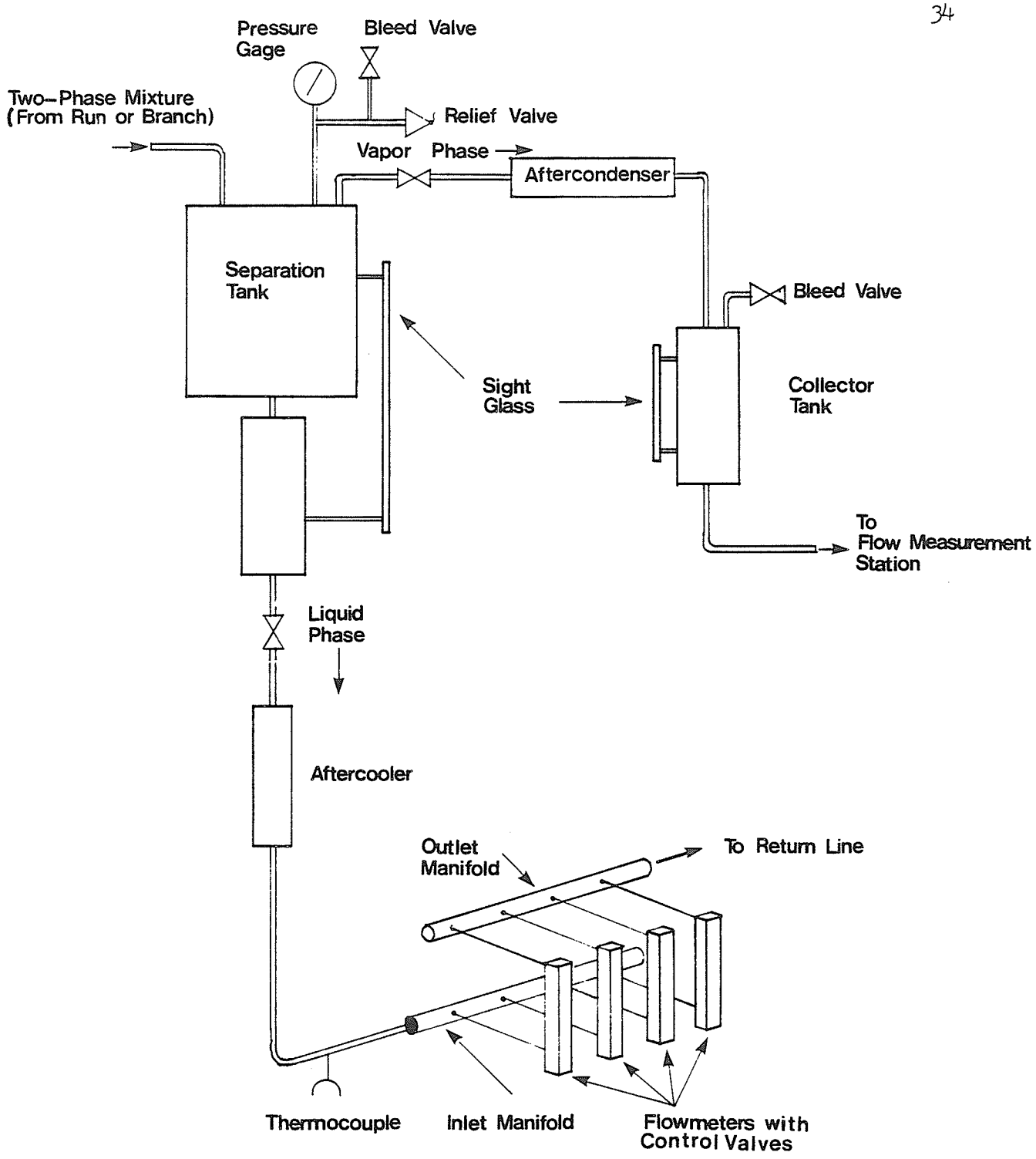

Fig. 3.6 Schematic diagram of the flow arrangement at the run or branch discharge sides

ter, 30-mm long steel pipe. The inside of the entire assembly was galvanized to prevent corrosion and all fittings connecting the steel tanks to the copper tubes were "Dielectric Unions." A 480-mm long sight glass was installed vertically, with a scale, used to maintain a constant liquid level in the tanks. Each tank had a pressure gage, a bleed valve and a safety relief valve (set at 200 kPa absolute) mounted on the top cover. The entire separation tank assemblies, except the sight glass, were insulated with 63.5-mm thick fiberglass insulation.

3.3.6 Aftercoolers and Aftercondensers

The liquid phase discharging from the bottom of the tanks was subcooled in an aftercooler before entering the flow rate measuring stations. The aftercoolers were double-pipe, counter-current flow heat exchangers. A 13.4-mm I.D. 15.9-mm O.D. type K copper tube was used as the inner pipe and a 18.9-mm I.D. 22.2-mm O.D. type K copper tube was used for the outer pipe. A total heat transfer length of 2.0 m was used for each aftercooler.

The steam removed from the top of the separation tanks was condensed in an aftercondenser and passed through a small collector tank before entering the flow rate measuring stations. The aftercondensers were identical to the aftercoolers in tube sizes, but 4.5 m was used for the total heat transfer length of each.

The liquid levels in the collector tanks, as well as the separation tanks, had to remain constant with time before steady-state could be assumed. A variation in these levels with time would mean that the flowmeter readings were not equal to the actual flow rates of the vapor and liquid into the separation tanks.

3.3.7 Flow Rate Measurement

The flow rates of each stream, from the aftercoolers and aftercondensers, were measured by variable area flowmeters ("Cole-Parmer" type R-3217). Each flow measurement station consisted of four flowmeters in parallel: one no. 18 (44.74 $cm^3/min.$ maximum capacity), one no. 26 (215.8 $cm^3/min.$ maximum capacity) and two no. 36 (1812 $cm^3/min.$ maximum capacity). Each flow measurement station, therefore, was capable of accurate flow rate measurement within the range of 5 to 3800 $cm^3/min.$ The above combination of flowmeters in each flow measurement station was chosen to accommodate the wide variation in flow rates anticipated as a result of different combinations of inlet mass flux, inlet quality and extraction rates to be covered in this investigation.

3.4 Pre-Test Preparation

Before any testing began, the following pre-test preparations were performed on the experimental apparatus:

1. All thermocouples were calibrated against precision thermometers over a temperature range between 25 °C and 120 °C. For each thermocouple, equations relating the true temperature (thermometer reading) to the corresponding digital potentiometer reading were obtained. These equations were used to correct the recorded temperatures in the data reduction.
2. All pressure gages were calibrated against a dead weight tester, over the range of each pressure gage. Since the differences between the true pressure (that of the dead weight tester) and the corresponding pressure gage reading were indistinguishable, the recorded pressure gage readings were used in the data reduction.
3. All flowmeters were calibrated by collecting an amount of water for a specified period of time (between one and five minutes). For the cooling-water flowmeters (on the precondenser side), equations relating the true flow rate (measured) to the scale reading were obtained. These equations were used in the data reduction. As for the test-fluid flowmeters (downstream from the aftercondensers and aftercoolers), the measured flow rates came very close (mostly within ±5 percent and never outside ±10 percent at full scale) to the manufacturer's calibration charts, hence the latter were chosen to be used in the data reduction.

4. The criterion for the absence of leaks was that the system was required to maintain a constant pressure of 310 kPa absolute (except for the separation tanks which maintained a pressure of 190 kPa absolute due to the safety relief valves) for a period of 24 hours.

3.5 Experimental Procedure

3.5.1 Start-Up Procedure

Due to the complexity of the apparatus, several steps were required to start up the system. The following is a list of steps, in order, which were performed each time the system was run.

1. The steam-trap drain valves were closed.
2. The bleed valves on the separation tanks and collector tanks were checked to ensure that they were open.
3. The digital potentiometer was switched on.
4. The cooling-water reservoir was filled to the overflow level.
5. The cooling-water pump was turned on with the by-pass valve fully opened.
6. The by-pass valve of the cooling-water pump was partially closed until the required cooling water passed through the cooling-water flowmeter upstream of the precondenser.

7. The building-steam supply valve was slowly opened to full opening.
8. The by-pass line valve allowing building steam into the heating coils was slowly opened.
9. The main-line valve allowing building steam into the heating coils was slowly opened one quarter of a turn.
10. The by-pass line valve allowing building steam into the heating coils was closed.
11. The system inlet valve was closed.
12. The superheater bleed valve was opened until all air and condensed steam was discharged. This valve was closed when steam exited from it.
13. The system inlet valve was slowly opened to the desired setting allowing steam into the system.
14. When the liquid levels in the separation tanks began to rise the liquid flowmeters were activated to keep the levels steady.
15. The test fluid circulating pump was turned on and the by-pass line was adjusted to maintain a relatively constant liquid level in the liquid receiver tank.
16. The throttling valves on the branch and run sides were adjusted to give the desired extraction rate.
17. The main-line valve allowing building steam into the heating coils was opened to the required setting.

18. The needle valve allowing building steam into the superheater was opened to the required setting.
19. The separation-tank bleed valves were closed when steam exited from each one.
20. The steam flow meters were activated when the liquid levels in the collector tanks began to rise.
21. The collector-tank bleed valves were closed.

Continuous monitoring of the liquid levels in the separation tanks, collector tanks, and the liquid receiver tank was maintained and necessary adjustments were made to the branch and run liquid test fluid flowmeters and the by-pass line on the liquid receiver until the system reached steady-state.

3.5.2 Steady-State Conditions

It was very important that steady-state had been reached before any data were recorded. The following conditions were continuously monitored until no change had occurred for at least 30 minutes.

1. The liquid levels in the separation tanks.
2. The liquid levels in the collector tanks.
3. The liquid level in the liquid receiver tank.
4. The boiler pressure.
5. The steam temperature and pressure at the outlet of the precondenser.
6. The cooling-water flow rate in the precondenser.

7. The inlet and exit temperature of the cooling water in the precondenser.

Typically, the system required at least two hours of continuous operation and adjustments before steady-state was reached. Additional runs, where only the extraction rate was changed, would require about one hour. Some runs, particularly at very low mass fluxes, would require considerably more time; in fact, four hours could be anticipated before steady-state was reached.

3.5.3 Recording of Data

The pressure gages and digital potentiometer provided readings in the British System of units (i.e. psig and °F, respectively). All these readings were later converted to the S.I. system.

After steady-state conditions had been reached, the following measurements were recorded:

1. The boiler pressure in kPa.
2. The superheater exit pressure in kPa and exit temperature in °C.
3. The precondenser inlet pressure in kPa and inlet temperature in °C.
4. The precondenser exit pressure in kPa and exit temperature in °C.
5. The separation tanks pressure in kPa.

6. The precondenser cooling-water flow rate as a percentage scale reading.
7. The precondenser cooling-water inlet and exit temperatures in °C.
8. The test fluid temperature at the inlet to each flow measurement station in °C.
9. The test fluid flowmeters as a percentage scale reading.
10. The observed flow patterns at the inlet, run and branch visual sections based on the descriptions given later in Section 3.6.

3.5.4 Shut-Down Procedure

When all measurements were recorded for the last run of a particular day, the following steps were followed, in order, to shut the system down:

1. The building-steam supply valve was closed.
2. The bleed valves on the separation tanks and collector tanks were opened when the system pressure was near atmospheric pressure.
3. The superheater bleed valve was opened.
4. The test fluid circulating pump was turned off.
5. All test fluid flowmeters were closed.
6. The by-pass line on the cooling-water pump was fully opened when the system had cooled down sufficiently.
7. The cooling-water pump was turned off.
8. The digital potentiometer was switched off.

9. The main-line valve allowing building steam into the heating coils was closed.
10. The steam-trap drain valves were opened.
11. The cooling-water reservoir was drained.

3.6 Flow Patterns

It was very important to classify properly the observed flow patterns, particularly in the inlet visual section. In the present investigation, three major and one transitional flow patterns were visually observed. The following descriptions were used to identify the different flow patterns:

Stratified flow: The liquid flows along the bottom of the tube and the vapor on top of it with a smooth interface.

Wavy flow: The two phases are separated with liquid flowing at the bottom of the tube. The vapor-liquid interface is wavy, apparently due to a difference between the vapor and liquid velocities.

Semiannular-Wavy flow: Similar to wavy flow in appearance, although the liquid begins to rise up the tube wall forming a film. The film is very thin and most of the liquid appears as a thick stratum at the bottom.

Semiannular flow: A stable liquid film covers the lower part of the tube wall and the upper portion of the tube appears dry. The liquid film thickness increas-

es around the perifery with a maximum at the bottom of the tube. Some of the liquid phase may appear as droplets entrained in the vapor.

Figure 3.7 shows a diagram illustrating the observed flow patterns. In the remaining part of the thesis, the names of the flow patterns are often abbreviated in order to conserve space. These abbreviations are used consistently:

ST = Stratified

W = Wavy

SA-W = Semiannular-Wavy

SA = Semiannular

3.7 Data Reduction

The data recorded during each run were reduced using an Amdahl 5850 digital computer. A data reduction program was written using FORTRAN WATFIV language. Figure 3.8 shows a schematic diagram of the system with the parameters relevant to the data reduction. The following is a list of the procedure used to reduce the data into the required phase-distribution parameters.

1. The vapor and liquid mass flow rates in the run and branch were found from the appropriate flowmeters and the total run and branch mass flow rates were determined by

$$W_2 = W_{G2} + W_{L2} \tag{3.1}$$

$$W_3 = W_{G3} + W_{L3} \tag{3.2}$$

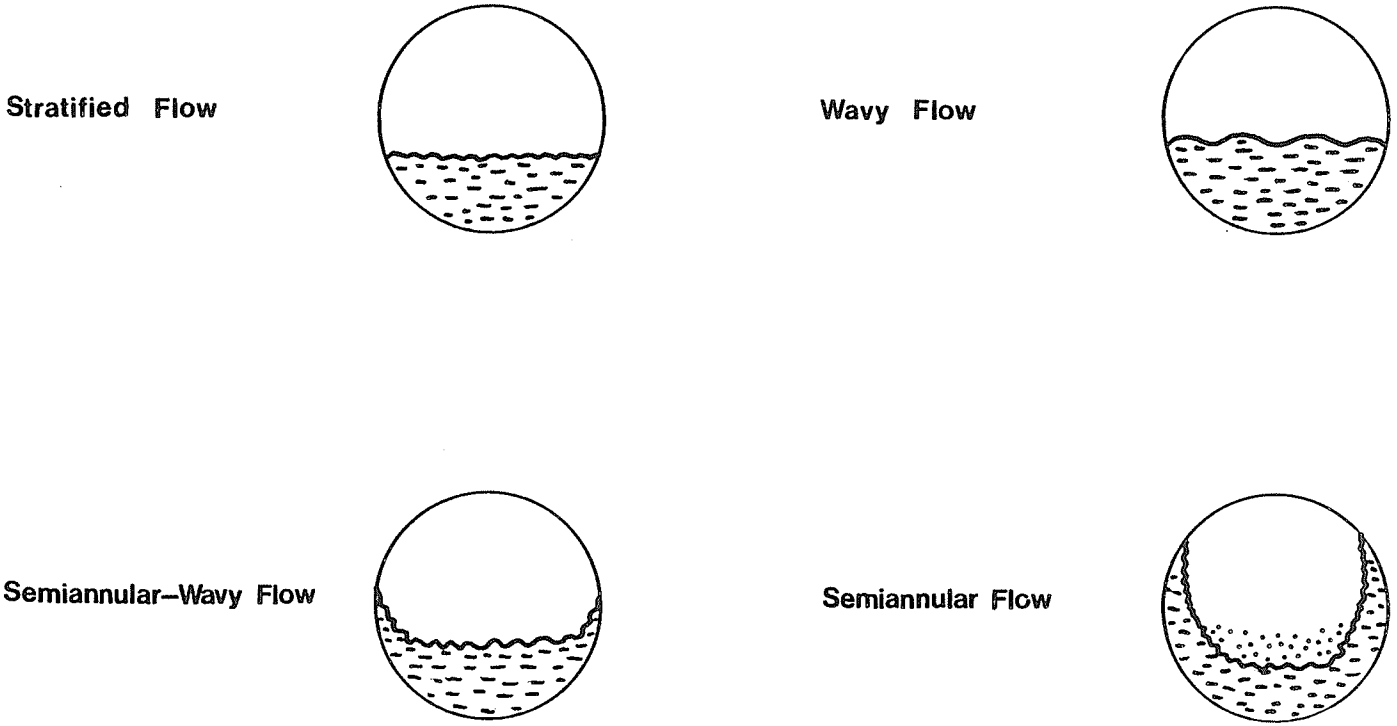

Fig. 3.7 Diagram illustrating the observed flow patterns

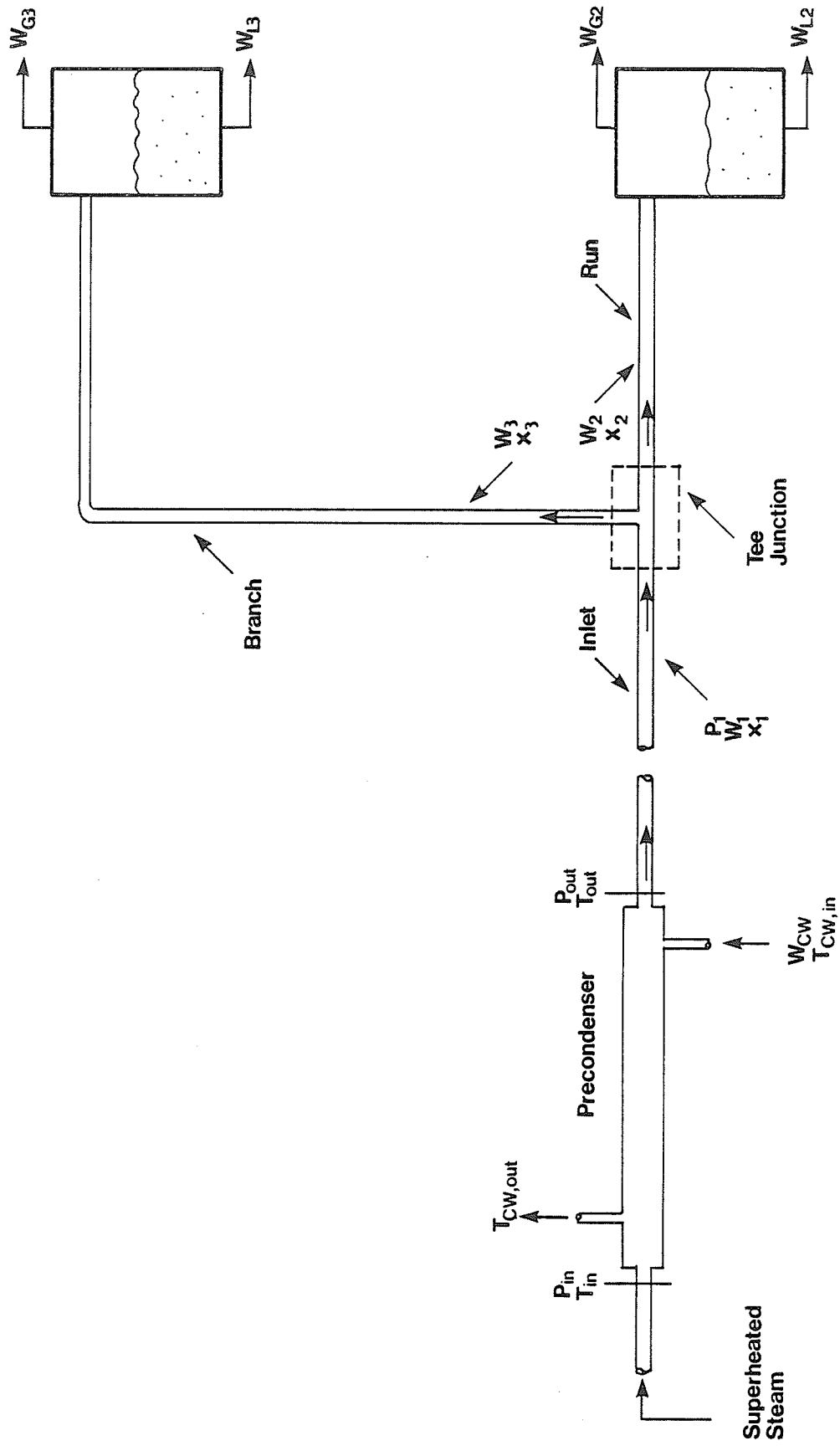

16. Fig. 3.8 Schematic diagram showing relevant flow parameters

2. The total inlet mass flow rate and inlet vapor flow rate were determined from

$$W_1 = W_2 + W_3 \tag{3.3}$$

$$W_{G1} = W_{G2} + W_{G3} \tag{3.4}$$

3. The inlet and branch qualities were computed as

$$x_1 = W_{G1} / W_1 \tag{3.5}$$

$$x_3 = W_{G3} / W_3 \tag{3.6}$$

4. A heat balance, performed on the precondenser, gave

$$- W_{CW} c_p (T_{CW,in} - T_{CW,out}) = W_1 (h_{in} - h_{out}) \tag{3.7}$$

where

W_{CW} = cooling-water flow rate in kg/s

c_p = cooling-water specific heat in kJ/kg.K

$T_{CW,in}$ = cooling-water inlet temperature in °C

$T_{CW,out}$ = cooling-water exit temperature in °C

h_{in} = superheated steam inlet enthalpy in kJ/kg (evaluated at P_{in} and T_{in})

h_{out} = saturated mixture exit enthalpy in kJ/kg.

From (3.7), h_{out} was computed.

5. The calculated precondenser exit quality was evaluated from

$$x_{1C} = (h_{out} - h_f)/h_{fg} \tag{3.8}$$

where

h_f is the saturated liquid enthalpy in kJ/kg, evaluated at the precondenser exit pressure (P_{out})

h_{fg} is the enthalpy of vaporization in kJ/kg, evaluated at the precondenser exit pressure (P_{out})

6. The heat balance error was found by

$$E = (x_1 - x_{1C})/x_1 \qquad (3.9)$$

Only runs with E within the range of ±10% were accepted. In this investigation, 64% of the runs were actually within ±5%.

7. For runs with heat balance errors within ±10%, the following parameters were calculated:

$$G_1 = W_1/(\pi D_1^2/4) \qquad (3.10)$$

$$G_3 = W_3/(\pi D_3^2/4) \qquad (3.11)$$

$$V_{GS} = G_1 x_1/\rho_G \qquad (3.12)$$

$$V_{LS} = G_1(1 - x_1)/\rho_L \qquad (3.13)$$

where

x_1 is the inlet quality evaluated from (3.5)

ρ_G is the vapor density in kg/m^3,
evaluated at P_1 (assuming that $P_1 = P_{out}$)

ρ_L is the liquid density in kg/m^3,
evaluated at P_1 (assuming that $P_1 = P_{out}$).

8. The fraction of total vapor entering the branch and the fraction of total liquid entering the branch were found from

$$F_{BG} = W_{G3}/W_{G1} \qquad (3.14)$$

$$F_{BL} = W_{L3}/W_{L1} \qquad (3.15)$$

9. Finally, the extraction rate W_3/W_1 (or G_3/G_1) and the ratio of the branch to inlet quality x_3/x_1 were computed.

Chapter 4

RESULTS AND DISCUSSION

4.1 Data Range

In the present experimental investigation, a total of 111 data points (runs) were obtained covering the range of operating conditions shown in Table 4.1. These data points comprise a total of 19 groups, each of which has the following characteristic operating conditions: a fixed amount of building steam entering the boiler, a fixed amount of building steam entering the superheater and a fixed amount of cooling water supplied to the precondenser. In each group, therefore, the extraction rate was the only independent parameter. With any variation in the extraction rate (variation in the fluid resistance), a change in the system pressure resulted; and as a result, the inlet mass flux and inlet quality also changed. Nominal (average) values of the inlet pressure ($\bar{P}_1$), inlet mass flux ($\bar{G}_1$) and inlet quality ($\bar{x}_1$) were computed for each group and are listed in Appendix A. The deviations from the actual inlet mass fluxes and inlet qualities to the respective nominal values are all within ±10% in each group. As well, the inlet flow pattern remained fixed for all runs in a particular group, for all groups.

Table 4.1

Ranges of Operating Conditions

Total number of runs	111
Inlet Flow Patterns	ST W SA-W SA
Inlet pressure P_1 (kPa)	116-207
Inlet mass flux G_1 ($kg/m^2.s$)	16.6-50.3
Inlet quality x_1 (%)	23.3-82.8
Extraction rate G_3/G_1	0.15-0.80

Based on the nominal operating conditions, the nominal inlet superficial gas velocity and nominal inlet superficial liquid velocity were determined for each group and plotted on the flow pattern map proposed by Mandhane et al. [16] (shown in Fig. 4.1). The transition lines appearing on this map were computed for the present operating conditions and test fluids based on the recommendation by Mandhane et al. [16]. This figure shows good agreement between the predicted and visually observed (as outlined in Section 3.6) inlet flow patterns over the entire range of operating conditions. A complete list of the operating conditions and the phase-distribution data for each run is given in Appendix B.

4.2 Presentation of Data

In this section, the experimental data will be presented in a number of ways in an attempt to isolate the individual effects of important independent parameters. As well, comparisons with previous investigations will be included as they become relevant.

4.2.1 Effect of Inlet Quality

In Figs. 4.2 (a-e), the present data are plotted using x_3/x_1 and G_3/G_1 as coordinates. Since $D_3=D_1$ in our case, the extraction rate W_3/W_1 is equal to G_3/G_1. In each figure, the lines of even phase distribution and the line BC (in Fig. 2.2a) are shown. The purpose of these figures is

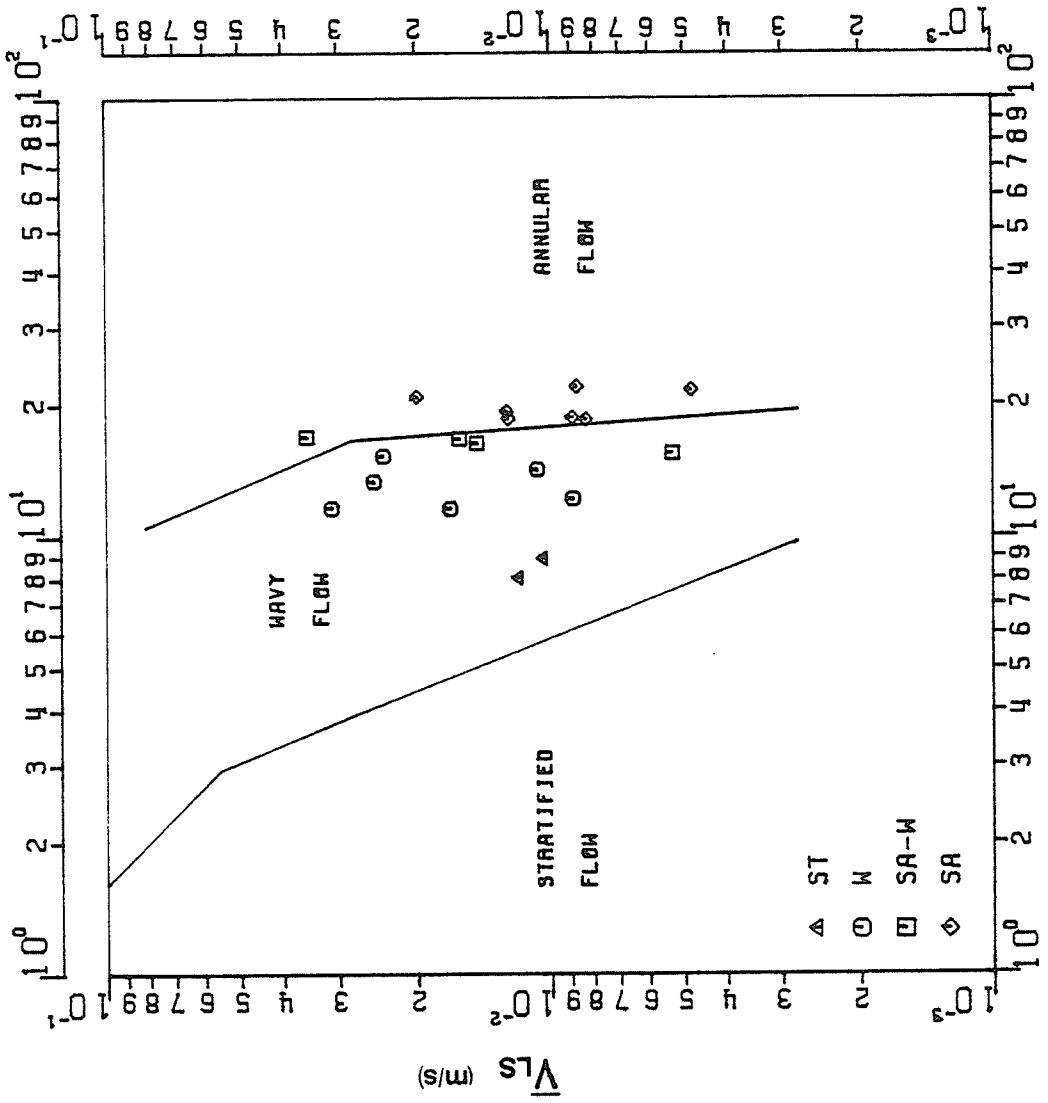

Fig. 4.1 The present range of operating conditions plotted on the Mandhane et al. [16] flow pattern map

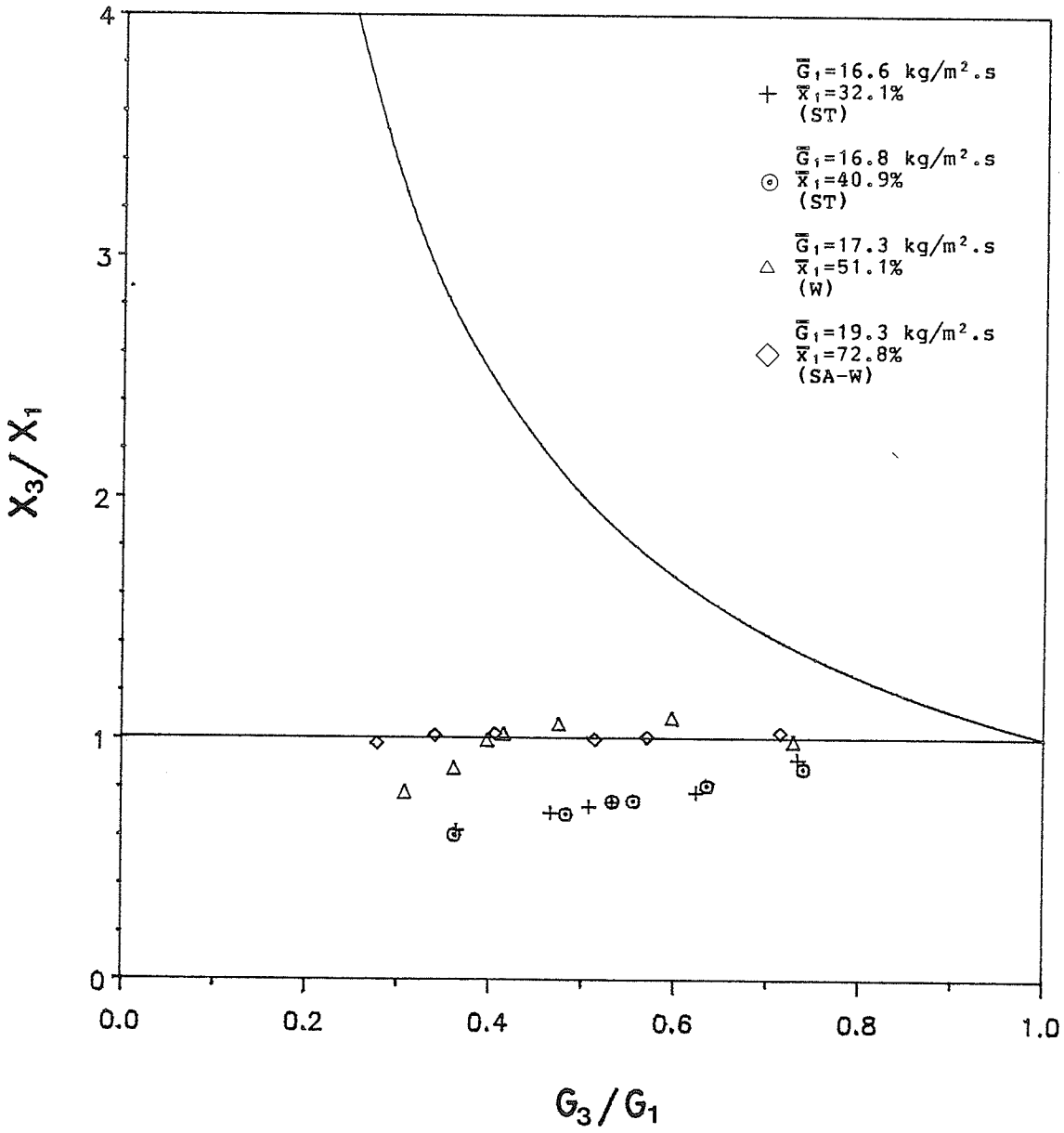

(a)

Fig. 4.2 Effect of inlet quality on the phase distribution

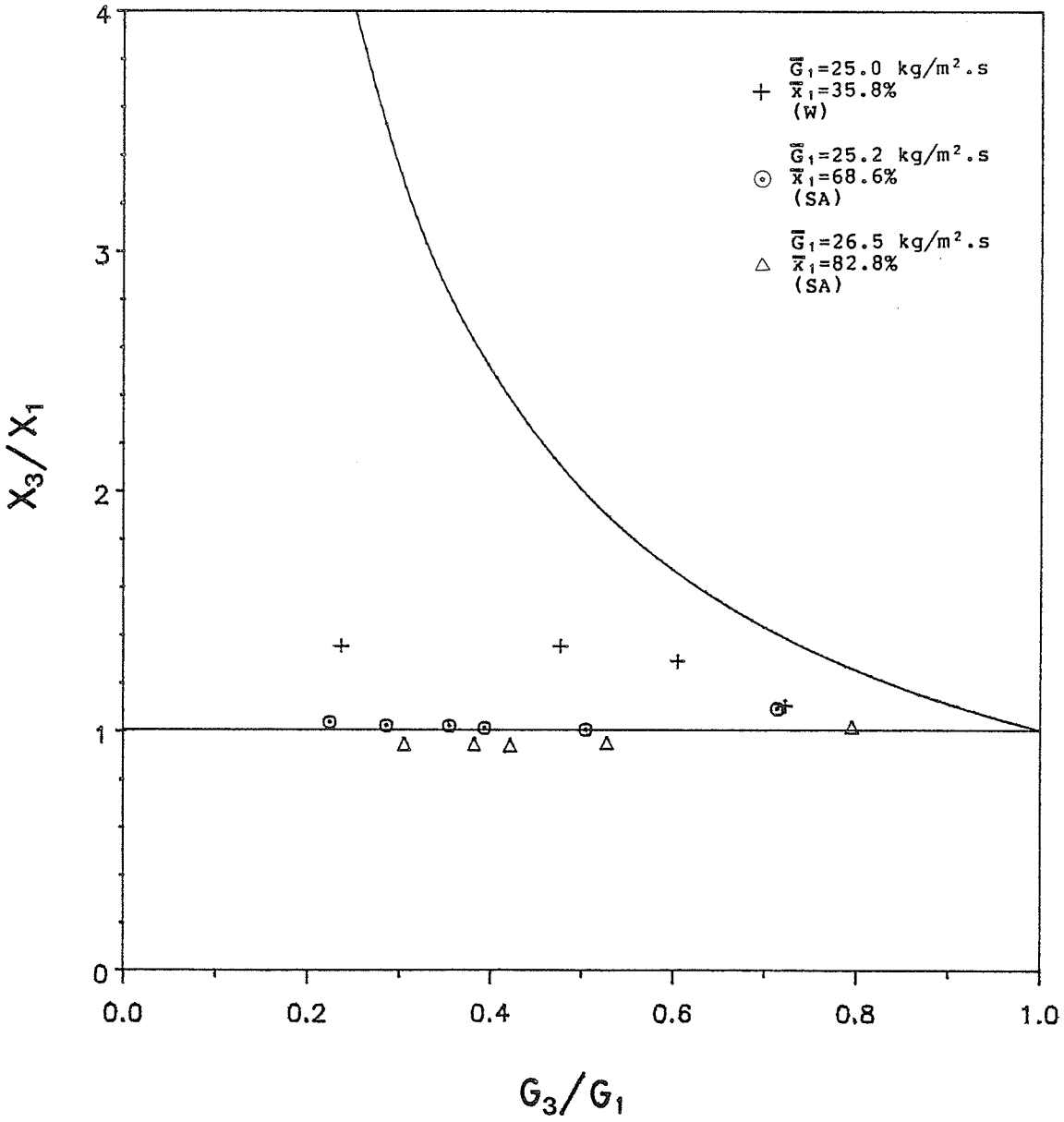

(b)

Fig. 4.2 Effect of inlet quality on the phase distribution

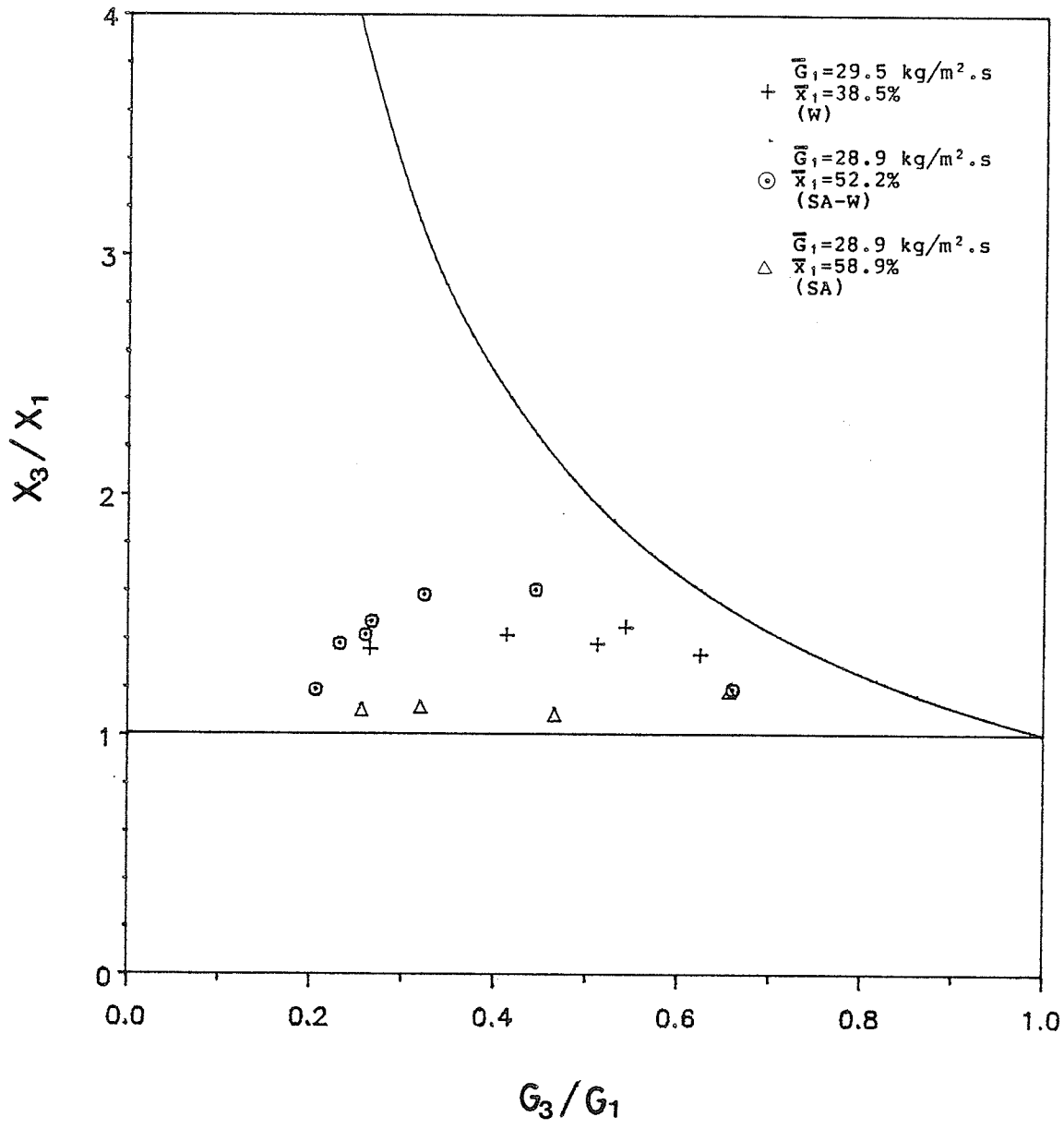

(c)

Fig. 4.2 Effect of inlet quality on the phase distribution

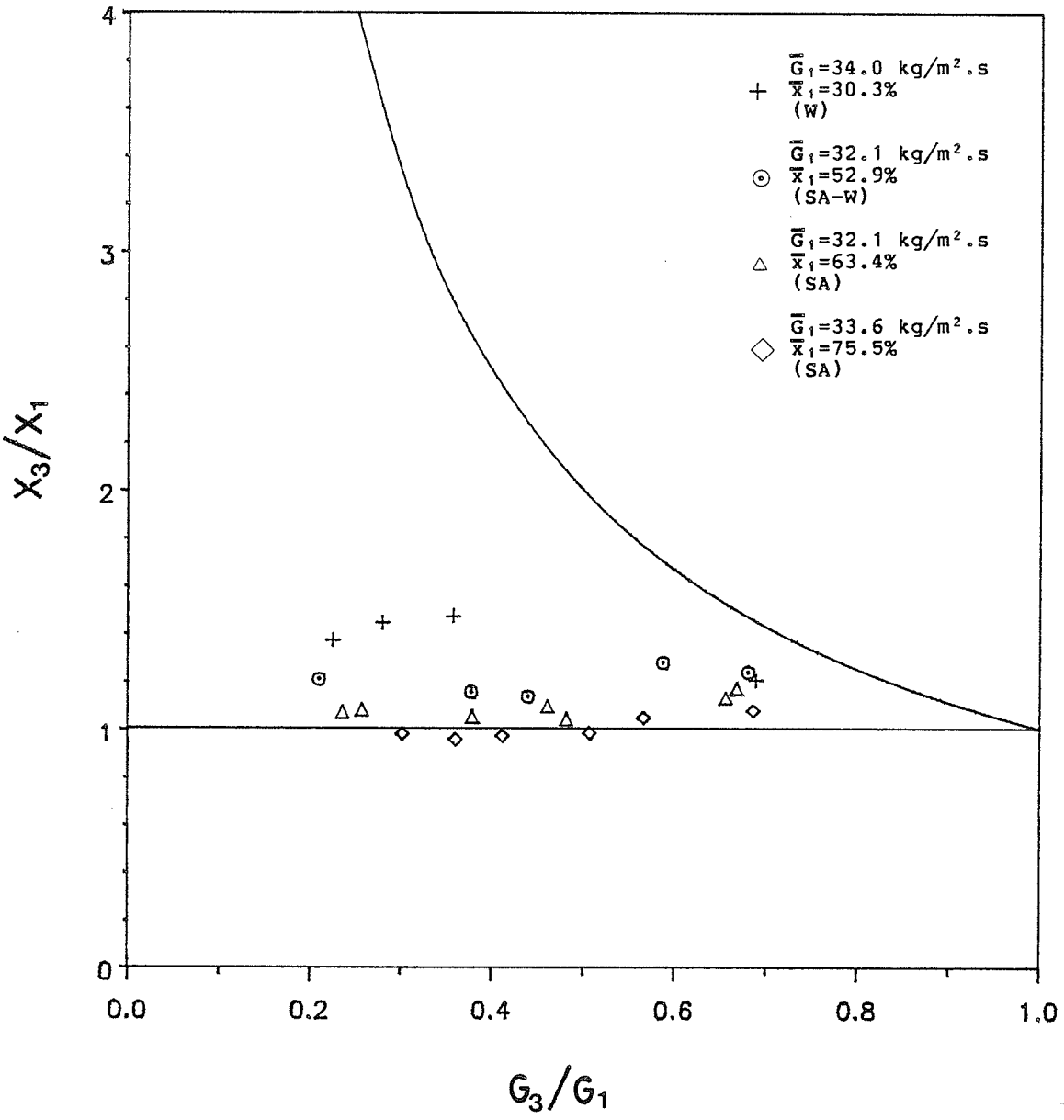

(d)

Fig. 4.2 Effect of inlet quality on the phase distribution

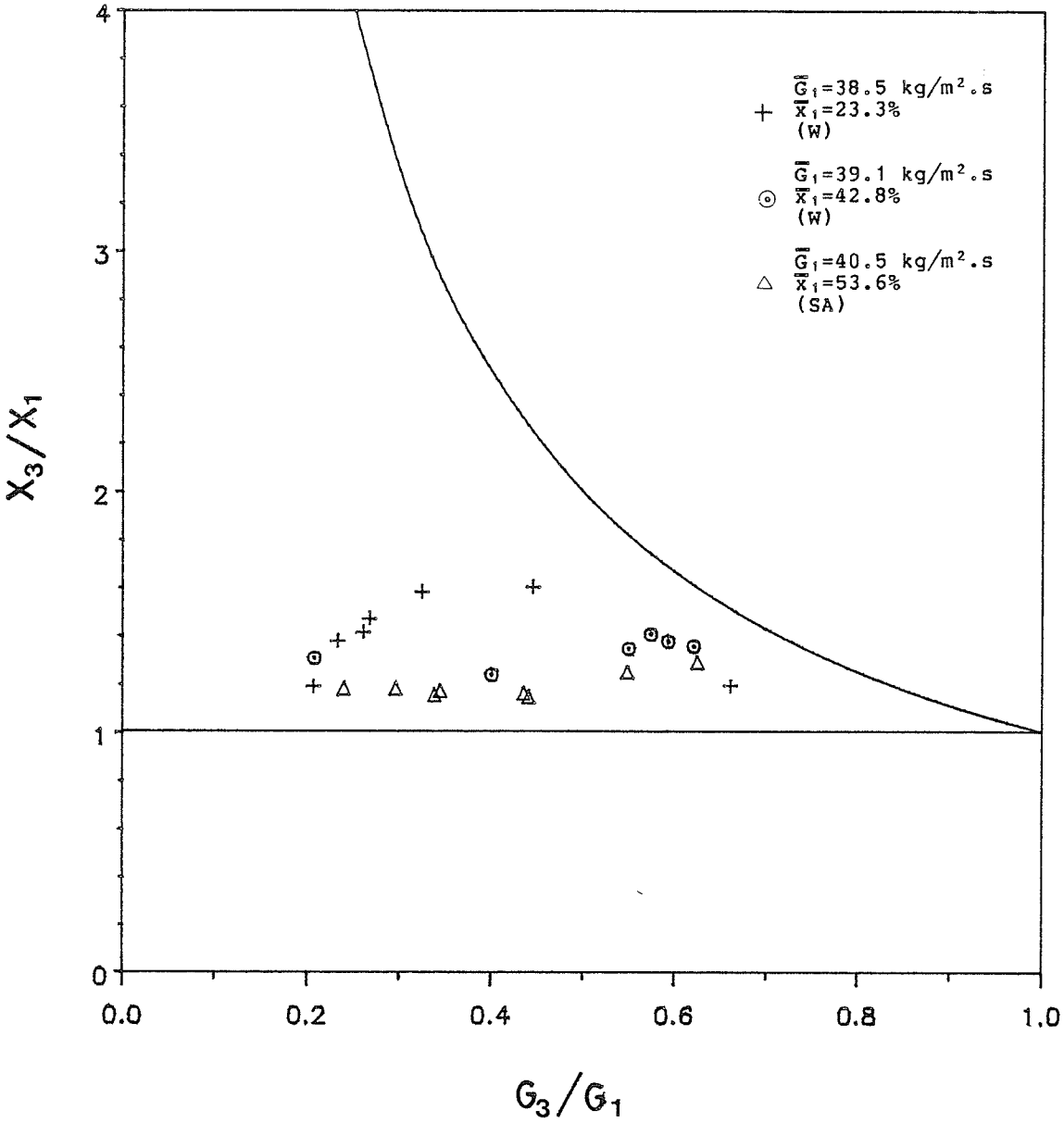

(e)

Fig. 4.2 Effect of inlet quality on the phase distribution

to isolate the effect of x_1, on the phase distribution, by presenting groups of data which cover a wide range of x_1 but maintain an approximately constant G_1. It must be understood that changing x_1 while keeping G_1 constant may result in changes in the inlet flow pattern. It will be shown later (Section 4.2.3), that the inlet flow pattern can have an effect on the phase distribution.

From Figs. 4.2(b-e), it is evident that x_3/x_1 decreases with increasing x_1. Figure 4.2(a), however, shows that at the lowest values of G_1 the effect of x_1 on the phase distribution is reversed (i.e. x_3/x_1 increases with increasing x_1). This reversal in the phase distribution will be discussed further in Section 4.2.4. In an investigation of the effect of x_1 on the phase distribution conducted by Collier [3], the results showed that at lower qualities (2 - 17 percent), x_3/x_1 increased with increasing x_1 and then decreased with any further increase in x_1 (17 - 50 percent).

4.2.2 Effect of Inlet Mass Flux

Figures 4.3(a-d) are similar to Figs. 4.2(a-e) except that an attempt to investigate the effect of G_1 on the phase distribution is made by maintaining an approximately constant x_1 and allowing G_1 to vary. These figures show that for a fixed x_1, when the data from different flow patterns are plotted on the same graph, there is an effect of G_1 on the phase distribution. This effect is largest at the

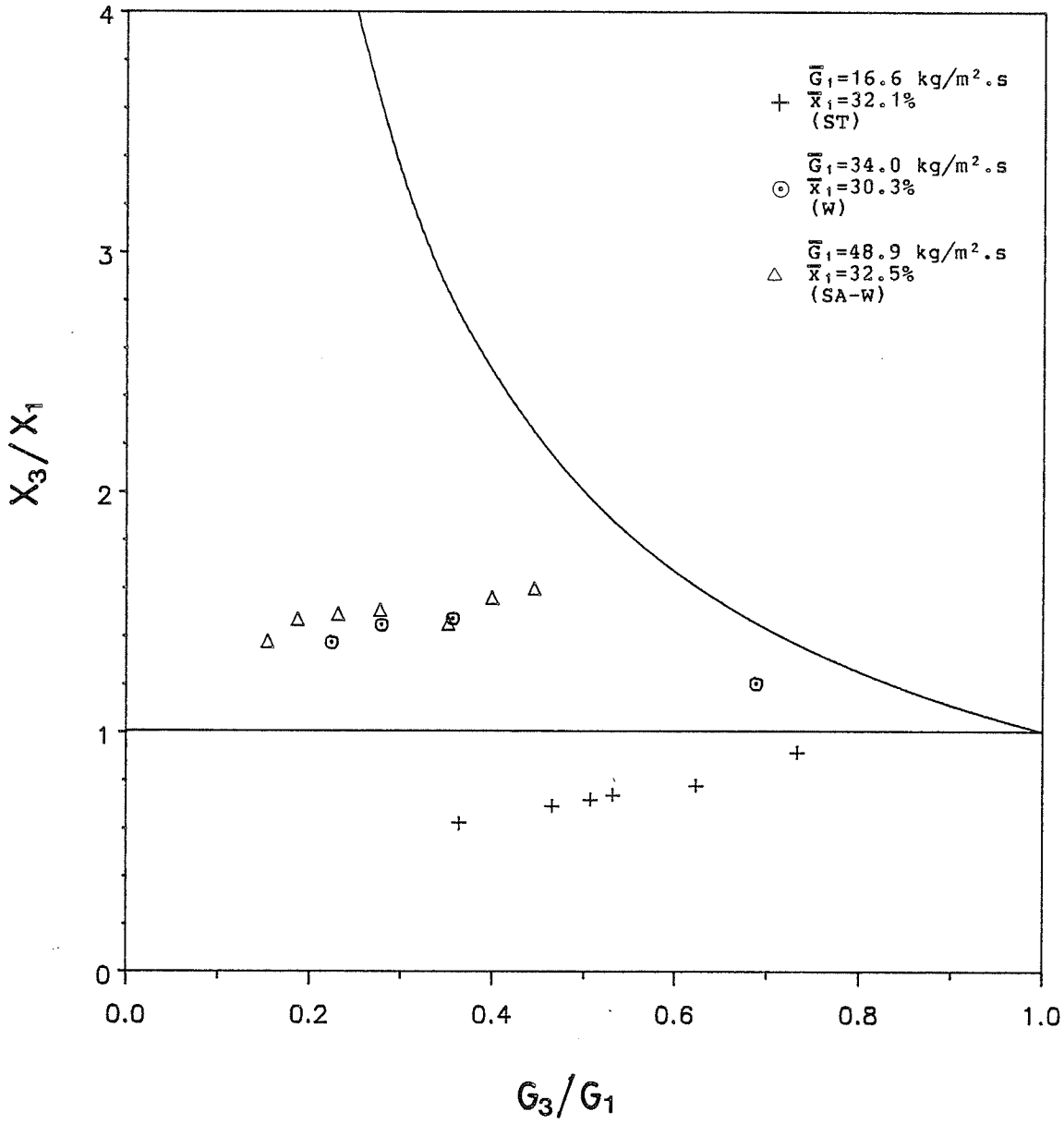

(a)

Fig. 4.3 Effect of inlet mass flux on the phase distribution

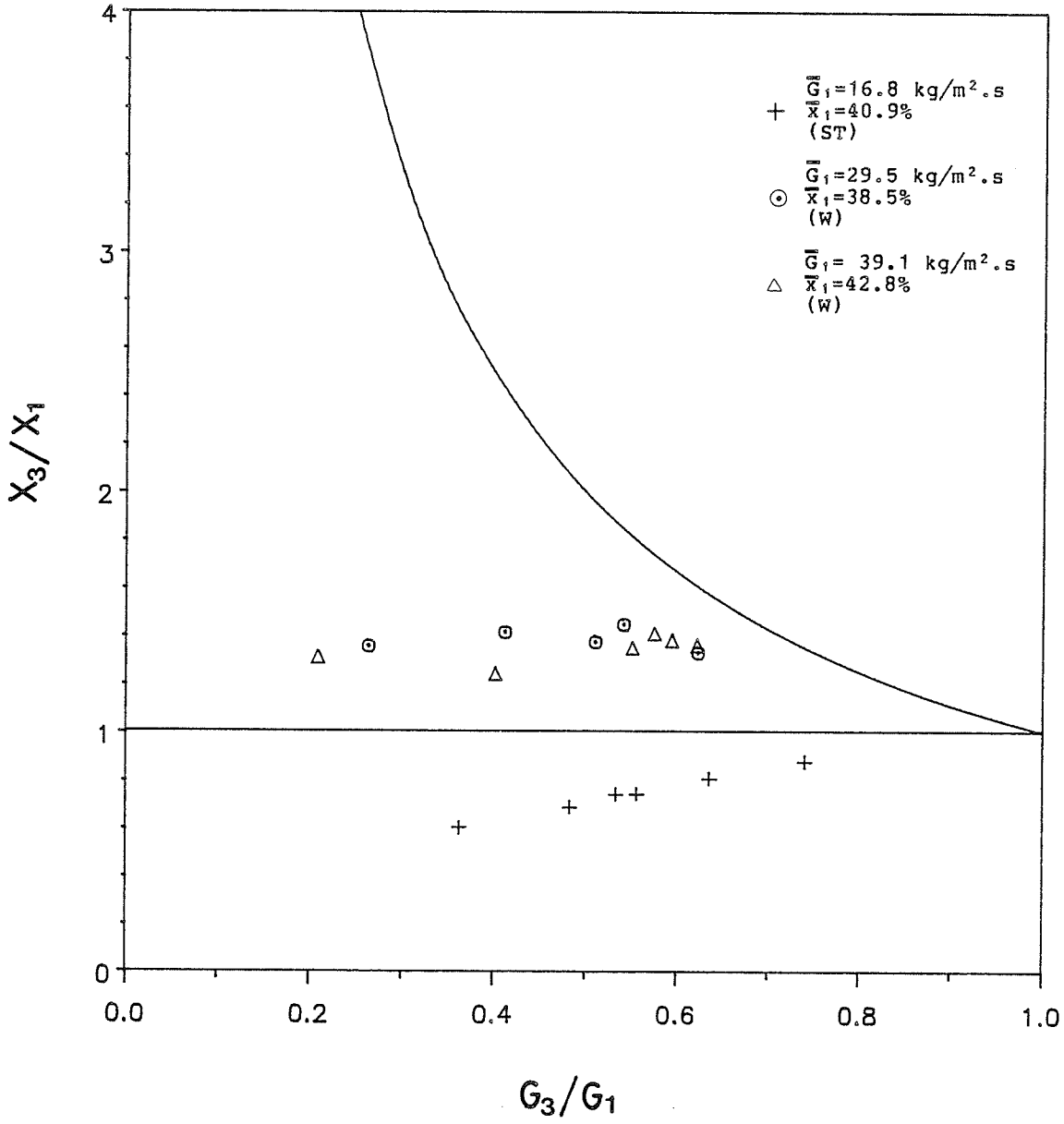

(b)

Fig. 4.3 Effect of inlet mass flux on the phase distribution

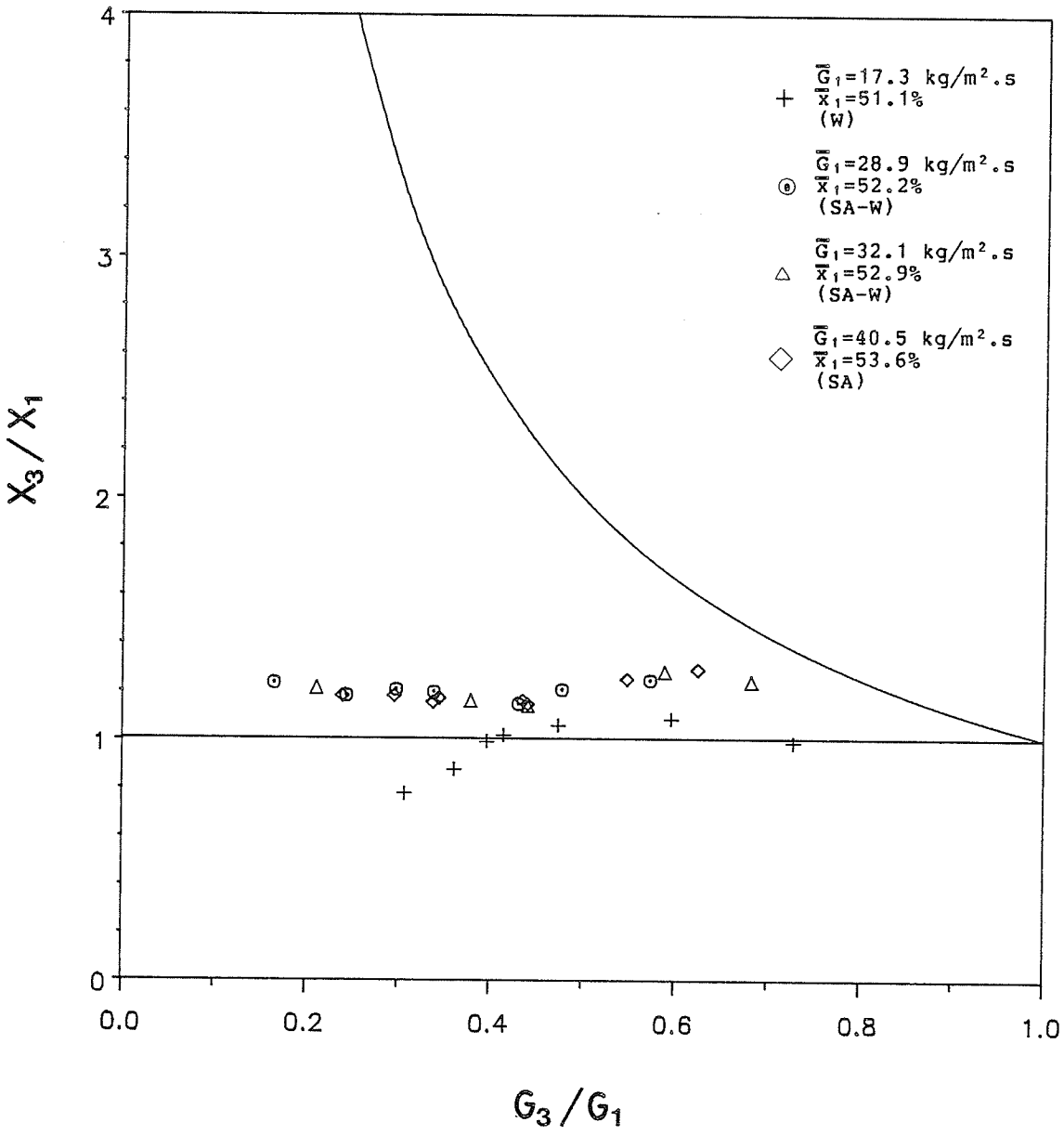

(c)

Fig. 4.3 Effect of inlet mass flux on the phase distribution

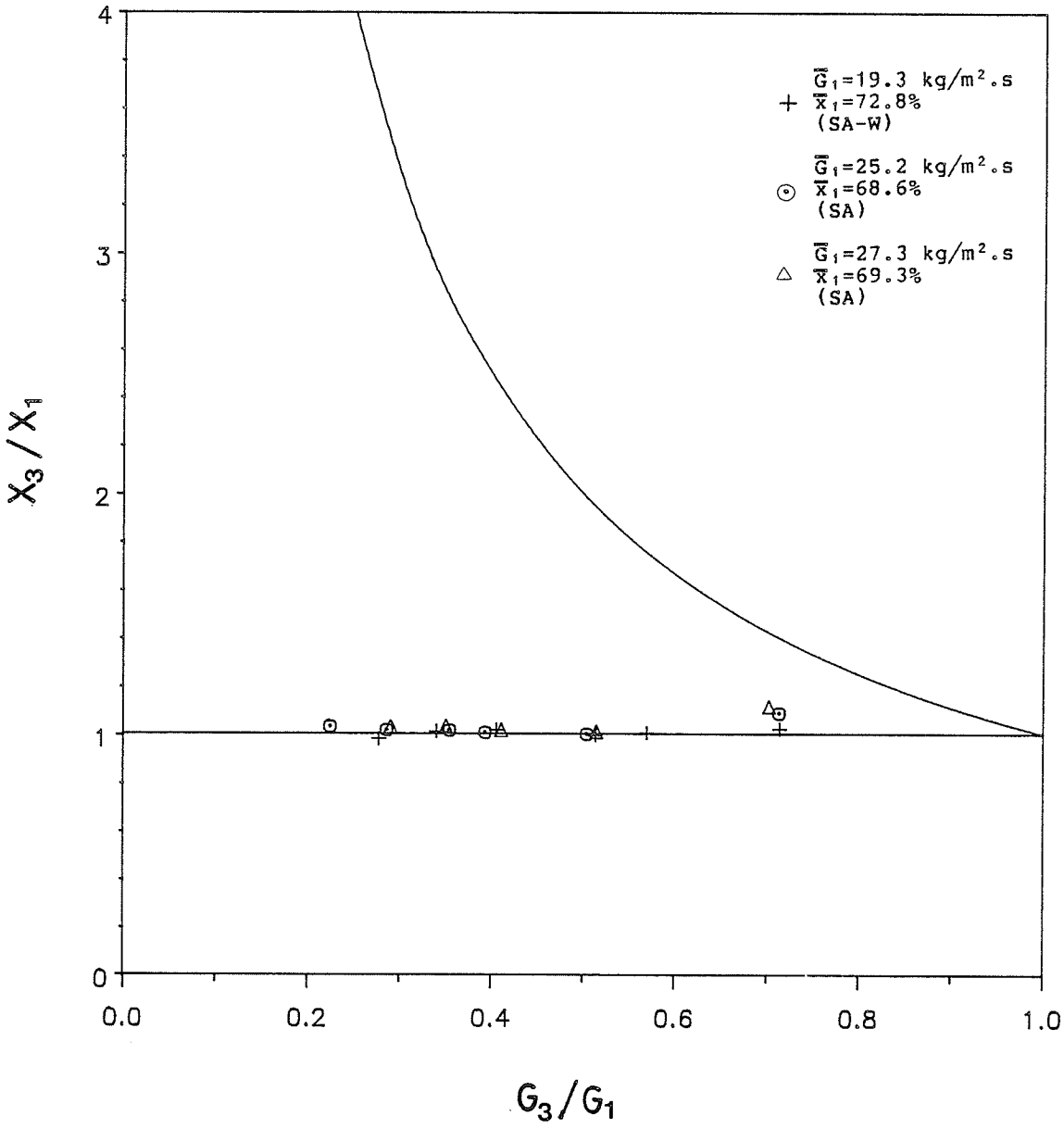

(d)

Fig. 4.3 Effect of inlet mass flux on the phase distribution

smallest $\bar{x}_1$ and indiscernible at the largest $\bar{x}_1$. However, a closer examination reveals that the change in the inlet flow pattern may be the dominant influence, since there does not appear to be any effect of $\bar{G}_1$ on the phase distribution within one inlet flow pattern. It must be emphasized that the range of G_1 covered in the present investigation (for the same x_1 and the same inlet flow pattern) is not very wide, and therefore, the above observation may not always apply to operating conditions outside those of the present investigation. Previous investigations (Saba and Lahey [12]) also did not cover a very wide range of G_1, since in most cases it is not possible to remain within the same inlet flow pattern if x_1 is kept constant and G_1 varies widely. In this investigation, the results showed very little effect of G_1 on the phase distribution for the entire range of x_1 (0.1 - 1.0 percent) tested. Henry [6] reported a strong phase distribution dependence on G_1, although the junction geometry ($D_3/D_1 = 0.2$) and range of W_3/W_1 (≥ 0.06) investigated were extremely different from the present investigation. It is therefore very difficult to include his results in a comparative discussion.

4.2.3 Effect of Inlet Flow Pattern

In Figs. 4.2(a-e) and Figs. 4.3(a-d), the variation of the inlet operating conditions ($\bar{x}_1$ and $\bar{G}_1$, respectively) resulted in a change (or changes) in the inlet flow pattern.

In this section, an attempt to isolate the effect of the inlet flow pattern on the phase distribtuion is made; that is, where the phase-distribution data exist within each inlet flow pattern.

In Figs. 4.4(a-g), F_{BG} and F_{BL} are used as the coordinates. In each figure the line of even phase distribution is shown. The data of stratified flow are shown in Fig. 4.4(a). All the data of stratified flow lie below the line of even phase distribution. Figs. 4.4(b and c), on the other hand, show that most of the data corresponding to wavy flow exist above this line. One group of wavy flow, however, is below the line of even phase distribution for part of the range of F_{BG} investigated. This becomes interesting when this group is located on the Mandhane et al. [16] flow pattern map (Fig. 4.1). This group corresponds to the wavy point which is located nearest to the stratified points. Since this wavy point is the closest to the stratified points, it could be expected that similarities in the phase distribution between them exist. The semiannular-wavy flow are shown in Fig. 4.4(d). Here, it can be seen that most of the data lie above the line of even phase distribution. The semiannular flow data, shown in Figs. 4.4(e and f), lie both above and below this line.

Figure 4.4(g) shows a composite drawing illustrating the regions which are occupied by the stratified, wavy and semi-

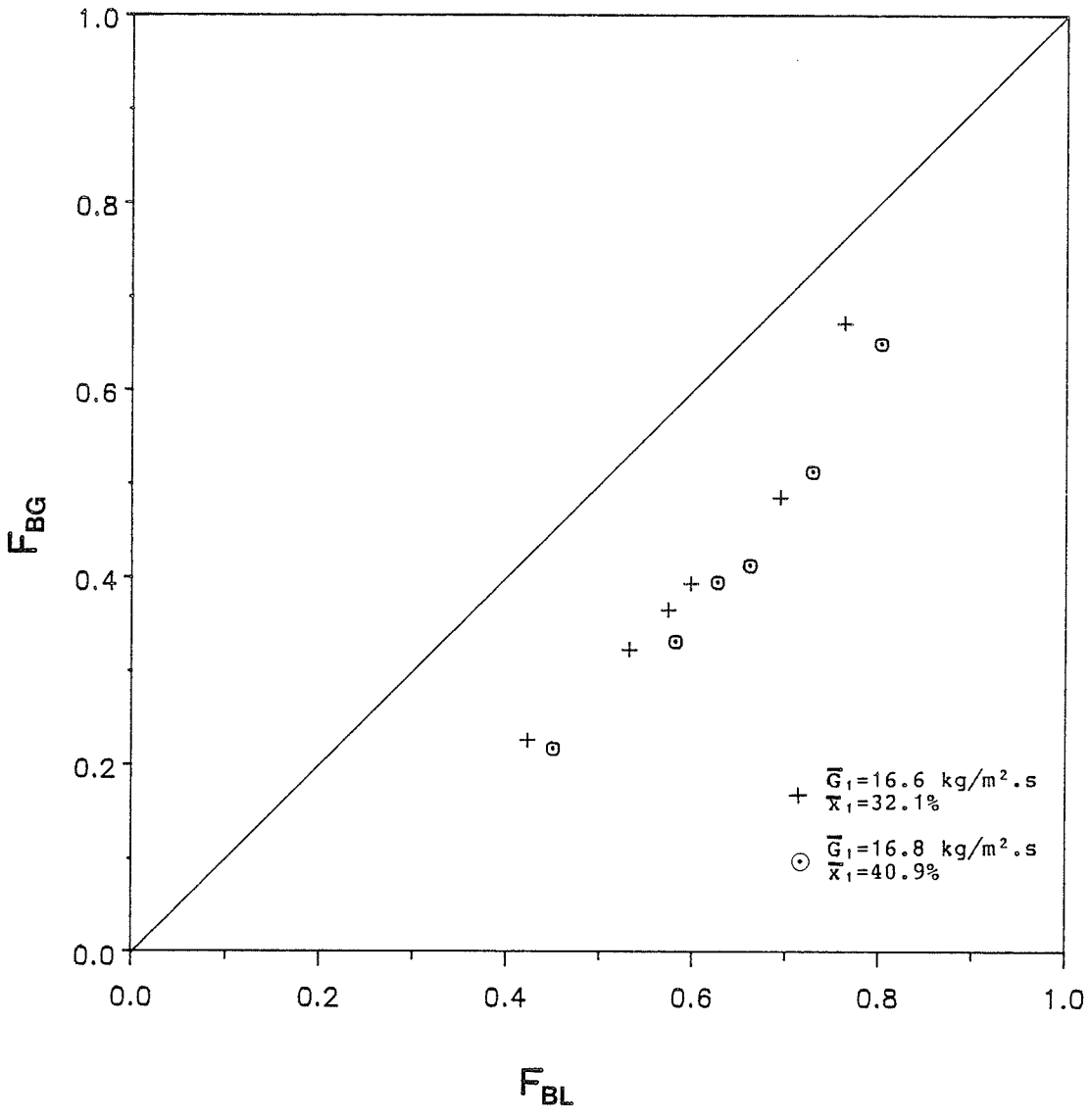

(a)

Stratified

Fig. 4.4 Effect of inlet flow pattern on the phase distribution

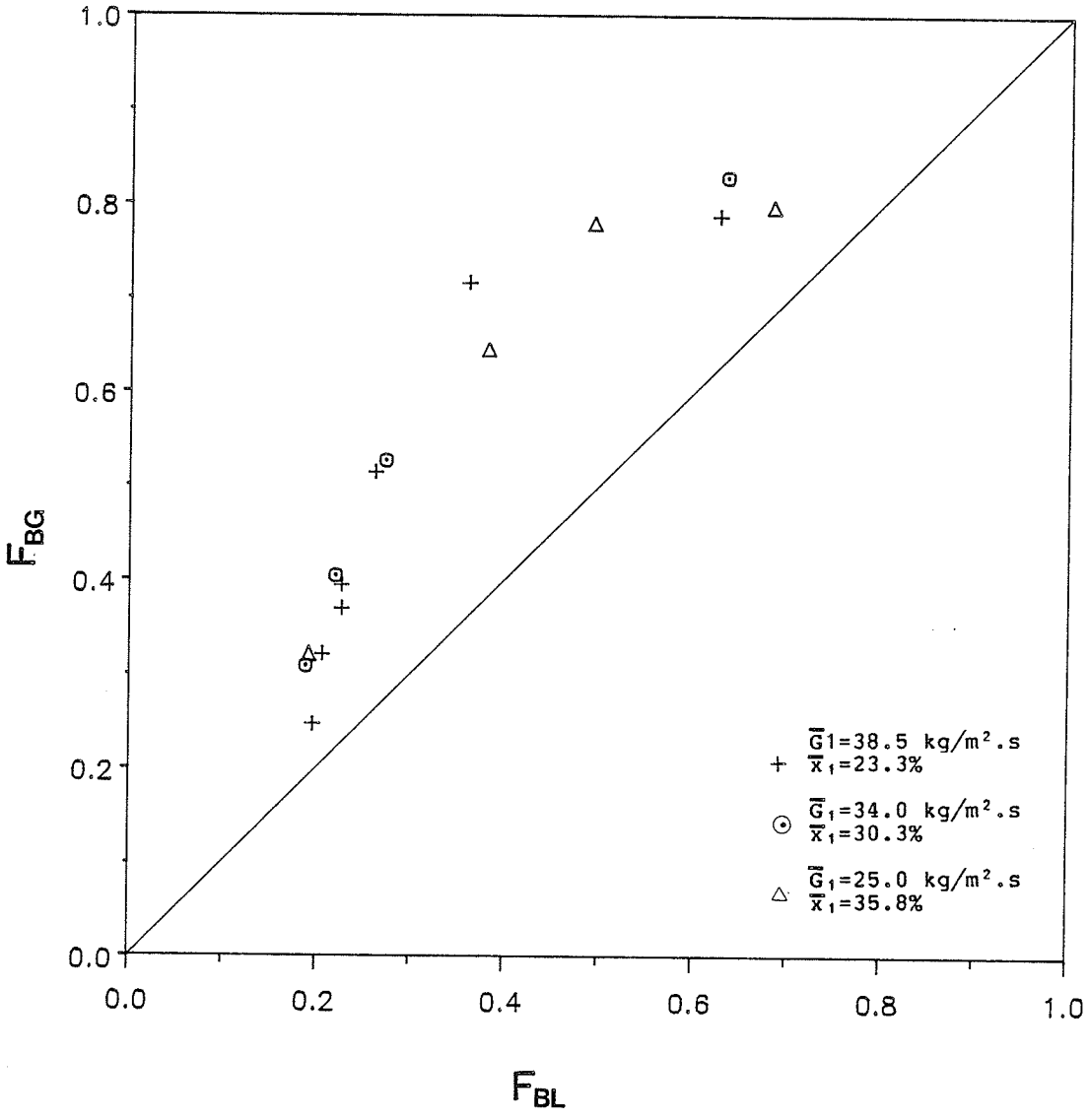

(b)

Wavy

Fig. 4.4 Effect of inlet flow pattern on the phase distribution

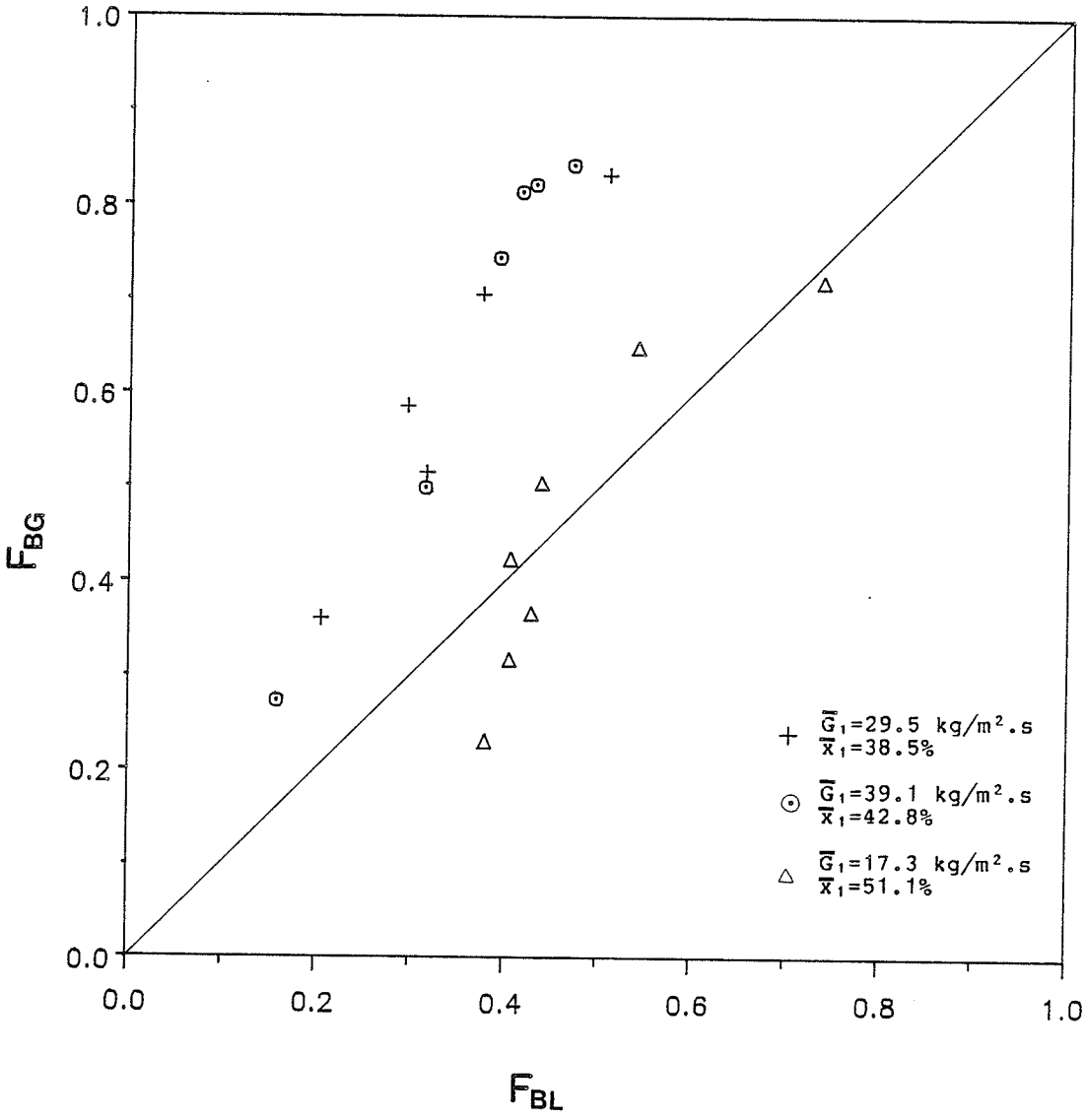

(c)

Wavy

Fig. 4.4 Effect of inlet flow pattern on the phase distribution

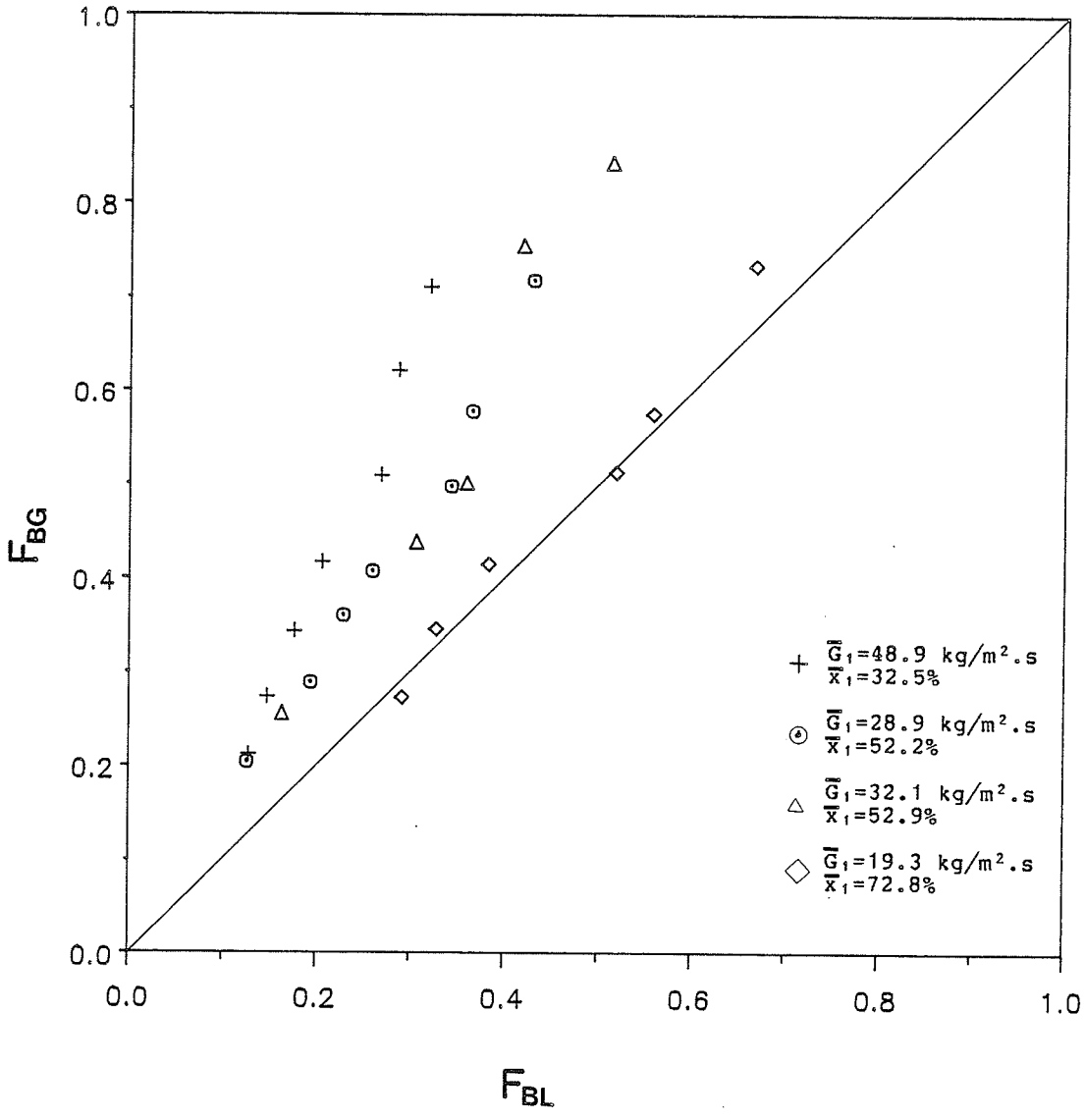

(d)

Semiannular-wavy

Fig. 4.4 Effect of inlet flow pattern on the phase distribution

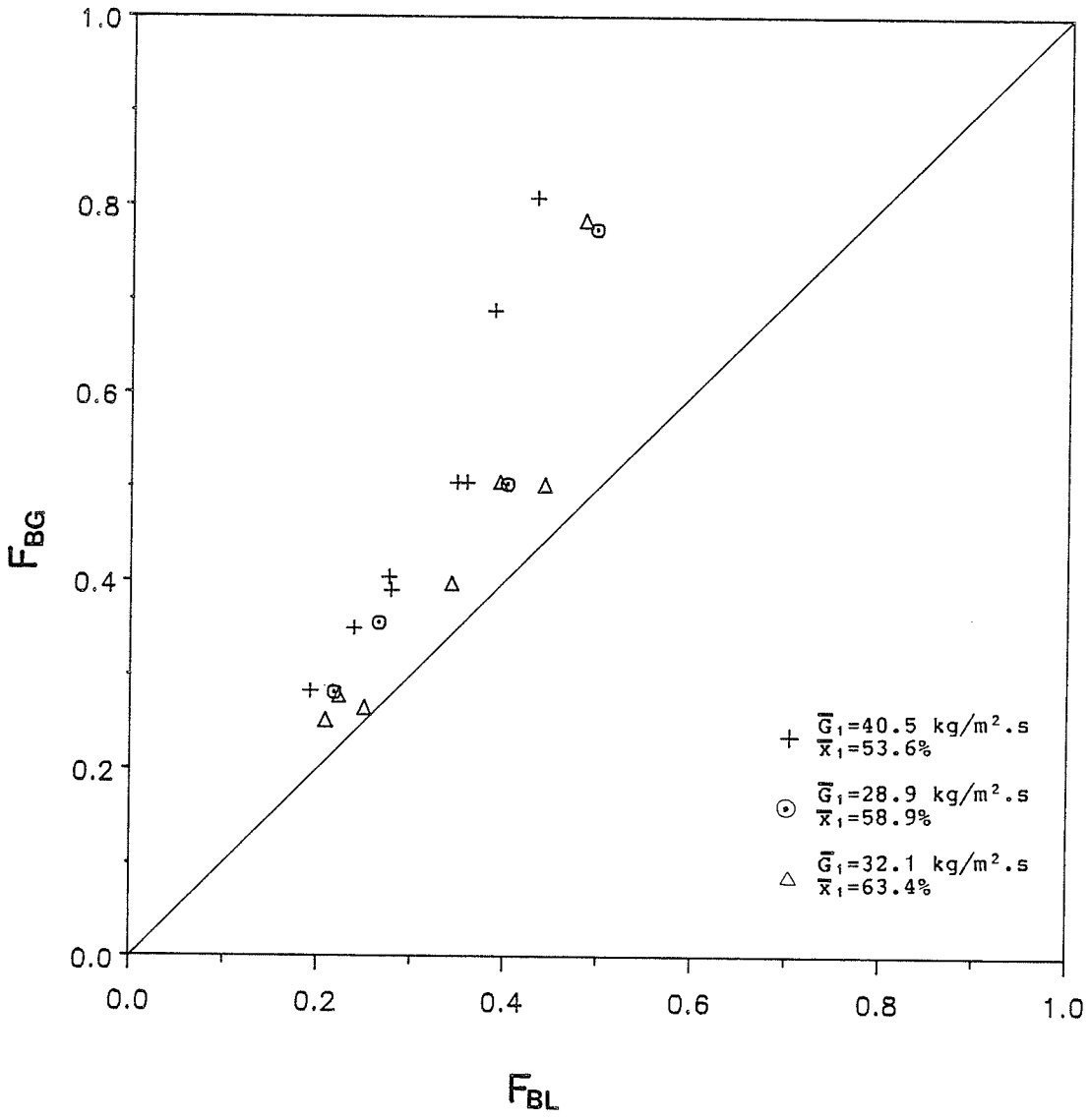

(e)

Semiannular

Fig. 4.4 Effect of inlet flow pattern on the phase distribution

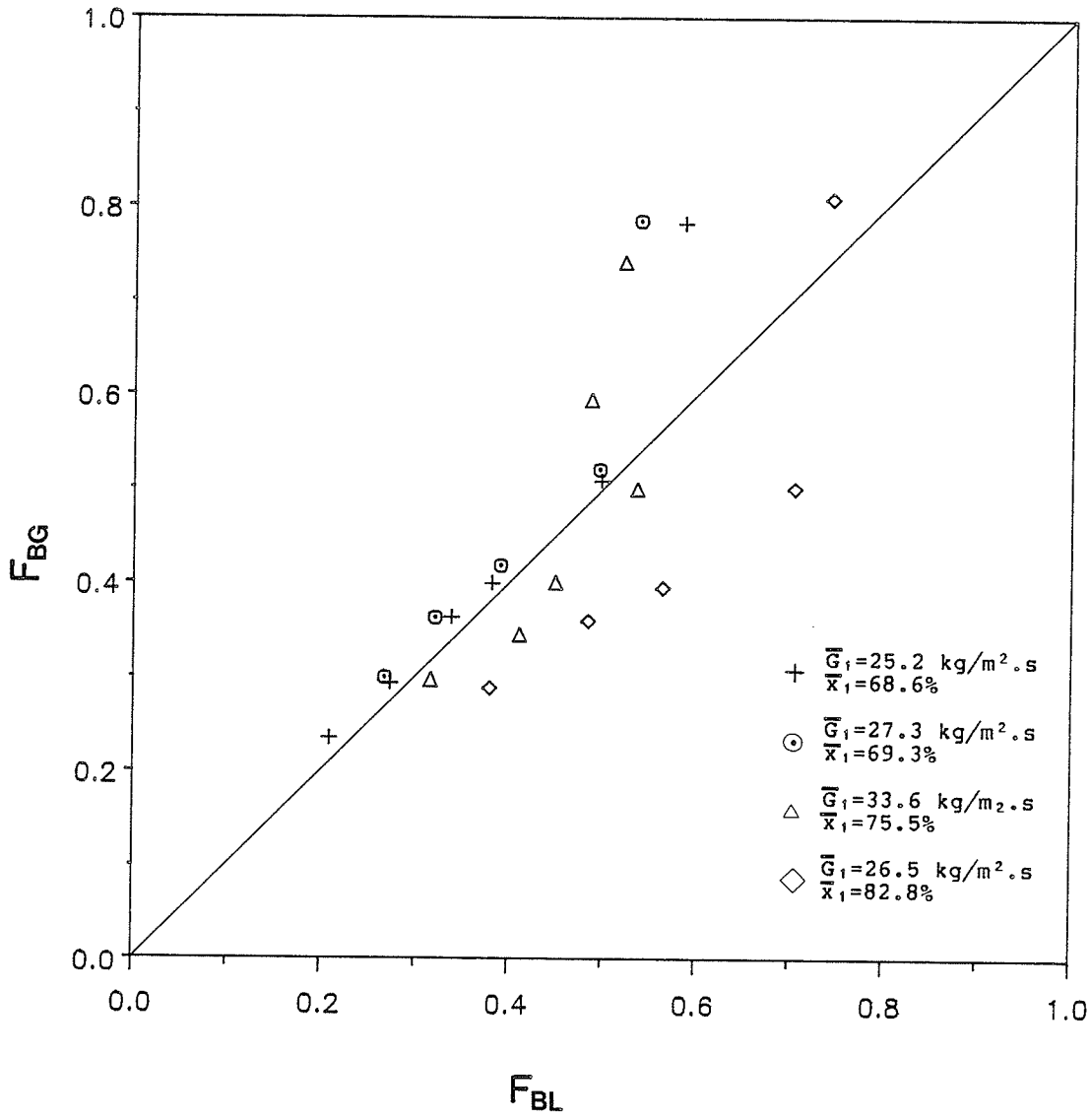

(f)

Semiannular

Fig. 4.4 Effect of inlet flow pattern on the phase distribution

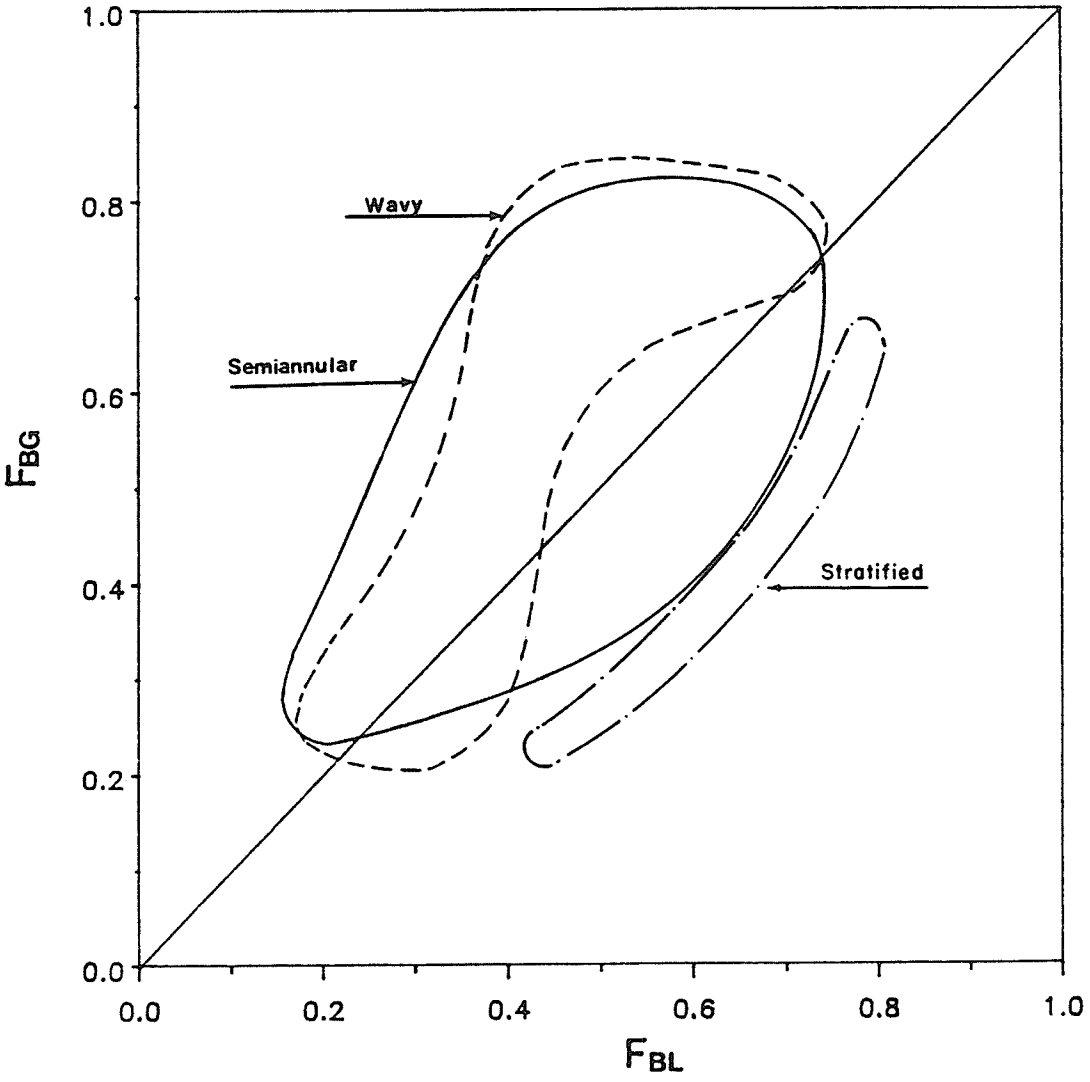

(g)

Composite drawing of stratified, wavy and semiannular flow data

Fig. 4.4 Effect of inlet flow pattern on the phase distribution

annular flow data for the present range of operating conditions.

4.2.4 Effect of Inlet Superficial Liquid Velocity

Within each group, the variation of the inlet pressure (P_1), with varying G_3/G_1, was quite high in some cases. This resulted in deviations of the inlet superficial vapor velocity (V_{GS}) and the inlet superficial liquid velocity (V_{LS}) greater than ±10% of the computed nominal values ($\bar{V}_{GS}$ and $\bar{V}_{LS}$, respectively), within particular groups. To maintain a high degree of confidence in the presented data, a criterion was set to ensure all deviations in V_{GS} and V_{LS} were within ±10% of $\bar{V}_{GS}$ and $\bar{V}_{LS}$, respectively. This resulted in presenting data which are not necessarily within one group, but rather, where V_{GS} and V_{LS} are within ±10% of their nominal values. These new data groups are listed in Appendix C.

Figures 4.5(a-d) use F_{BG} and F_{BL} as the coordinates. In each figure, a range of $\bar{V}_{LS}$ are presented for fixed values of $\bar{V}_{GS}$. Each figure may contain different inlet flow patterns. The results of all figures clearly show that F_{BL} decreases with increasing $\bar{V}_{LS}$ at a fixed F_{BG}. Furthermore, this trend is continuous irrespective of the inlet flow conditions. Referring back to Fig. 4.2(a) now reveals an interesting observation. It was noted that the phase-distribution behavior, in this figure, was not the same as in

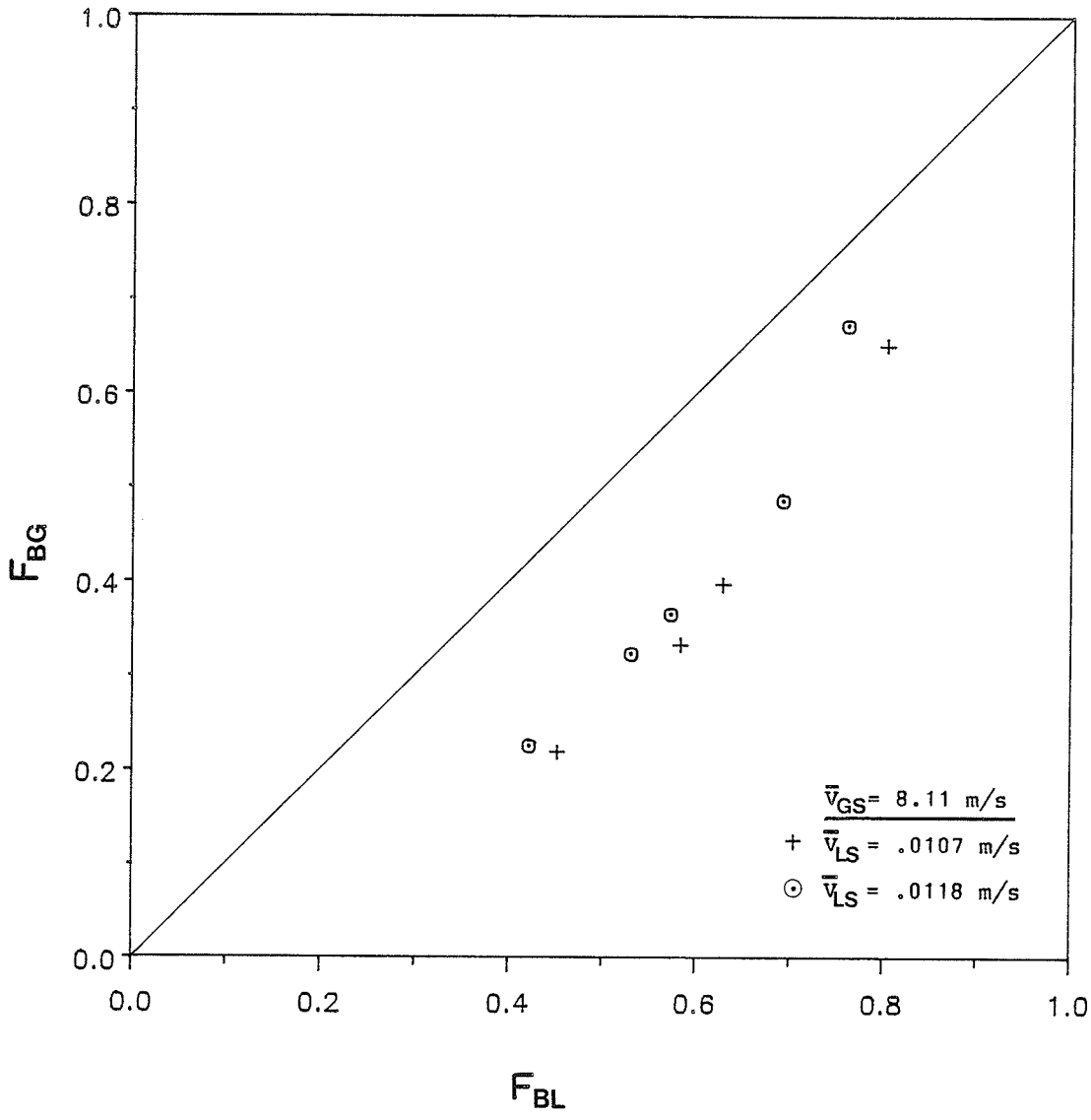

(a)

Fig. 4.5 Effect of superficial liquid velocity on the phase distribution

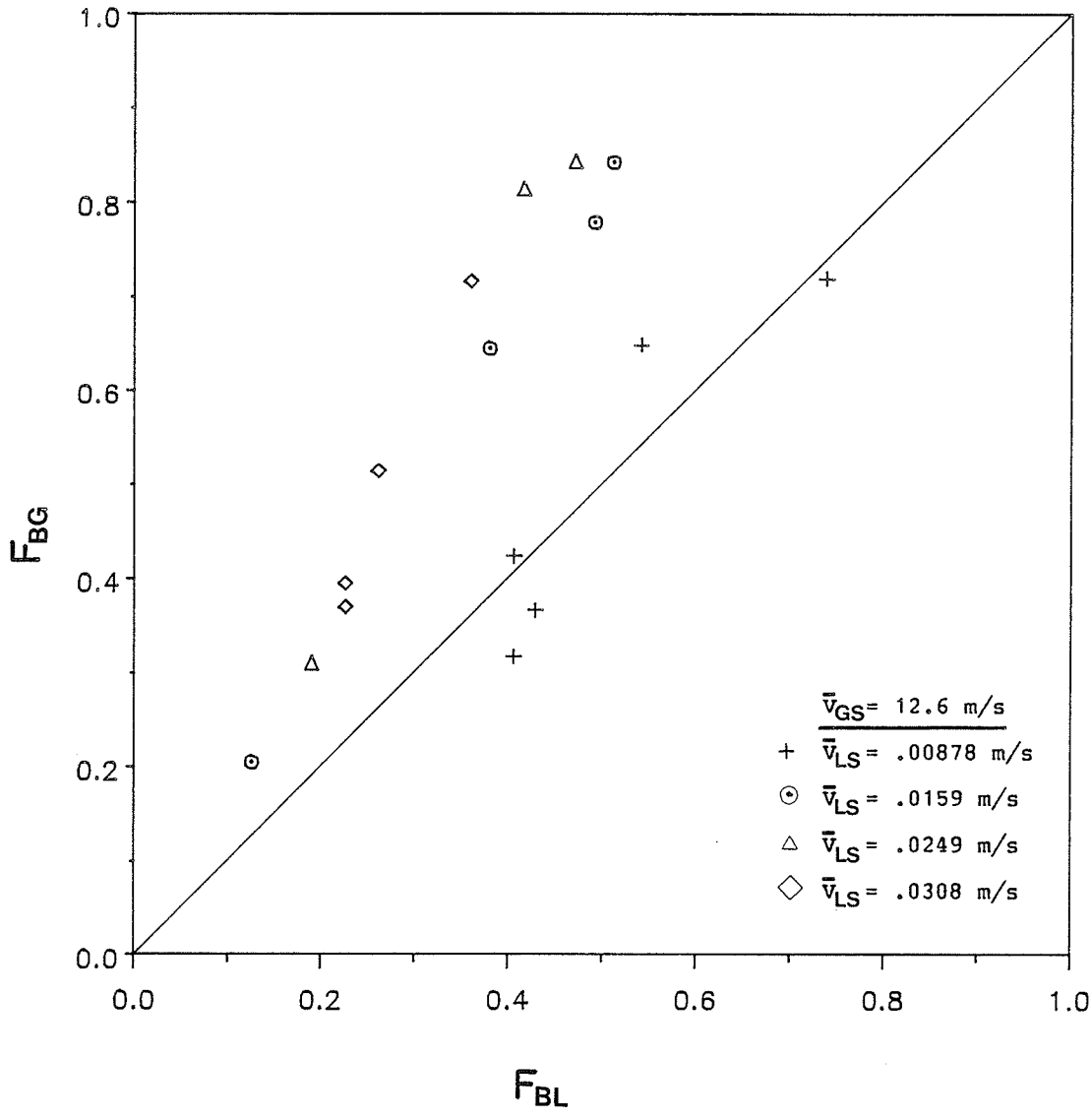

(b)

Fig. 4.5 Effect of superficial liquid velocity on the phase distribution

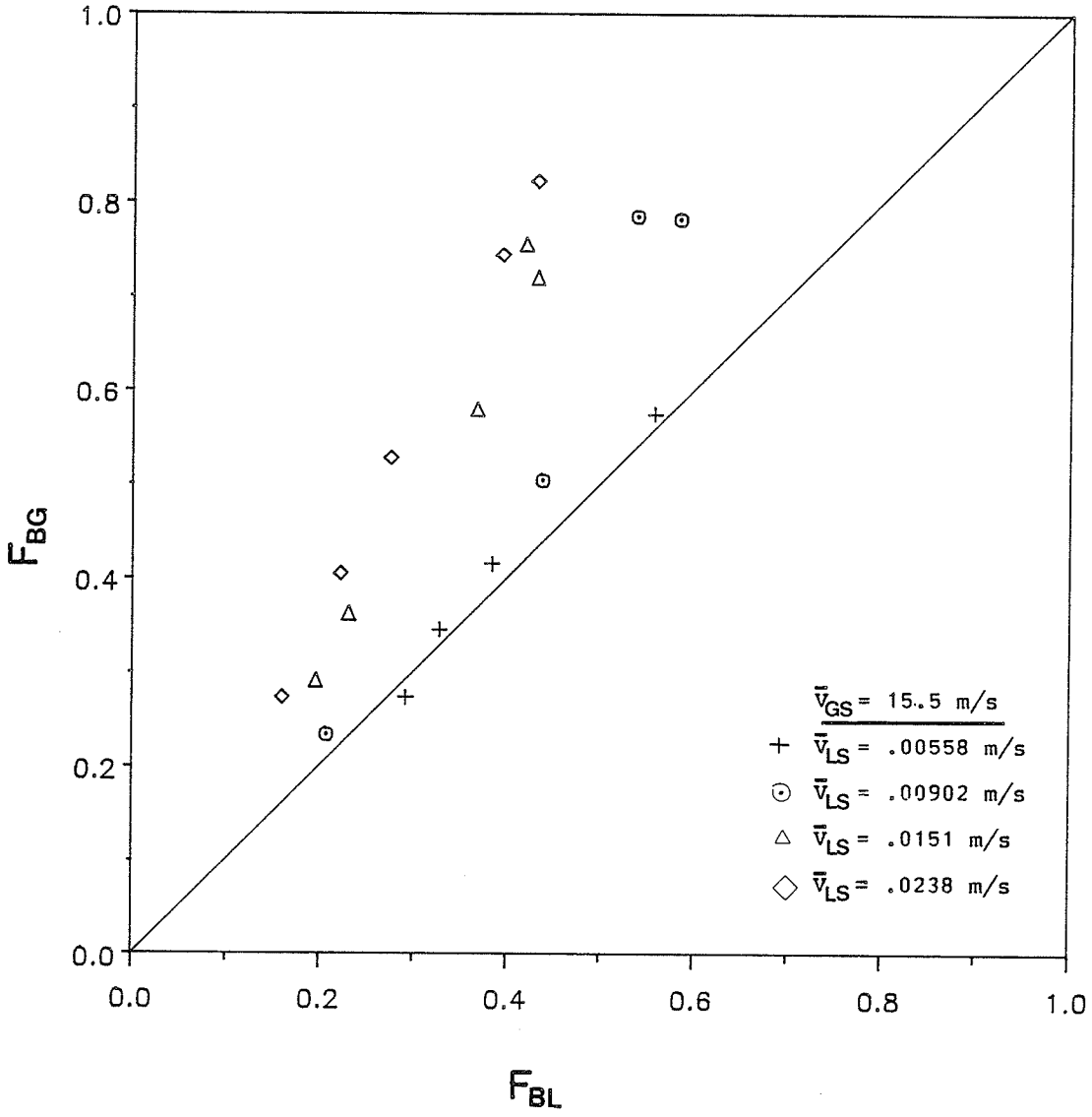

(c)

Fig. 4.5 Effect of superficial liquid velocity on the phase distribution

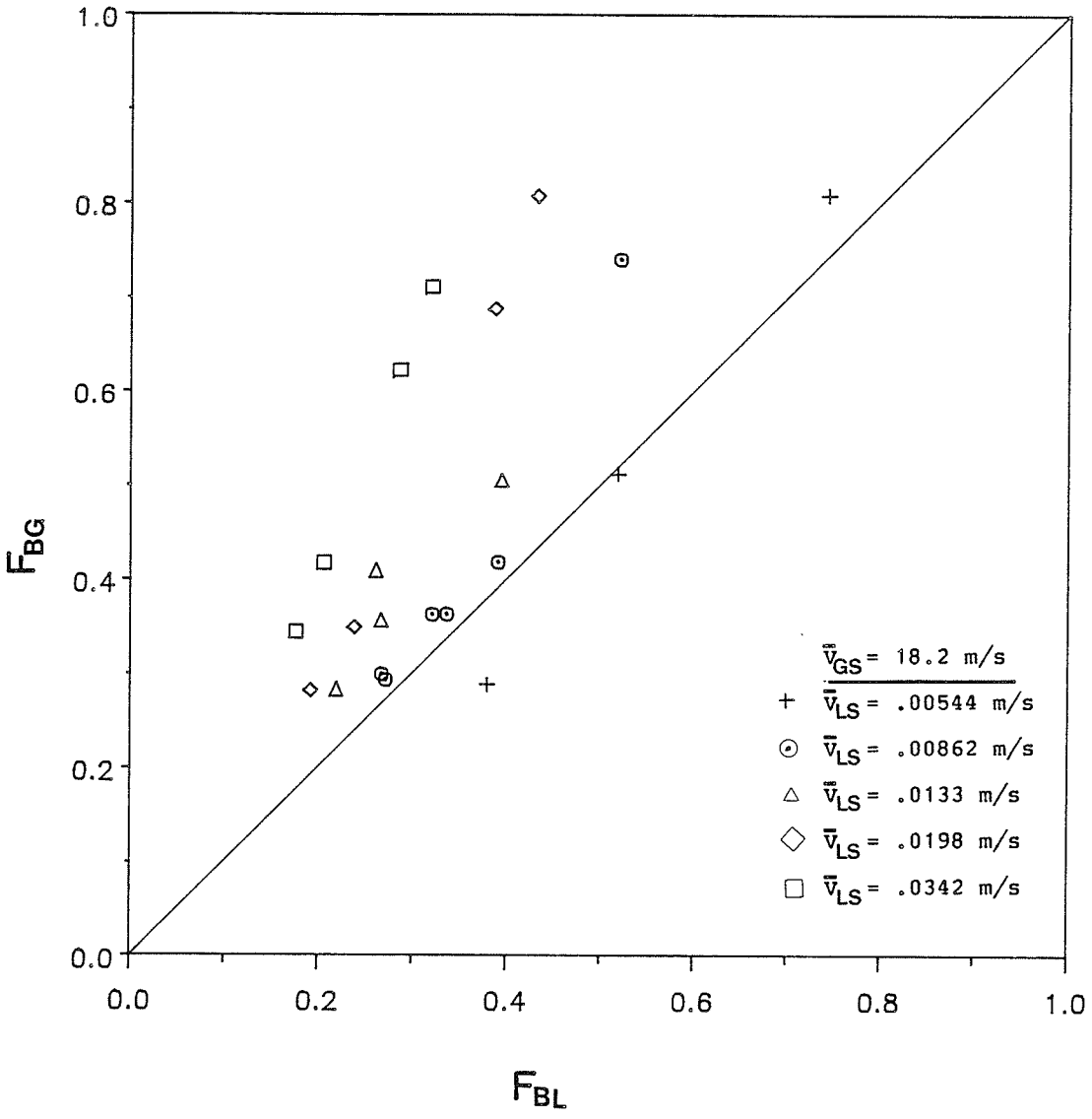

(d)

Fig. 4.5 Effect of superficial liquid velocity on the phase distribution

Figs. 4.2(b-e). However, when most of these data (those meeting the criteria for plotting in Figs. 4.5(a-d)) were replotted in Figs. 4.5(a,b and c), the behavior is seen to be consistent with all other data; that is, for a fixed $\bar{V}_{GS}$, F_{BL} decreases with increasing $\bar{V}_{LS}$. The investigations of both Hong [4] and Seeger et al. [14] showed the same effect on the phase distribution due to V_{LS}, for operating conditions covering inlet qualities similar to the present investigation. The inlet flow patterns in these previous investigations included wavy and annular flow (Hong [4]) and stratified, dispersed bubble, slug and annular flow (Seeger et al. [14]).

4.3 Comparison with Existing Phase-Distribution Correlations

In this section, existing phase-distribution correlations were tested against the present experimental data. One correlation is the phase-distribution model proposed by Azzopardi and Whalley [7]. This model is a simple geometrical phenomenologically based model developed for annular flow. Although in the present investigation annular flow was not observed, the data of semiannular flow may provide an interesting test of the model by Azzopardi and Whalley [7]. The second phase-distribution correlation tested was proposed by Seeger et al. [14]. This correlation consists of a set of empirically derived equations for different branch orienta-

tions, based on their phase-distribution data. Although the operating conditions, P_1 and G_1, from which these equations were derived are much different from the present values, this correlation was tested due to the wide range of inlet qualities on which it was based.

4.3.1 The Azzopardi and Whalley [7] Model

The phase-distribution model proposed by Azzopardi and Whalley [7] is geometrically based for annular flow. The model assumes that the portion of liquid removed through the branch comes from the same segment of the tube as the removed gas. Furthermore, the model assumes that the liquid which is removed comes from the liquid film; that is, the liquid which exists as entrained droplets travel straight on into the run. This is shown schematically in Fig. 4.6. For the special case which assumes that the liquid film is uniform over the entire tube periphery, the model reduces to

$$\frac{G_3 x_3}{G_1 x_1} = \frac{1}{2\pi}\left\{\left\{\frac{2\pi \quad G_3(1-x_3)}{(1-E_1)G_1(1-x_1)}\right\} - \sin\left\{\frac{2\pi \quad G_3(1-x_3)}{(1-E_1)G_1(1-x_1)}\right\}\right\} \qquad (4.1)$$

where E_1 is the fraction of inlet liquid which exists as entrained droplets.

Azzopardi [11] later proposed a correction term which takes into account the ratio of the branch to inlet tube diameter (D_3/D_1). Substituting this correction term into (4.1) gives

$$\frac{G_3 x_3}{G_1 x_1} = \frac{1}{2\pi}\left\{\left\{\frac{2\pi}{(1-E_1)1.2(D_3/D_1)^{0.4}} \quad \frac{G_3(1-x_3)}{G_1(1-x_1)}\right\}\right. \qquad (4.2)$$

$$\left. -\sin\left\{\frac{2\pi}{(1-E_1)1.2(D_3/D_1)^{0.4}} \frac{G_3(1-x_3)}{G_1(1-x_1)}\right\}\right\}$$

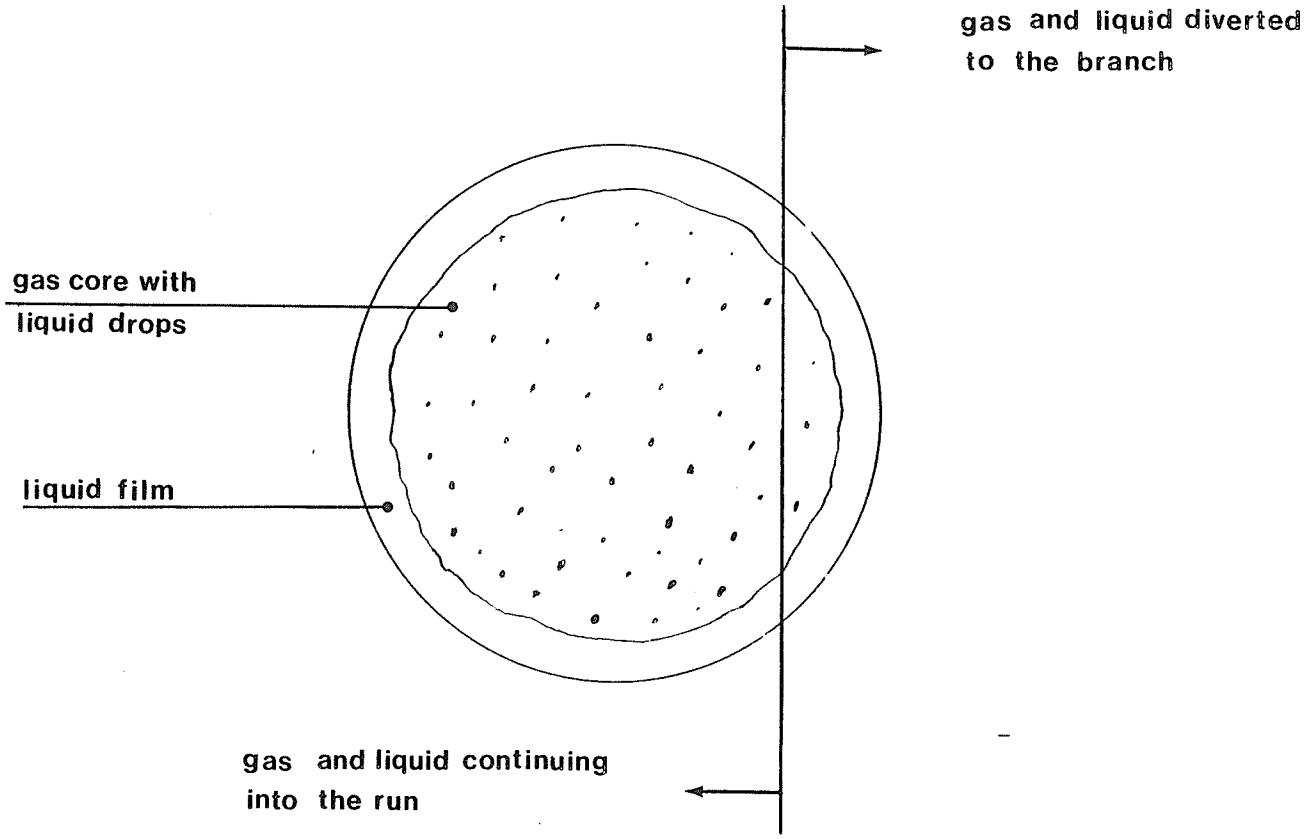

Fig. 4.6 Schematic diagram illustrating the basis of the Azzopardi and Whalley [7] model

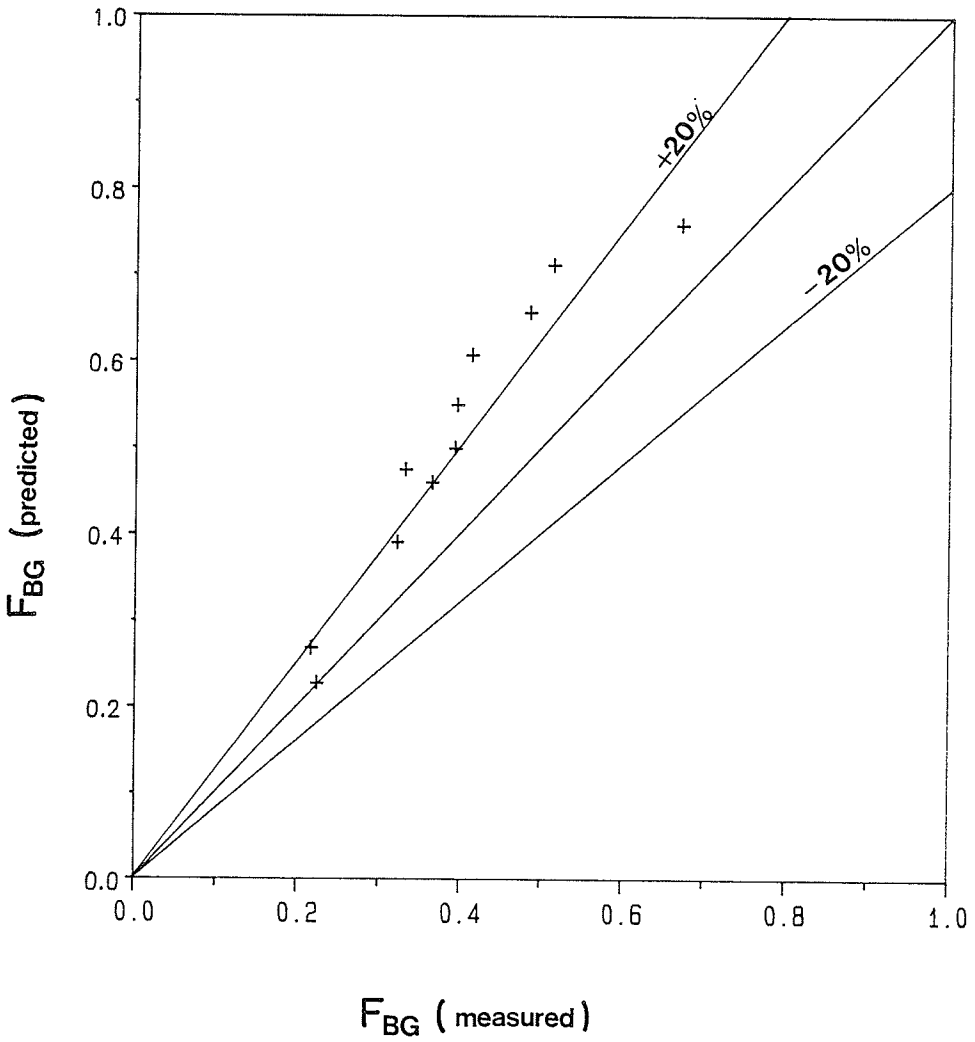

$E_1 = 0.0$

Fig. 4.7 Comparison between the data of stratified flow and the model by Azzopardi and Whalley [7]

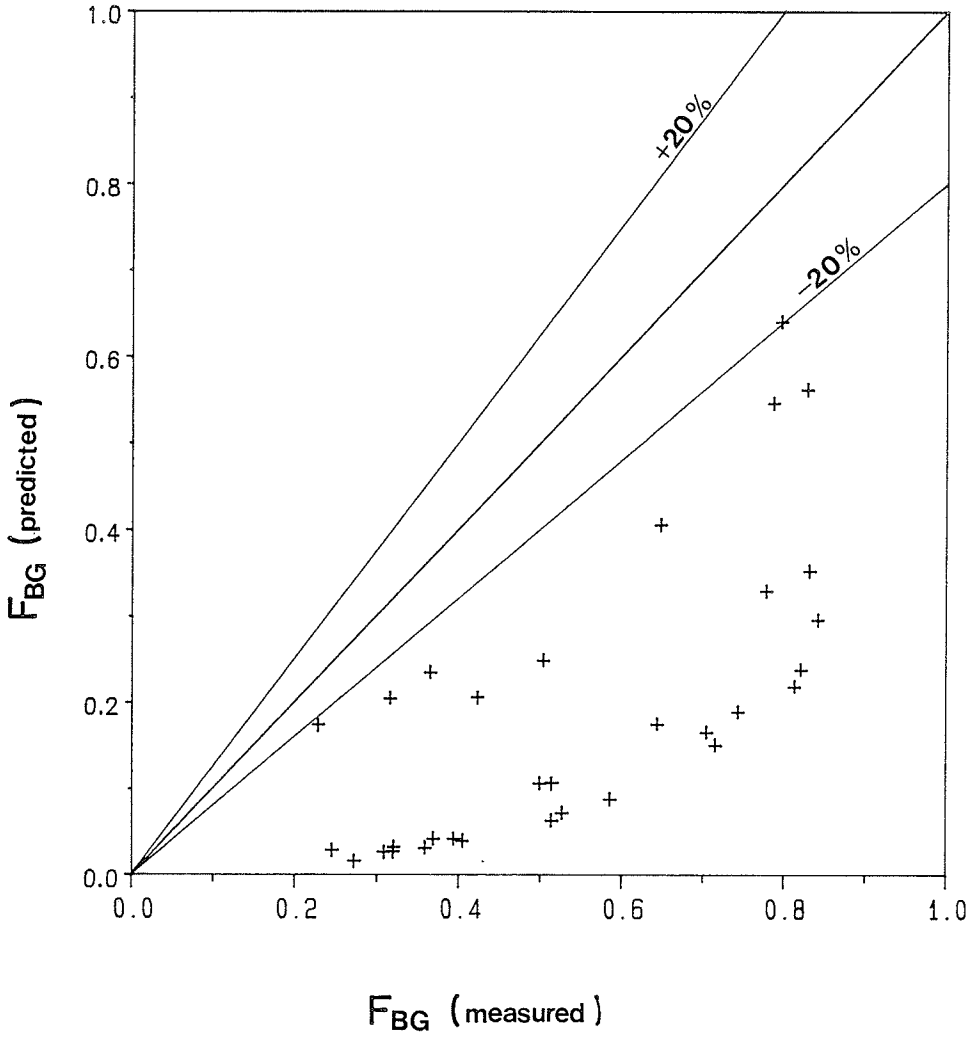

$E_1 = 0.0$

Fig. 4.8 Comparison between the data of wavy flow and the model by Azzopardi and Whalley [7]

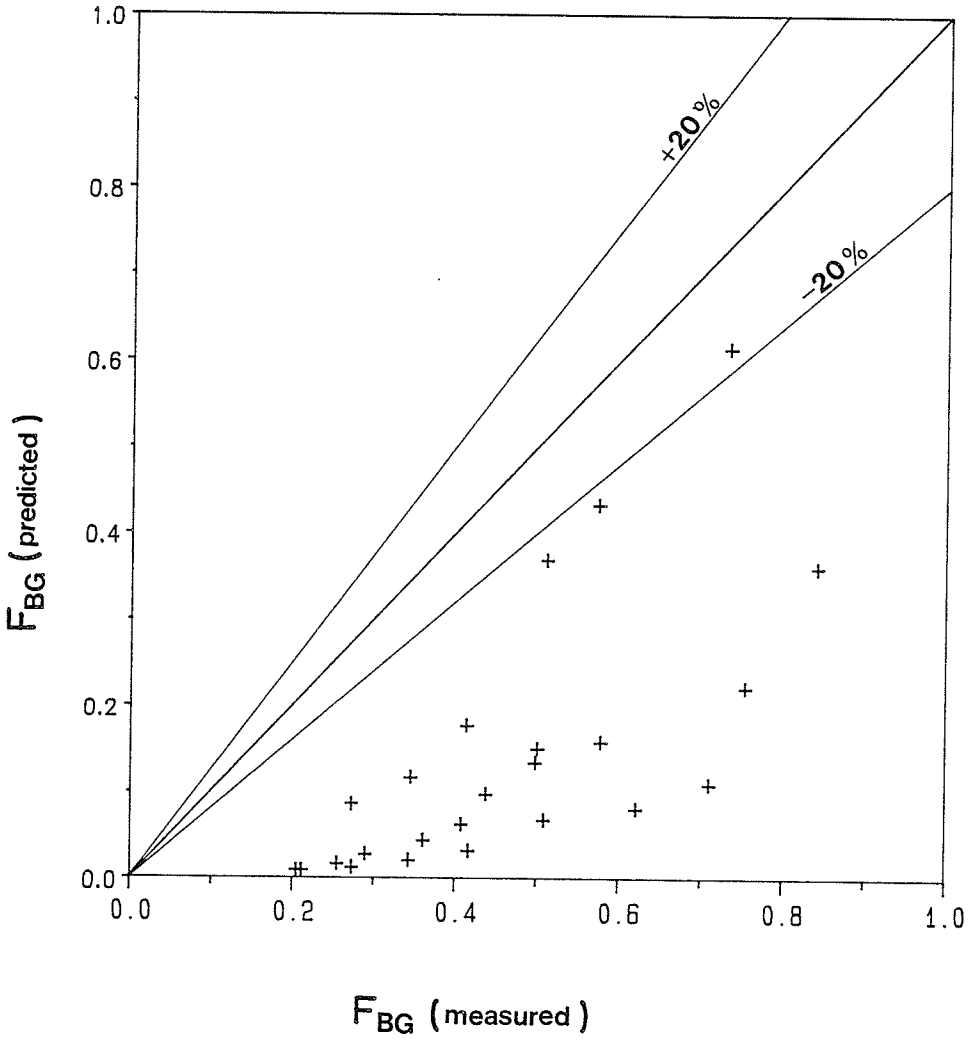

$E_1 = 0.0$

Fig. 4.9 Comparison between the data of semiannular-wavy flow and the model by Azzopardi and Whalley [7]

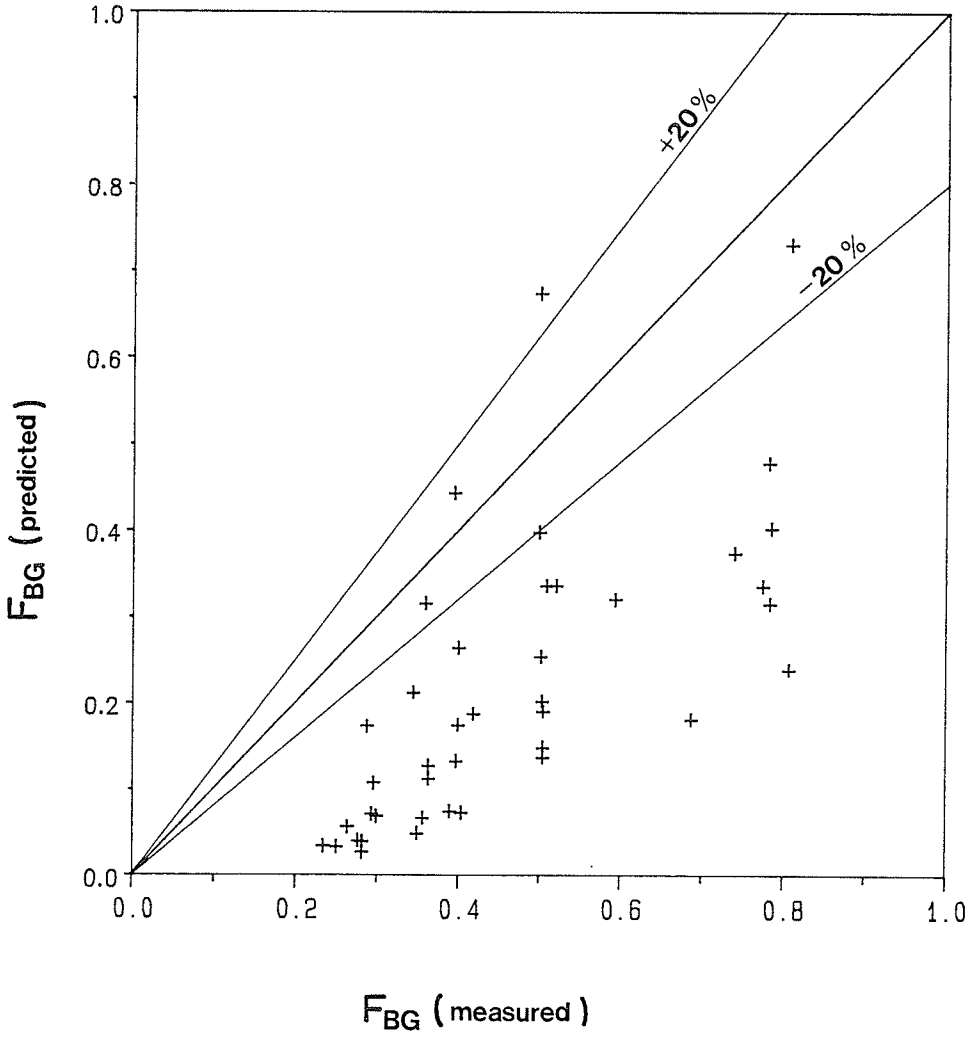

$E_1 = 0.0$

Fig. 4.10 Comparison between the data of semiannular flow and the model by Azzopardi and Whalley [7]

Substituting (3.14) and (3.15) into (4.2), and rearranging, gives (for $D_3 = D_1$)

$$F_{BG} = \frac{1}{2\pi}\left\{\left\{\frac{1.67\pi \quad F_{BL}}{(1-E_1)}\right\} - \sin\left\{\frac{1.67\pi \; F_{BL}}{(1-E_1)}\right\}\right\} \qquad (4.3)$$

Equation (4.3) was tested by substituting all of the experimentally obtained values of F_{BL} into (4.3) to obtain the corresponding predicted values for F_{BG}. Figures 4.7 to 4.10 show the predicted values of F_{BG} plotted against the measured values, for the same F_{BL}. All figures show the predictions for a fixed inlet flow pattern and for each flow pattern the liquid entrainment was assumed to be negligible (i.e. $E_1 = 0$). It is apparent from these figures that the model generally predicts poorly, particularily for wavy and semiannular-wavy flow. All the data is underpredicted; that is, for a fixed F_{BL}, the model predicts a lower value of F_{BG} than the experimental value. Since the model was developed for annular flow, the predicted values of F_{BG} would be expected to be lower than the corresponding experimental values of F_{BG}. Although the agreememnt with the stratified flow data is quite good, this is likely fortuitous since the geometry of stratified flow is very different from annular flow. Most of the semiannular flow data fall outside the ±20% error lines, although some points do fall close to or within these lines.

To investigate further the operating conditions which led to a better agreement between the model and the experimental data, most of the semiannular flow data were replotted indicating the nominal inlet conditions for each group. Here, the values of $\bar{V}_{GS}$, $\bar{V}_{LS}$ and $\bar{V}_{GS}/\bar{V}_{LS}$ are based on groups rather than the criterion set in Section 4.2.4. Figure 4.11 shows that the model's prediction becomes increasingly better as both $\bar{x}_1$ and $\bar{V}_{GS}/\bar{V}_{LS}$ increase. Based on the nominal inlet conditions of the semiannular flow data, values for E_1 were determined from the correlation proposed by Katoka and Ishii [17] and compared with experimentally obtained values of Gill and Hewitt [18]. The agreement between the predicted values of Katoka and Ishii [17], for the present operating conditions and the experimental values of Gill and Hewitt [18] were found to be quite good, considering Gill and Hewitt [18] investigated liquid entrainment for air-water annular flow in a vertical tube (38.1-mm I.D.). The maximum value of E_1 was found to be less than 0.15 for the operating conditions corresponding to semiannular flow in this investigation. Figure 4.12 shows the groups of semiannular flow as in Fig. 4.11 except that in Fig. 4.12, the value E_1 = 0.15 was used. Although most of the data are still underpredicted, the points are all shifted towards better agreement.

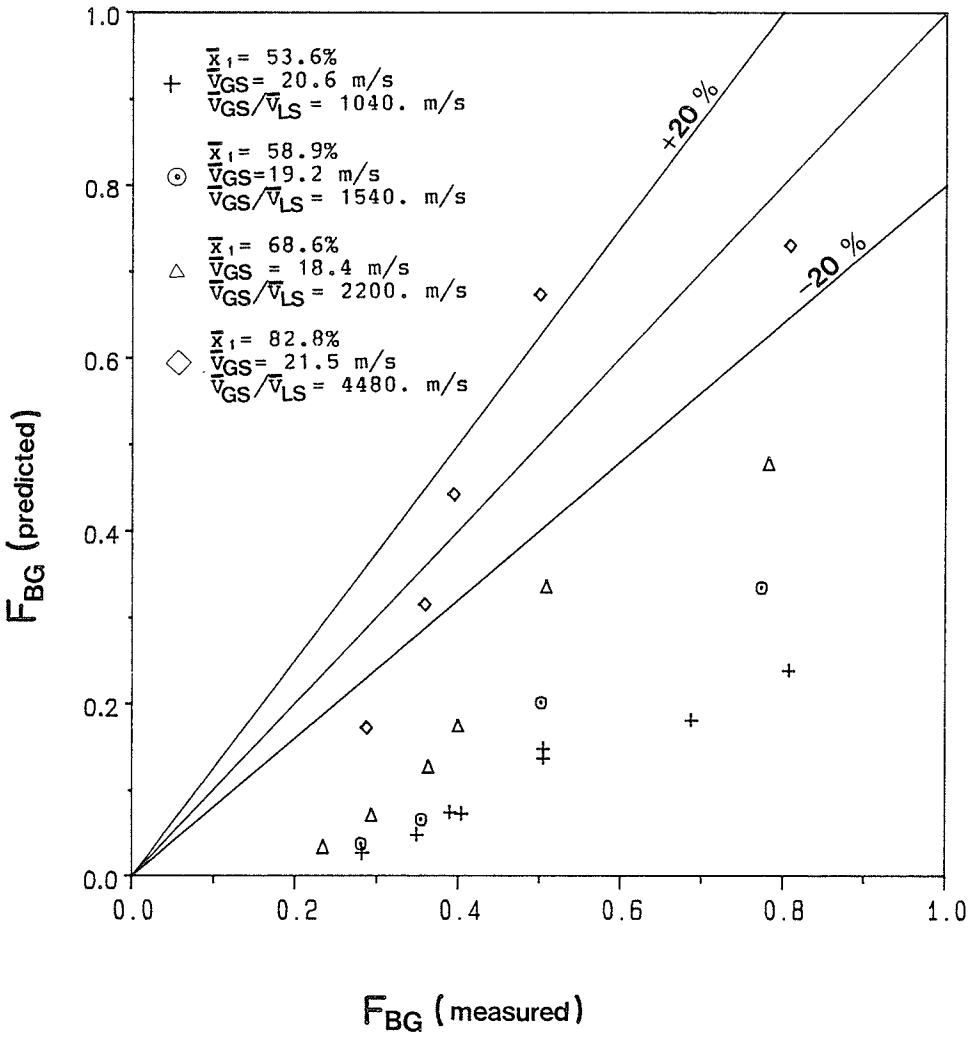

Fig. 4.11 Effect of inlet conditions on the predictions of Azzopardi and Whalley [7] for semiannular flow (E_1 = 0.0)

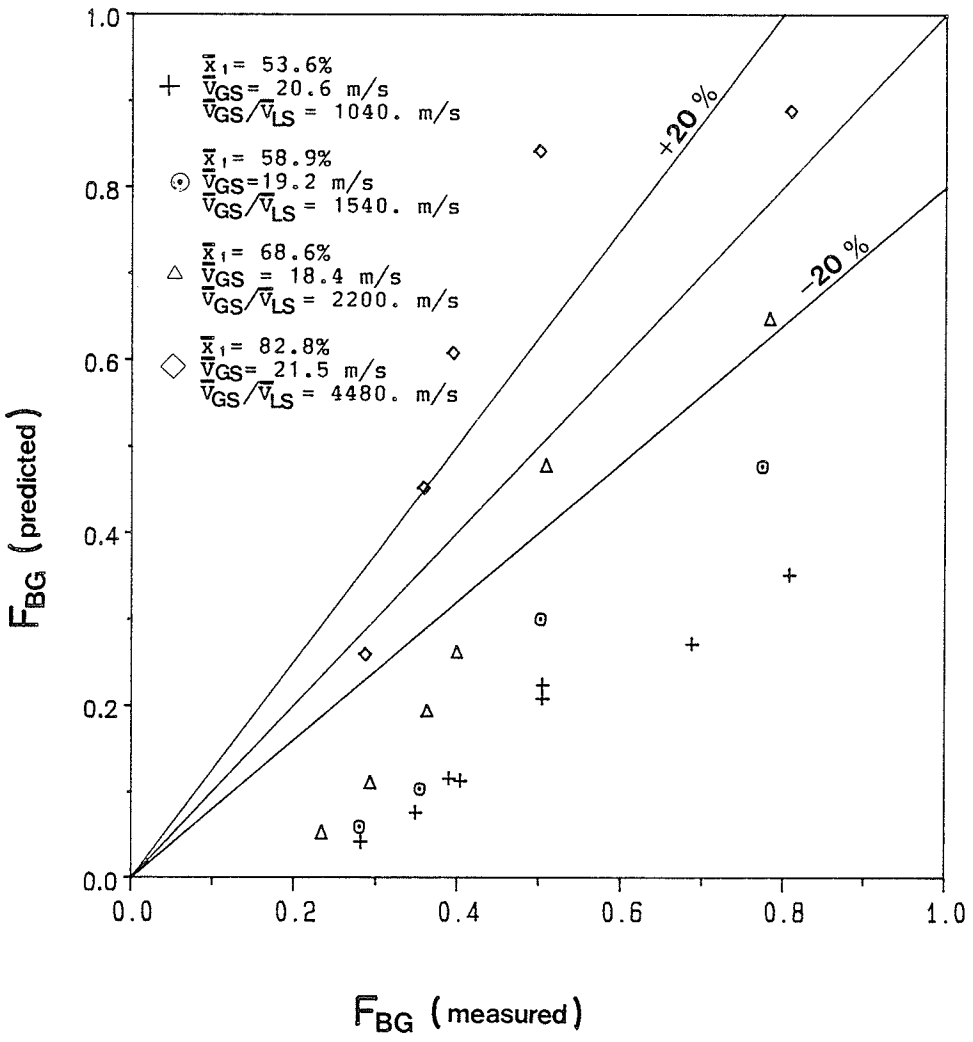

Fig. 4.12 Effect of inlet conditions on the predictions of Azzopardi and Whalley [7] for semiannular flow (E_1 = 0.15)

4.3.2 The Seeger et al. [14] Correlation

For a horizontal main tube, Seeger et al. [14] derived three phase-distribution correlations for the following branch orientations: vertically upwards, horizontal and vertically downwards. The equation for a horizontal branch for any inlet flow pattern other than dispersed bubble is

$$\frac{x_3}{x_1} = 5\left(\frac{G_3}{G_1}\right) - 6\left(\frac{G_3}{G_1}\right)^2 + 2\left(\frac{G_3}{G_1}\right)^3 + a\left(\frac{G_3}{G_1}\right)\left(\frac{1-G_3}{G_1}\right)^4 \qquad (4.4)$$

where

$$a = 13.9\left\{\left[\left[\frac{\rho_G}{\rho_L}\right]S_1^2\right]^{0.26} - 1\right\} \qquad (4.5)$$

$$S_1 = \rho_L\left(\frac{1}{(1-x_1)}\right)\left(\frac{1+\ 0.12(1-x_1)}{\rho_H}\ \ \frac{V_{rel}}{G_1}\ \ \frac{x_1}{\rho_G}\right) \qquad (4.6)$$

$$\rho_H = \left(\frac{x_1}{\rho_G} + \frac{(1-x_1)}{\rho_L}\right)^{-1} \qquad (4.7)$$

$$V_{rel} = \frac{1.18}{\rho_L^{0.5}}\left(g\ (\rho_L - \rho_G)\right)^{0.25} \qquad (4.8)$$

Equation (4.4) was tested against the present experimental data by substituting all experimental values of G_3/G_1 from each group into (4.4) to obtain the corresponding predictions of x_3/x_1.

In Fig. 4.13, the predicted values of x_3/x_1 are plotted against the measured values, at the same G_3/G_1 for $x_1 \geq 40\%$ and $G_3/G_1 \geq 0.4$. It is evident from Fig. 4.13 that equation (4.4) predicted the experimental values of x_3/x_1 remarkably

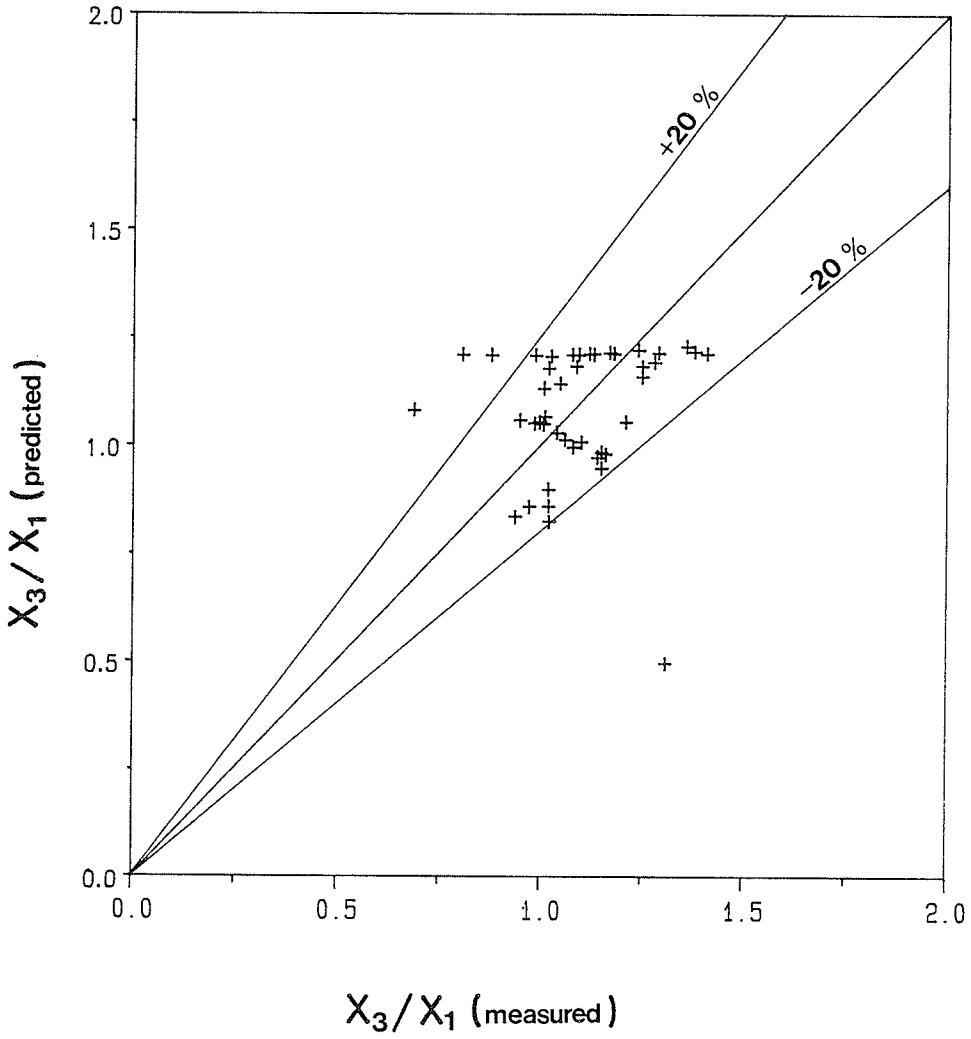

Fig. 4.13 Comparison between the correlation by Seeger et al. [14] and the present data for $x_1 \geq 40\%$ and $G_3/G_1 \geq 0.4$

well. Most predictions are within ±20% of the corresponding measured values. This is a very encouraging result considering the differences in the operating conditions between the present investigation and those from which equation (4.4) was derived. In Fig. 4.14, most of the predicted values of x_3/x_1 are within ±40% for the entire range of x_1 investigated and for $G_3/G_1 \geq 0.3$. Figure 4.15, however, shows that for all x_1 and $G_3/G_1 < 0.3$, most of the predicted values of x_3/x_1 fall outside the ±40% error lines. It is not surprising that equation (4.4) failed to predict x_3/x_1 for low values of G_3/G_1, since the limit of equation (4.4) at $G_3/G_1 = 0.0$ is $x_3/x_1 = 0.0$. This limitng value may not be true for all flow patterns and is very difficult to establish since reliable data at low extraction rates are quite scarce.

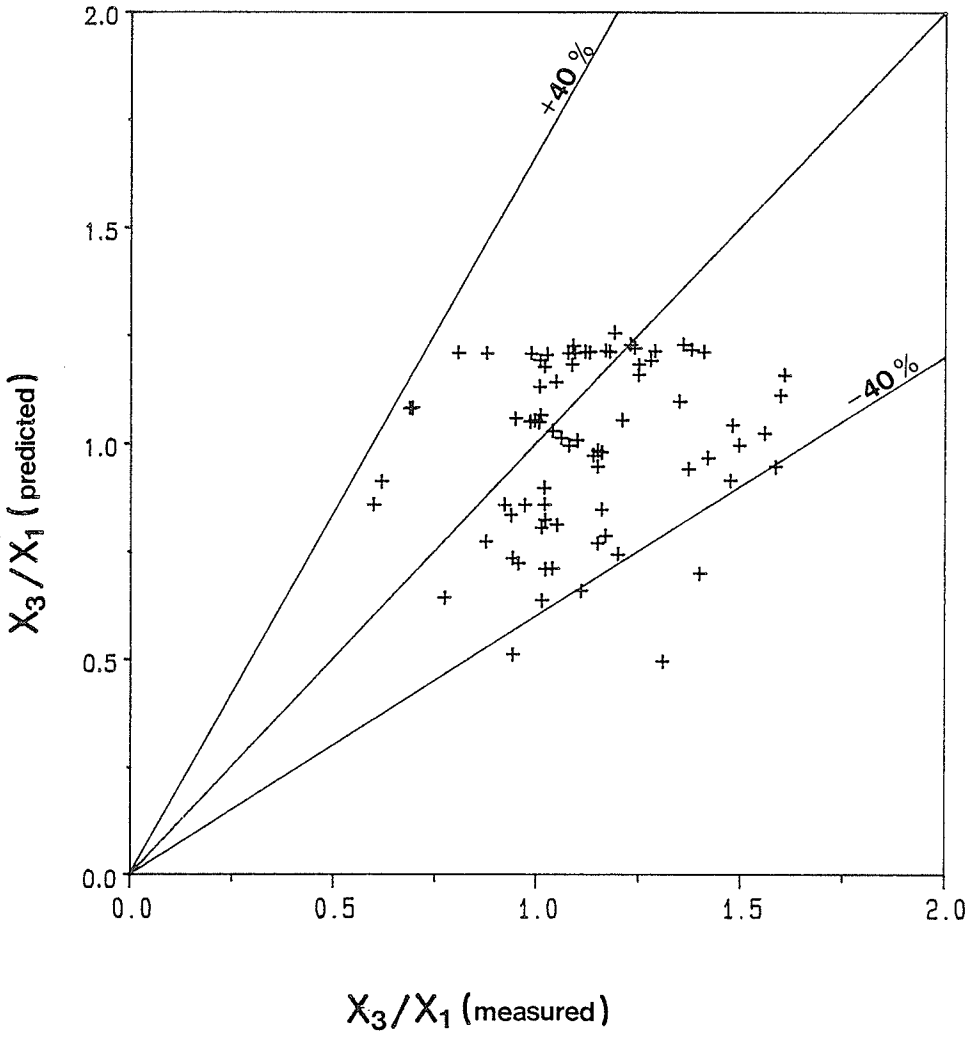

Fig. 4.14 Comparison between the correlation by Seeger et al. [14] and the present data for all x_1 and $G_3/G_1 \geq 0.3$

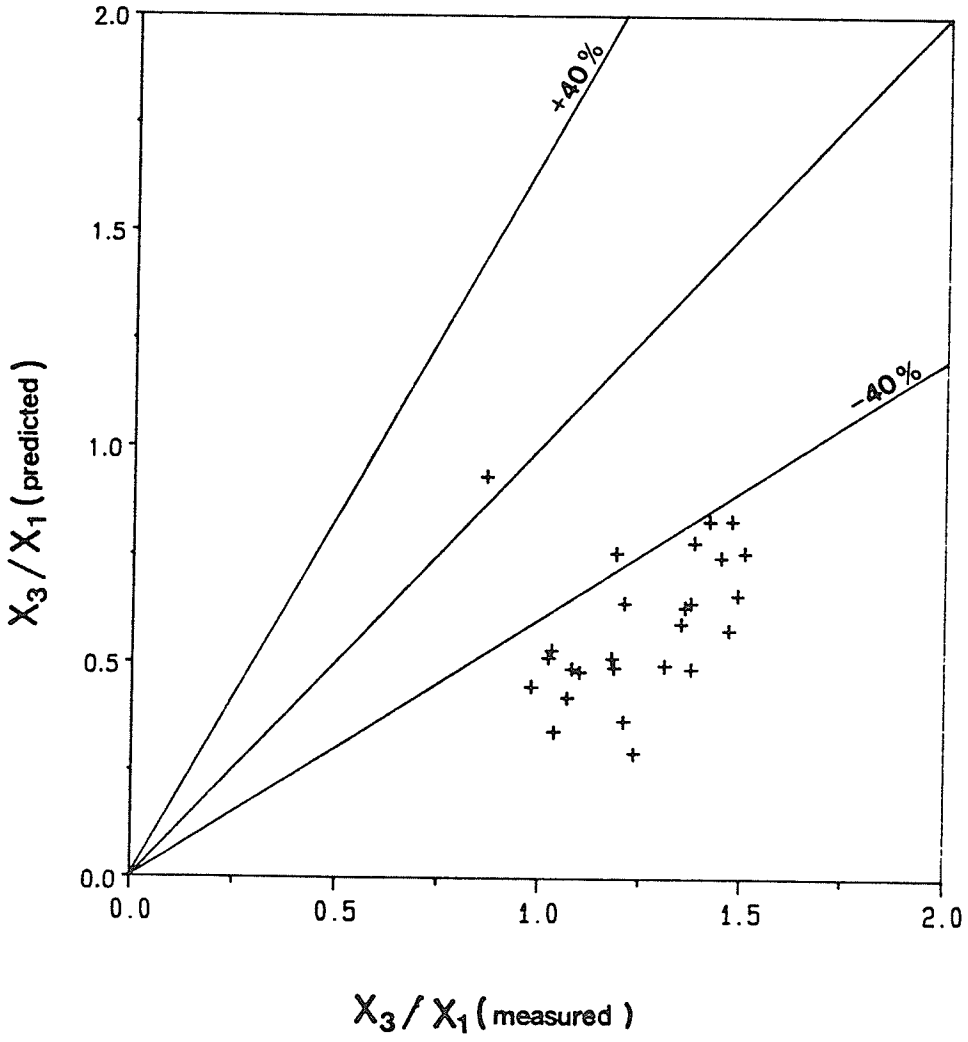

Fig. 4.15 Comparison between the correlation by Seeger et al. [14] and the present data for all x_1 and $G_3/G_1<0.3$

Chapter 5

CONCLUSIONS AND RECOMMENDATIONS

5.1 Conclusions

In the present investigation, the phase distribution of two-phase flow through a tee junction was studied. The investigation included: obtaining phase-distribution data for steam-water flow through a horizontal tee junction with an equal diameter horizontal branch; a qualitative discussion of the present phase-distribution results, as well as results from previous investigations; and a quantitative comparison of the present experimental results with existing phase-distribution correlations. For the range of operating conditions in the present investigation, a number of conclusions can be drawn.

1. The phases did not, in general, distribute themselves evenly through the tee junction.
2. All stratified flow data were below the line of even phase distribution. Most of the wavy and semiannular-wavy flow data were above this line, whereas the semiannular flow data were both above and below it.
3. For a fixed G_1, x_3/x_1 decreased with increasing x_1, except however, at the lowest inlet mass fluxes investigated where this trend was reversed.

4. For a fixed inlet flow pattern and a fixed $\bar{x}_1$, there was no apparent effect of $\bar{G}_1$ on the phase distribution.
5. For any fixed $\bar{V}_{GS}$, F_{BL} decreased with increasing $\bar{V}_{LS}$, irrespective of the inlet flow pattern.
6. Although the model developed by Azzopardi and Whalley [7] failed to predict the present phase-distribution data, the predictions became increasingly better as the inlet $\bar{x}_1$ and $\bar{V}_{GS}/\bar{V}_{LS}$ increased.
7. The Seeger et al. [14] correlation predicted the present phase-distribution data remarkably well over the entire range of operating conditions and where $G_3/G_1 \geq 0.3$. This correlation failed, however, to predict the data for $G_3/G_1 < 0.3$.

5.2 Recommendations for Future Work

The present investigation is one of few experimental studies undertaken in this extremely important two-phase flow research topic. Not unlike previous investigations, only a narrow range of phase-distribution data could be added to that which already exists. While this investigation succeeded in answering some questions, and in some cases verifying previously investigated questions, many new questions were raised. The questions which we face now must be understood before any generalized mathematical models can be developed. It is hoped that this investigation will motivate others to undertake experimental investigations at previously untested operating conditions, in an effort to better understand the following:

1. The influence of the operating conditions on the phase distribution; those being, x_1, G_1, P_1, G_3/G_1 and the inlet flow pattern.
2. The influence of the junction geometry (D_1, D_3, D_3/D_1) on the phase distribution.
3. The influence of the junction orientation on the phase distribution.
4. The influence of the junction itself; that is, between tees and wyes of different configurations.

REFERENCES

1. Azzopardi, B.J., "Two-Phase Flow in Junctions," Encyclopedia of Fluid Mechanics, Chapter 25, Gulf, 1986.

2. Tsuyama, M., and Taga, M., "On the Flow of the Air-Water Mixture in the Branch Pipe - 1. Experiment on the Horizontal Branch which is Equal to the Main One in Diameter," Bull. JSME, Vol. 2, pp. 151-156, 1959.

3. Collier, J.G., "Single-Phase and Two-Phase Flow Behavior in Primary Circuit Components,"Proceedings of NATO Advanced Study Institute on Two-Phase Flow and Heat Transfer, Istanbul, Turkey, 1976.

4. Hong, K.C., "Two-Phase Flow Splitting at a Pipe Tee," Journal of Petroleum Technology, pp. 270-296, 1978.

5. Johansen, S.E.,"Experimental Study of Gas-Liquid Flow in a Pipe Tee," M.Sc. Thesis, University of Tulsa, 1979.

6. Henry, J.A.R., "Dividing Annular Flow in a Horizontal Tee," Int. J. Multiphase Flow, Vol. 7, pp. 343-355, 1981.

7. Azzopardi, B.J., and Whalley, P.B., "The Effect of Flow Patterns on Two-Phase Flow in a T Junction," Int. J. Multiphase Flow, Vol. 8, pp. 497-507, 1982.

8. Whalley, P.B., and Azzopardi, B.J., "Two-Phase Flow in a 'T'Junction," UKAEA Report AERE-R 9699, 1980.

9. Whalley, P.B., and Fells, N.S., "Further Measurements of Two-Phase Flow in a T Junction," UKAEA Report AERE-M 3149, 1981.

10. Azzopardi, B.J., and Baker, D.R., "Two-Phase Flow in a T Junction: The Effect of Flow Pattern in Vertical Upflow," UKAEA Report AERE-R 10174, 1981.

11. Azzopardi, B.J., "The Effect of Side Arm Diameter on the Two-Phase Flow Split at a "T" Junction," Int. J. Multiphase Flow, Vol. 10, pp. 509-512, 1984.

12. Saba, N., and Lahey, R.T., "The Analysis of Phase Separation in Branching Conduits," Int. J. Multiphase Flow, Vol. 10, pp.1-20, 1984.

13. Lahey, R.T., "Current Understanding of Phase Separation Mechanisms in Branching Conduits," Presented at the Japanese/U.S. Symposium on Transient Two-Phase Flow, 1984.

14. Seeger, W., Reimann, J., and Mueller, U., "Phase Separation in a T-Junction with a Horizontal Inlet," 2nd Int. Conference on Multi-Phase Flow, London, England, June 1985.

15. Honan, T.J., and Lahey, R.T., The Measurement of Phase Separation in Wyes and Tees," Nuclear Eng. and Design, Vol. 64, pp. 93-102, 1981.

16. Mandhane, J. M., Gregory, G.A., and Aziz, K. "A Flow Pattern Map of Gas-Liquid Flow in Horizontal Pipes," Int. J. Multiphase Flow, Vol. 1, pp. 537-553, 1974.

17. Katoaka, I., and Ishii, M., "Entrainment and Deposition Rates of Droplets in Annular Two-Phase Flow," ASME/JSME, Thermal Engineering Joint Conference Proceedings, Vol.1, pp. 69-80, 1983.

18. Gill, L.E., and Hewitt, G.F., "Further Data on the Upwards Annular Flow of Air-Water Mixtures," UKAEA Report AERE-R 3935, 1962.

Appendix A

NOMINAL INLET FLOW PARAMETERS

Table A.1 summarizes the nominal inlet operating conditions for the different experimental groups.

Legend

No.	Group number
Inlet F.P.	Inlet flow pattern
$\bar{P}_1$	Nominal inlet pressure (kPa)
$\bar{G}_1$	Nominal inlet mass flux ($kg/m^2.s$)
$\bar{x}_1$	Nominal inlet quality (%)

Table A.1

Nominal Inlet Flow Parameters

No.	Inlet F.P.	$\bar{P}_1$ (kPa)	$\bar{G}_1$ (kg/m^2.s)	$\bar{x}_1$ (%)
1	W	141	29.5	38.5
2	SA-W	179	32.1	52.9
3	W	135	25.0	35.8
4	W	194	39.1	42.8
5	SA	196	32.1	63.4
6	SA	187	40.5	53.6
7	SA	207	33.6	75.5
8	SA	180	27.3	69.3
9	SA	156	28.9	58.9
10	SA	182	26.5	82.8
11	SA-W	159	19.3	72.8
12	SA	166	25.2	68.6
13	W	134	34.0	30.3
14	W	134	38.5	23.3
15	SA-W	159	48.9	32.5
16	W	126	17.3	51.1
17	ST	116	16.6	32.1
18	ST	134	16.8	40.9
19	SA-W	163	28.9	52.2

Appendix B

OPERATING CONDITIONS AND PHASE-DISTRIBUTION DATA

Table B.1 provides a listing of the operating conditions and corresponding phase-distribution data for all test runs.

Legend

No.	Run number
P_1	Inlet pressure (kPa)
G_1	Inlet mass flux ($kg/m^2.s$)
x_1	Inlet quality (%)
G_3/G_1	Extraction rate
x_3/x_1	Ratio of branch to inlet quality
Error	Heat balance error (%)
F_{BG}	Fraction of total vapor entering branch
F_{BL}	Fraction of total liquid entering branch
$\bar{V}_{GS}$	Superficial vapor velocity (m/s)
$\bar{V}_{LS}$	Superficial liquid velocity (m/s)

Table B.1

Operating Conditions and Phase-Distribution Data

No.	P_1 (kPa)	G_1 (kg/m².s)	x_1 (%)	G_3/G_1	x_3/x_1	Error (%)	F_{BG}	F_{BL}	V_{GS} (m/s)	V_{LS} (m/s)	BRANCH FLOW PATTERN	RUN FLOW PATTERN
1-1	136	29.6	38.7	.265	1.36	-4.79	.360	.205	14.6	.0191	ST	ST
1-2	125	28.6	40.5	.413	1.42	-6.10	.586	.295	16.0	.0179	ST	ST
1-3	150	32.1	41.6	.512	1.38	-7.56	.705	.374	15.5	.0197	W	ST
1-4	150	28.8	36.0	.542	1.45	-0.46	.514	.316	12.0	.0194	ST	ST
1-5	142	28.5	35.7	.624	1.33	-3.56	.832	.508	12.4	.0192	W	ST
2-1	124	32.5	51.4	.211	1.21	-4.31	.255	.164	23.2	.0166	ST	W
2-2	167	32.5	54.4	.378	1.16	-1.48	.438	.307	18.5	.0157	ST	W
2-3	156	33.0	56.8	.440	1.14	-1.64	.501	.360	20.9	.0150	W	W
2-4	181	31.7	50.5	.588	1.28	-2.61	.754	.419	15.4	.0166	W	ST
2-5	205	30.7	51.2	.682	1.24	+0.58	.842	.513	13.5	.0159	W	ST
3-1	143	25.3	34.6	.236	1.35	-9.52	.320	.192	10.6	.0174	ST	W
3-2	129	24.9	35.7	.476	1.35	-6.26	.644	.382	11.9	.0168	ST	ST
3-3	129	25.2	38.6	.604	1.29	-4.65	.779	.494	13.0	.0162	ST	ST
3-4	139	24.5	34.2	.722	1.10	-6.59	.797	.684	10.42	.0169	W	ST
4-1	194	37.8	43.2	.209	1.31	+5.74	.273	.160	14.8	.0228	ST	W
4-2	156	39.8	43.5	.402	1.24	-3.77	.499	.317	20.7	.0224	W	W
4-3	194	39.2	44.9	.551	1.35	-3.10	.744	.394	16.0	.0228	W	ST
4-4	208	38.9	39.8	.575	1.41	-3.68	.814	.417	13.1	.0249	W	ST
4-5	201	39.5	41.7	.594	1.38	-4.26	.822	.431	14.4	.0244	W	ST
4-6	208	39.4	40.5	.622	1.36	-4.55	.842	.471	13.5	.0249	W	ST
5-1	205	31.3	62.8	.235	1.07	-2.22	.252	.209	16.9	.0124	ST	W
5-2	211	31.2	62.5	.257	1.08	-2.01	.277	.223	16.3	.0124	ST	W
5-3	184	33.2	64.4	.378	1.05	-6.31	.397	.343	20.4	.0125	ST	W
5-4	170	32.0	60.1	.461	1.10	-6.44	.505	.395	19.8	.0135	W	W
5-5	170	32.9	65.9	.481	1.04	-8.60	.501	.443	22.3	.0119	W	W
5-6	218	32.1	66.8	.656	1.13	-3.45	.743	.482	17.4	.0113	W	ST
5-7	215	31.7	61.5	.668	1.17	-4.68	.783	.484	16.0	.0130	W	ST

Table B.1 (continued)

No.	P_1 (kPa)	G_1 (kg/m².s)	x_1 (%)	G_3/G_1	x_3/x_1	Error (%)	F_{BG}	F_{BL}	V_{GS} (m/s)	V_{LS} (m/s)	BRANCH FLOW PATTERN	RUN FLOW PATTERN
6-1	204	39.3	52.5	.239	1.18	+1.41	.281	.192	17.8	.0198	ST	W
6-2	198	39.3	51.7	.296	1.18	+1.30	.349	.238	18.1	.0201	ST	W
6-3	184	41.1	53.7	.338	1.15	+3.48	.390	.278	21.1	.0202	ST	W
6-4	187	41.4	53.7	.344	1.17	-1.87	.404	.275	20.9	.0203	ST	W
6-5	170	43.0	55.8	.435	1.16	-3.13	.504	.348	24.7	.0201	ST	ST
6-6	163	42.2	56.2	.440	1.15	+6.42	.504	.358	25.4	.0195	W	W
6-7	187	39.0	53.6	.548	1.25	+1.34	.687	.387	19.6	.0192	W	ST
6-8	204	38.7	51.3	.624	1.29	+2.96	.807	.432	17.2	.0200	W	ST
7-1	222	33.6	71.7	.302	.980	-3.41	.296	.317	19.2	.0101	ST	SA
7-2	210	32.8	76.3	.360	.956	+0.17	.344	.412	21.0	.00825	ST	SA
7-3	197	33.7	76.3	.412	.972	-1.62	.400	.450	23.0	.00846	ST	SA
7-4	177	34.3	78.5	.507	.984	-1.46	.499	.537	26.7	.00780	W	W
7-5	205	35.0	74.5	.566	1.05	-1.51	.594	.487	22.4	.00947	W	ST
7-6	232	32.4	75.4	.687	1.08	+1.19	.740	.522	18.7	.00849	SA	ST
8-1	187	26.5	68.5	.290	1.03	-5.93	.299	.269	17.1	.00885	ST	W
8-2	184	27.8	68.6	.350	1.04	-8.48	.363	.323	18.2	.00924	ST	W
8-3	170	27.4	70.2	.411	1.02	-6.62	.418	.392	19.8	.00862	ST	ST
8-4	156	28.1	73.0	.514	1.01	-5.67	.521	.498	22.9	.00799	ST	ST
8-5	201	26.9	66.2	.702	1.12	-8.42	.785	.540	15.6	.00966	W	ST
9-1	163	28.6	58.1	.256	1.10	-8.34	.282	.219	17.8	.0127	ST	W
9-2	156	29.4	59.1	.320	1.11	-9.41	.356	.267	19.4	.0127	ST	W
9-3	135	29.1	61.4	.465	1.08	-8.62	.503	.404	22.8	.0118	ST	ST
9-4	170	28.3	57.1	.656	1.18	-7.88	.775	.498	16.6	.0128	W	ST
10-1	191	25.8	81.0	.305	.943	-0.64	.288	.379	19.2	.00518	ST	W
10-2	181	26.0	82.1	.382	.941	-0.02	.359	.485	20.7	.00493	ST	W
10-3	173	26.4	84.4	.421	.937	+0.01	.394	.564	22.6	.00435	ST	W
10-4	156	28.0	86.8	.527	.949	+0.47	.500	.705	27.2	.00390	ST	W
10-5	211	26.4	79.8	.795	1.02	+1.11	.808	.743	17.6	.00565	W	ST

Table B.1 (continued)

No.	P_1 (kPa)	G_1 (kg/m².s)	x_1 (%)	G_3/G_1	x_3/x_1	Error (%)	F_{BG}	F_{BL}	V_{GS} (m/s)	V_{LS} (m/s)	BRANCH FLOW PATTERN	RUN FLOW PATTERN
11-1	167	19.1	71.9	.278	.981	-5.97	.272	.292	14.4	.00567	ST	ST
11-2	158	19.5	72.4	.340	1.01	-6.50	.345	.328	15.5	.00566	ST	ST
11-3	156	20.0	72.3	.406	1.02	-7.68	.414	.384	16.1	.00583	ST	ST
11-4	153	20.2	74.1	.514	.997	-6.89	.512	.519	17.0	.00550	ST	ST
11-5	153	18.9	74.1	.570	1.01	-4.58	.574	.558	15.9	.00515	ST	ST
11-6	167	18.1	71.9	.714	1.03	-3.91	.733	.667	13.6	.00536	ST	ST
12-1	181	24.3	66.2	.225	1.04	-7.08	.234	.209	15.6	.00868	ST	W
12-2	170	24.5	67.8	.287	1.02	-6.49	.293	.273	17.1	.00833	ST	W
12-3	163	25.3	69.3	.355	1.02	-7.75	.363	.338	18.8	.00820	ST	W
12-4	156	25.7	71.2	.394	1.01	-6.00	.399	.381	20.4	.00779	ST	W
12-5	143	26.0	71.2	.505	1.01	-9.11	.508	.498	22.4	.00787	ST	ST
12-6	184	25.4	65.7	.715	1.09	-7.79	.782	.585	15.9	.00922	W	ST
13-1	132	33.5	29.0	.225	1.37	-7.25	.309	.190	12.7	.0250	ST	ST
13-2	129	33.7	31.7	.280	1.45	-4.45	.405	.222	14.3	.0241	ST	ST
13-3	122	34.8	32.7	.357	1.48	-9.57	.527	.275	16.0	.0245	ST	ST
13-4	153	34.1	27.8	.689	1.20	-9.36	.829	.636	10.8	.0260	ST	ST
14-1	143	38.1	21.4	.207	1.19	-7.83	.246	.196	9.88	.0315	ST	ST
14-2	136	38.1	23.0	.233	1.38	-4.17	.321	.206	11.2	.0308	ST	ST
14-3	132	38.3	23.8	.261	1.42	-4.05	.370	.227	11.9	.0307	ST	ST
14-4	129	38.8	24.5	.267	1.47	-4.93	.394	.226	12.7	.0307	ST	ST
14-5	122	38.4	24.7	.324	1.59	-6.80	.514	.262	13.3	.0303	ST	ST
14-6	132	39.3	23.9	.445	1.61	-8.62	.716	.360	12.3	.0314	ST	ST
14-7	143	38.5	21.6	.661	1.19	-9.96	.787	.626	10.1	.0317	ST	ST
15-1	184	49.1	30.8	.153	1.38	+1.93	.211	.128	14.4	.0360	ST	W
15-2	170	49.6	30.4	.186	1.47	-4.33	.273	.148	15.5	.0365	ST	W
15-3	163	49.0	32.9	.230	1.49	+3.61	.343	.177	17.3	.0347	ST	W
15-4	149	48.3	33.5	.277	1.51	-1.69	.417	.206	18.9	.0338	ST	ST
15-5	143	50.3	34.3	.351	1.45	-3.04	.509	.269	20.9	.0348	ST	W
15-6	150	48.5	33.5	.399	1.56	-2.69	.621	.287	18.8	.0340	ST	ST
15-7	156	47.7	32.0	.445	1.60	-1.99	.711	.320	17.1	.0342	W	ST

Table B.1 (continued)

No.	P_1 (kPa)	G_1 (kg/m².s)	x_1 (%)	G_3/G_1	x_3/x_1	Error (%)	F_{BG}	F_{BL}	V_{GS} (m/s)	V_{LS} (m/s)	BRANCH FLOW PATTERN	RUN FLOW PATTERN
16-1	132	17.1	48.0	.308	.774	-4.75	.229	.380	10.7	.00934	ST	ST
16-2	129	16.8	50.3	.361	.877	+1.20	.317	.406	11.3	.00874	ST	ST
16-3	127	17.1	51.3	.397	.922	-0.98	.366	.429	11.9	.00873	ST	ST
16-4	122	17.3	51.9	.415	1.02	-3.20	.423	.406	12.7	.00872	ST	ST
16-5	115	17.8	54.3	.474	1.06	-6.98	.504	.439	14.4	.00851	ST	ST
16-6	129	17.9	51.5	.596	1.09	-5.74	.648	.542	12.3	.00913	ST	ST
16-7	129	16.8	51.2	.728	.987	+1.33	.719	.738	11.5	.00858	ST	ST
17-1	122	16.5	30.0	.364	.618	-4.30	.225	.424	6.99	.0121	ST	ST
17-2	115	16.1	31.8	.466	.694	+3.09	.323	.532	7.63	.0115	ST	ST
17-3	115	16.5	32.1	.507	.720	+4.84	.365	.574	7.86	.0117	ST	ST
17-4	115	16.8	32.2	.532	.739	+2.91	.393	.598	8.03	.0119	ST	ST
17-5	111	16.9	34.0	.623	.779	+1.54	.485	.694	8.84	.0117	ST	ST
17-6	116	16.5	32.6	.733	.917	+0.67	.672	.763	7.96	.0117	ST	ST
18-1	143	16.8	37.9	.363	.600	-7.97	.218	.452	7.72	.0110	ST	ST
18-2	136	16.6	39.7	.484	.688	-4.14	.333	.583	8.40	.0105	ST	ST
18-3	136	17.2	40.6	.534	.742	-9.33	.396	.628	8.87	.0107	ST	ST
18-4	129	16.9	42.7	.557	.744	-4.02	.414	.663	9.64	.0102	ST	ST
18-5	122	16.5	43.4	.636	.808	-3.47	.514	.730	10.1	.00975	ST	ST
18-6	136	16.8	41.2	.741	.879	-1.76	.651	.803	8.79	.0104	ST	ST
19-1	177	27.5	49.2	.166	1.24	+4.01	.205	.128	13.4	.0148	ST	W
19-2	170	28.6	52.0	.245	1.19	+1.52	.290	.196	15.3	.0145	ST	W
19-3	160	28.9	52.0	.298	1.21	-3.96	.361	.230	16.4	.0146	ST	W
19-4	156	29.3	53.2	.340	1.20	-4.86	.408	.261	17.4	.0144	ST	ST
19-5	143	30.0	56.2	.431	1.15	-5.92	.498	.345	20.4	.0138	ST	ST
19-6	160	29.3	52.8	.479	1.21	-4.39	.578	.367	16.9	.0146	ST	ST
19-7	174	28.7	49.7	.574	1.25	-2.59	.718	.432	14.4	.0153	W	ST

Appendix C

DATA USED IN FIGS. 4.5(a-d)

Table C.1 provides a listing of the group numbers associated with the data of Figs. 4.5(a-d).

Legend

Figure	Figure number
$\bar{V}_{GS}$	Nominal superficial vapor velocity (m/s)
$\bar{V}_{LS}$	Nominal superficial liquid velocity (m/s)
No.	Datum number

Table C.1

Data used in Figs. 4.5(a-d)

Figure	$\bar{V}_{GS}$ (m/s)	$\bar{V}_{LS}$ (m/s)	No.
4.5(a)	8.11	0.0107	18-1 18-2 18-3 18-6
		0.0118	17-1 17-2 17-3 17-5 17-6
4.5(b)	12.6	0.00878	16-2 16-3 16-4 16-6 16-7
		0.0159	2-5 3-2 3-3 19-1
		0.0249	4-4 4-6 13-1
		0.0308	14-3 14-4 14-5 14-6
4.5(c)	15.5	0.0058	11-1 11-2 11-3 11-5

Table C.1 (continued)

Figure	$\bar{V}_{GS}$ (m/s)	$\bar{V}_{LS}$ (m/s)	No.
4.5(c) (cont.)		0.00902	8-5 12-1 12-6 16-4
		0.0151	2-4 19-2 19-3 19-6 19-7
		0.0238	4-1 4-3 4-5 13-2 13-3
4.5(d)	18.2	0.00544	10-1 10-5 11-4
		0.00862	7-6 8-1 8-2 8-3 12-2 12-3
		0.0133	5-4 9-1 9-2 19-4
		0.0198	6-1 6-2 6-7 6-8
		0.0342	15-3 15-4 15-6 15-7